공학박사 학위논문

Nanocomposite Thin Films Containing Amyloid Fibrils Based on the Layer-by-Layer Assembly

다층적층법 기반으로 형성된 아밀로이드 나노복합체 박막의 구현

2014년 2월

서울대학교 대학원

화학생물공학부

이 지 혜

Nanocomposite Thin Films Containing Amyloid Fibrils Based on the Layer-by-Layer Assembly

다층적층법 기반으로 형성된 아밀로이드 나노복합체 박막의 구현

지도교수 차 국 헌

이 논문을 공학박사 학위논문으로 제출함

2013 년 10 월

서울대학교 대학원
화학생물공학부
이 지 혜

이지혜의 공학박사 학위논문을 인준함

2013 년 12 월

위 원 장 장 정 식 (인)
부 위 원 장 車 國 憲 (인)
위 원 백 승 렬 (인)
위 원 조 진 한 (인)
위 원 남 기 태 (인)

Abstract

Nanocomposite Thin Films Containing Amyloid Fibrils Based on the Layer-by-Layer Assembly

Ji-Hye Lee

School of Chemical and Biological Engineering

The Graduate School

Seoul National University

Protein aggregates including amyloid have recently received much attention on a variety of research fields such as medicine, food, nanotechnology, and soft matter science. Almost peptides and proteins are converted into insoluble amyloid fibrils under certain environmental conditions. This amyloid fibril has common properties including highly ordered nanostructure induced by hydrogen bonds between parallel or anti-parallel beta sheets stability to harsh environments. Therefore they are very stable over a wide range of pH, salt concentration, and temperature and resistant to proteases. The extensive hydrogen bond network and side-chain interactions in steric-zipper of tightly packed cross β-sheet structure could account for this extraordinary stability. In addition, they

have high mechanical stiffness comparable to silk and steel, and are easily functionalized for specific applications. Also, highly ordered amyloid aggregation of fibrils leads formation of complex networks of filaments, gels and films that may be suitable for immobilizing enzymes, small molecules and drugs. These merits make amyloid fibril as an attractive candidate for advanced functional nanomaterial to develop functional platforms. Therefore recently a number of researches about advanced materials incorporating amyloid fibrils have been constructed. In this thesis, nanocomposite thin film containing amyloid fibrils was demonstrated by layer-by-layer deposition. The brief introduce about amyloid fibril and layer-by-layer deposition methods are in Chapter 1.

In Chapter 2, we have investigated fibril formation kinetics of κ-casein and some factors affecting fibrillation kinetics, reduction of disulfide bonds within κ-casein, incubation temperature, and initial concentration of κ-casein. Unlike the fibril formed with nucleation-dependent mechanism, the rate-limiting step for fibrillation of κ-casein is dissociating multimeric κ-casein into monomeric, dimeric and trimeric κ-casein. Therefore the reduction of disulfide bonds is critical to induce fibrillation and the contour length of fibrils also elongated by reduction of disulfide bonds. Incubation temperature is, also, one of the most critical factors to change the fibrillation kinetics and fibril morphologies. In the initial step of fibrillation, the kinetics increases rapidly and sharply, and then the kinetics set as saturated at different values depended on the temperature. The slope of kinetics during early stage is dependent on the temperature. Therefore, incubation temperature affected on not only conversion rates into fibrils but

also kinetics (slopes of fluorescence intensity graph) of fibrillation of κ-casein. Also the morphologies was affected by the temperature, thus contour length and height increases as temperature increases due to degree of protein denaturation to have propensity to fibril forming by heating. As similar with fibril formed through nucleation depended mechanism, κ-casein showed that the degree of conversion from native protein to fibrillar structures increases by initial concentration increases. Also the contour length of the fibrils was elongated with increase of initial concentration. Fibrillation kinetics and morphology of κ-casein fibrils, induced by nucleation-depended mechanism, is controlled by reduction of disulfide bonds, temperature, and initial concentration.

In Chapter 3, we have demonstrated that nanocomposite film incorporating amyloid fibrils induced from a kind of milk protein, κ-casein, with dip-based layer-by-layer deposition. The matured fibrils of κ-casein were assembled with polyelectrolyte to fabricate nanocomposite films by attractive intermolecular interactions. The charge density of κ-casein fibrils is affected by pH value and it is negatively and positively charged when the fibrils are in acid and basic environmental condition, respectively. The charge density can be adjusted by changing the pH of the solvent which makes them excellent candidates for thin films or capsules by electrostatic interaction driven LbL film. Three different types of nanocomposite films were fabricated with negatively charged PSS and PAA at pH 3, and with positively charged PDAC at pH 8. (κ-casein fibril/PAA) film was assembled by combined force of hydrogen bonds and electrostatic interaction because more than 90% of carboxylic groups in PAA is protonated at pH 3, and the (κ-casein fibril/PSS) and (κ-casein fibril/PDAC) film were assembled by

electrostatic interaction at pH 3 and 8, respectively. The film based on electrostatic interaction showed linear film growth and increased surface roughness with the number of layer, while the film based on combined force of electrostatic interaction and hydrogen bonds showed exponential film growth and the consistent surface roughness with the number of the film layers. Also microcapsules were formed successfully with $(\kappa\text{-casein fibril/PEs})_{6.5}$ assembled at pH 3 and the thickness of the shell is correlated with film thickness assembled on silicon substrate. Our results suggest that all the film characteristics strongly depend on the method of its preparation. It is anticipated that nanocomposite film and capsule incorporated with amyloid could be applied to biomedical tissue engineering, drug, and food engineering.

In Chapter 4, we have explored the formation of *in-situ* nanocomposite films consisting of a weak PEs (PAA) and *κ*-casein, employed as biocompatible amyloid fibril precursors, constructed by the dip-based LbL deposition. The *κ*-casein was transformed into amyloid fibrils without film delamination by combined external stimuli such as pH, reductant, and heat. The aspect ratio as well as the fibril density of such amyloid fibrils within the multilayer films was controlled by incubation time. The formation of *in-situ* nanocomposite films, triggered by external stimuli, could open up new types of nanocomposite platforms suitable for a wide range of advanced materials and biomedical applications.

In Chapter 5, we demonstrated the fibrillation of κ-casein within LbL film and the fibrillation kinetics on the LbL film consisting of κ-casein and PAA. Although fibrillation

kinetics of κ-casein within LbL film was delayed when compared with fibrillation kinetics of κ-casein in solution, the contour length of fibrils grown on the LbL film was longer than three times. And also the fibrils were thickened and twined each other by extended thermal incubation, which were depended on the incubation temperature and reduction of disulfide bonds. In addition, this study provides a potential platform for fabricating structure controlled nanomaterials by self-assembly of functional group tailored peptides on the LbL films.

Keywords

Functional Thin Film, Multilayer Film, Layer-by-Layer, Amyloid, κ-Casein, Polyelectrolytes, Nanocomposite

Student Number: 2009-31263

Contents

Chapter 1. Introduction

Chapter 2. Fibrillation kinetics of κ-Casein in Bulk Solution

Chapter 3. Polymeric Nanocomposites Incorporating κ-Casein Amyloid Fibrils by Layer-by-Layer deposition

Chapter 4. In-Situ Fibrillation of κ-Casein within LbL Film by External Stimuli

List of Figures

List of Schemes

Chapter 1.

Introduction

1.1 Amyloids as Functional Nanomaterial

Protein aggregates including amyloid have recently received much attention on a variety of research fields such as medicine, food, nanotechnology, and soft matter science. In the early stage of amyloid research, the study was only focused on the controlling fibrillation kinetics of protein and finding the way to suppression of amyloid formation and elimination of amyloid in point of therapeutic view, since the amyloid was well known as protein aggregates associated with a number of neurodegenerative disease such as Alzheimer's, Parkinson's, and Huntington's diseases.[1,2] However, besides disease associated proteins, almost peptides and proteins are converted into insoluble amyloid fibrils under certain.[14] The functional group may be recruited at the amino acid side chain for applications such as receptor-ligand and gold-thiol interactions. Furthermore, highly ordered amyloid aggregation of fibrils leads formation of complex networks of filaments, gels and films that may be suitable for immobilizing enzymes, small molecules and drugs.[15,16] These merits make amyloid fibril as an attractive candidate for advanced functional nanomaterial to develop functional platforms. Therefore recently a number of researches about advanced materials incorporating amyloid fibrils have been constructed. For example, protein fibril-based nanocomposites which incorporate matured protein fibril within bulk matrices such as silicon elastomer (poly(dimethylsiloxane)),[17] poly(L-lactic acid),[18] poly(ethylene glycol)[19] and epoxy resin.[20] These new types of

nanocomposites, filled with optimal content of protein fibrils, possess tuned and balanced physical and mechanical properties such as stiffness and Young's modulus without sacrificing their thermal and elongation properties. More recently, nanocomposites containing protein fibrils and graphene sheets have been demonstrated to be biodegradable and highly conductive.[21] Although fibril-based nanocomposite have been introduced, understanding intermolecular interaction between fibrils and matrices and manufacturing various of types composite such as thin film and capsule are needed to apply a variety field such as drug and food carrier, scaffold for tissue engineering, protective film, and so on.

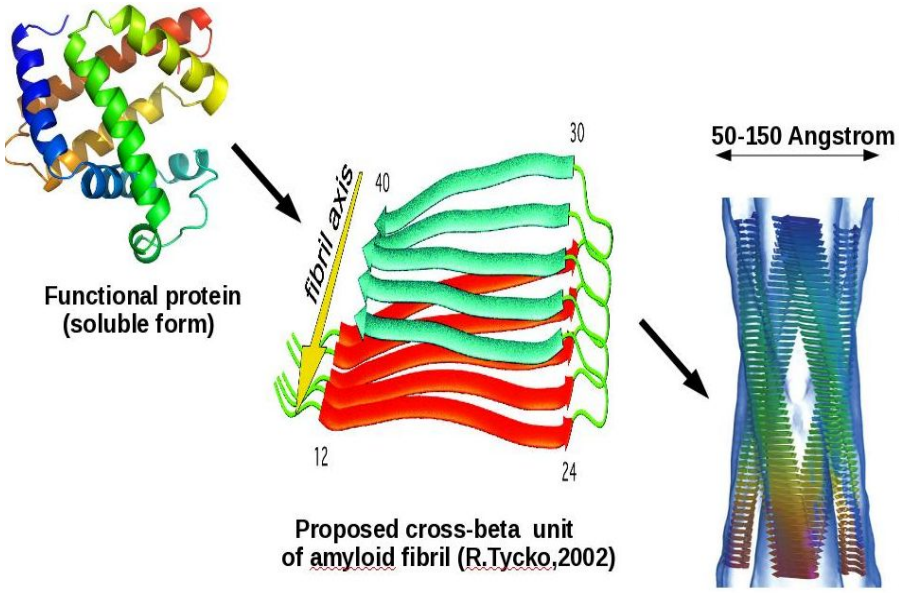

Scheme1.1. Molecular model of an amyloid fibril derived from cryo-EM analysis of fibrils showing one way in which regions of the polypeptide chain involved in β-sheet structure is assembled within the fibrils.

1.2 Layer-by-Layer Assembly

LbL assembly, involving the alternate deposition of species with complementary intermolecular interactions, is one of the most versatile methods to fabricate composite films. Although LbL assembly was introduced by the pioneering work of Iler in 1966,[22] its importance was not recognized until it was rediscovered by Decher and co-workers in the early 1990s.[23] Since then, much progress has been achieved in the field of LbL assembly. The building blocks of LbL assembly include, but are not limited to, synthetic polymers,[24-26] polymeric microgels,[27-29] biomacromolecules,[30,31] nanoparticles,[32] graphenes,[33,34] block copolymers,[35] and complexes of these species[24], and also these functional materials could be inserted at desired location within the multilayer film. The process of LbL deposition to fabricate composite films is quite simple and can be accurately controlled to allow finely tailored film growth with nanometer-scale resolution. Taking LbL assembly of oppositely charged species as an example, a multilayer film can be fabricated by alternately dipping a charged substrate into aqueous solutions of oppositely charged materials with intermediate steps of rinsing in water. This conventional assembly based on dipping method has been extended to spin-assisted,[36] spray-assisted,[37,38] and microfluidic-assisted LbL assembly.[39] LbL deposition can be driven by multiple weak interactions, including electrostatic interactions,[23] hydrogen-bonds,[40] charge-transfer interactions,[41] biospecific interactions,[42] cation–dipole interactions,[43] and the combined interaction of the above forces, etc. Also the LbL films could have external stimuli, including pH, salt, and temperature responsive properties depended on the kinds of incorporating material and intermolecular interactions between

pair materials within LbL films.[44] Multilayer film by LbL deposition methods have been received much attention to develop energy,[45] battery,[34] membrane, drug delivery system[29] due to its programmable properties.

1.3 Nanocomposite Thin Film Incorporating Amyloid by LbL Depositon Method

In this thesis, we focus on fabrication of nanocomposite thin film incorporating with amyloid fibrils induced from bovine κ-casein, a kind of food grade protein, as reinforcement and polyelectrolyte as matrix by layer-by-layer (LbL) deposition method. Prior to fabrication of nanocomosite with amyloid fibril, fibril formation and kinetics, and fibrillation mechanism of κ-casein are elucidated to utilize as reinforcement (Chapter2) in nanocomposite thin film. Since amyloid fibril induced from protein have isoelectric point, surface charge density of the fibril is affected by pH of their surrounding environment and can become more positively or negatively charged due to the loss or gain protons. Therefore the nanocomposite thin films incorporating amyloid fibril are easily fabricated in both of acid and basic environment using electrostatic interaction between fibrils and polyelectrolytes (charpter3). Beyond nanocomposite fulfilled with matured amyloid fibrils, we demonstrate in-situ nanocomposite induced by fibrillation of amyloid within multilayer thin film by controlling of intermolecular interaction between amyloid precursor protein and polyelectrolytes. Moreover the fibril formed within multilayer films from precursor of amyloid become thicker than fibrils formed in bulk solution by interfibrillar assembly (chapter4&5).

It is anticipated that our investigations, shown in this thesis, could contribute to establish an advanced new nanobio platform such as in-situ nanocomposite with biocompatible and robust mechanical property, which could be applied as robust drug carrier, tissue engineering matrix, and protective thin films.

1.4 References

(1) Chiti, F.; Dobson, C. M. *Annual review of biochemistry* **2006**, *75*, 333.

(2) Dobson, C. M. *Trends Biochem Sci* **1999**, *24*, 329.

(3) Dobson, C. M. *Philos T Roy Soc B* **2001**, *356*, 133.

(4) Swoboda, B. E. P.; Dobson, C. M.; Joniau, M.; Weissmann, C. *Philos T Roy Soc B* **2001**, *356*, 145.

(5) Fandrich, M.; Fletcher, M. A.; Dobson, C. M. *Nature* **2001**, *410*, 165.

(6) Chiti, F.; Webster, P.; Taddei, N.; Clark, A.; Stefani, M.; Ramponi, G.; Dobson, C. M. *P Natl Acad Sci USA* **1999**, *96*, 3590.

(7) Sunde, M.; Serpell, L. C.; Bartlam, M.; Fraser, P. E.; Pepys, M. B.; Blake, C. C. F. *J Mol Biol* **1997**, *273*, 729.

(8) Symmons, M. F.; Buchanan, S. G.; Clarke, D. T.; Jones, G.; Gay, N. J. *FEBS letters* **1997**, *412*, 397.

(9) Barnhart, M. M.; Chapman, M. R. *Annu Rev Microbiol* **2006**, *60*, 131.

(10) Fowler, D. M.; Koulov, A. V.; Balch, W. E.; Kelly, J. W. *Trends Biochem Sci* **2007**, *32*, 217.

(11) True, H. L.; Lindquist, S. L. *Nature* **2000**, *407*, 477.

(12) Sawaya, M. R.; Sambashivan, S.; Nelson, R.; Ivanova, M. I.; Sievers, S. A.; Apostol, M. I.; Thompson, M. J.; Balbirnie, M.; Wiltzius, J. J.; McFarlane, H. T.; Madsen, A. O.; Riekel, C.; Eisenberg, D. *Nature* **2007**, *447*, 453.

(13) Smith, J. F.; Knowles, T. P. J.; Dobson, C. M.; MacPhee, C. E.; Welland, M. E. *P Natl Acad Sci USA* **2006**, *103*, 15806.

(14) Cherny, I.; Gazit, E. *Angewandte Chemie* **2008**, *47*, 4062.

(15) Bhak, G.; Lee, S.; Park, J. W.; Cho, S.; Paik, S. R. *Biomaterials* **2010**, *31*, 5986.

(16) Chun, J.; Bhak, G.; Lee, S. G.; Lee, J. H.; Lee, D.; Char, K.; Paik, S. R. *Biomacromolecules* **2012**, *13*, 2731.

(17) Oppenheim, T.; Knowles, T. P. J.; Lacour, S. P.; Welland, M. E. *Acta Biomaterialia* **2010**, *6*, 1337.

(18) Byrne, N.; Hameed, N.; Werzer, O.; Guo, Q. P. *Eur Polym J* **2011**, *47*, 1279.

(19) Knowles, T. P. J.; Oppenheim, T. W.; Buell, A. K.; Chirgadze, D. Y.; Welland, M. E. *Nat Nanotechnol* **2010**, *5*, 204.

(20) Even, N.; Adler-Abramovich, L.; Buzhansky, L.; Dodiuk, H.; Gazit, E. *Small* **2011**, *7*, 1007.

(21) Li, C. X.; Adamcik, J.; Mezzenga, R. *Nat Nanotechnol* **2012**, *7*, 421.

(22) Iler, R. K. *Journal of colloid and interface science* **1966**, *21*, 569.

(23) Decher, G. *Science* **1997**, *277*, 1232.

(24) Guo, Y.; Geng, W.; Sun, J. *Langmuir : the ACS journal of surfaces and colloids* **2009**, *25*, 1004.

(25) Feldoto, Z.; Lundin, M.; Braesch-Andersen, S.; Blomberg, E. *Journal of colloid and interface science* **2011**, *354*, 31.

(26) Haberska, K.; Ruzgas, T. *Bioelectrochemistry* **2009**, *76*, 153.

(27) Clarke, K. C.; Lyon, L. A. *Langmuir : the ACS journal of surfaces and colloids* **2013**, *29*, 12852.

(28) Costa, E.; Lloyd, M. M.; Chopko, C.; Aguiar-Ricardo, A.; Hammond, P. T. *Langmuir* **2012**, *28*, 10082.

(29) De Geest, B. G.; Dejugnat, C.; Verhoeven, E.; Sukhorukov, G. B.; Jonas, A. M.; Plain, J.; Demeester, J.; De Smedt, S. C. *J Control Release* **2006**, *116*, 159.

(30) Elbakry, A.; Wurster, E. C.; Zaky, A.; Liebl, R.; Schindler, E.; Bauer-Kreisel, P.; Blunk, T.; Rachel, R.; Goepferich, A.; Breunig, M. *Small* **2012**, *8*, 3847.

(31) Saurer, E. M.; Flessner, R. M.; Sullivan, S. P.; Prausnitz, M. R.; Lynn, D. M. *Biomacromolecules* **2010**.

(32) Bae, W. K.; Kwak, J.; Lim, J.; Lee, D.; Nam, M. K.; Char, K.; Lee, C.; Lee, S. *Nano Lett* **2010**, *10*, 2368.

(33) Hong, J.; Char, K.; Kim, B. S. *J Phys Chem Lett* **2010**, *1*, 3442.

(34) Yu, A. P.; Park, H. W.; Davies, A.; Higgins, D. C.; Chen, Z. W.; Xiao, X. C. *J Phys Chem Lett* **2011**, *2*, 1855.

(35) Xu, L.; Zhu, Z. C.; Sukhishvili, S. A. *Langmuir : the ACS journal of surfaces and colloids* **2011**, *27*, 409.

(36) Cho, J.; Char, K.; Hong, J. D.; Lee, K. B. *Adv Mater* **2001**, *13*, 1076.

(37) Krogman, K. C.; Lowery, J. L.; Zacharia, N. S.; Rutledge, G. C.; Hammond, P. T. *Nat Mater* **2009**, *8*, 512.

(38) Krogman, K. C.; Zacharia, N. S.; Schroeder, S.; Hammond, P. T. *Langmuir : the ACS journal of surfaces and colloids* **2007**, *23*, 3137.

(39) Lee, M.; Park, W.; Chung, C.; Lim, J.; Kwon, S.; Ahn, K. H.; Lee, S. J.; Char, K. *Lab on a chip* **2010**, *10*, 1160.

(40) Zhuk, A.; Pavlukhina, S.; Sukhishvili, S. A. *Langmuir* **2009**, *25*, 14025.

(41) Shimazaki, Y.; Mitsuishi, M.; Ito, S.; Yamamoto, M. *Langmuir* **1998**, *14*, 2768.

(42) Takahashi, S.; Sato, K.; Anzai, J. *Anal Bioanal Chem* **2012**, *402*, 1749.

(43) Ogawa, Y.; Arikawa, Y.; Kida, T.; Akashi, M. *Langmuir* **2008**, *24*, 8606.

(44) Kharlampieva, E.; Kozlovskaya, V.; Zavgorodnya, O.; Lilly, G. D.; Kotov, N. A.; Tsukruk, V. V. *Soft Matter* **2010**, *6*, 800.

(45) Xiang, Y.; Lu, S. F.; Jiang, S. P. *Chem Soc Rev* **2012**, *41*, 7291.

Chapter 2.

Fibrillation kinetics of κ-Casein in Bulk Solution

2.1 . Introduction

Protein aggregation is one of the most challenging fields in biology and medicine due to its relation with diseases. However, non-disease-related amyloids are also important in other fields.[1-3] In material science, they provide functional and mechanical properties with applications ranging from medicine to electronics.[4] In food science and technology, protein fibrils offer desirable properties, especially for their interfacial and texture building feature.[5,6]

The casein is principal component of milk which constitutes over 70~80% of total bovine milk protein.[7] In milk, casein exists as large micelle-like particles that comprise four different types of proteins: α_{s1}-casein, α_{s2}-casein, β-casein, and κ-casein. Due to their high content of phosphate groups, α_{s1}-casein, α_{s2}-casein, β-casein have a strong tendency to bind metal ion, in particular calcium in milk. These calcium-binding caseins represent approximately 85% of total casein and are insoluble at calcium concentration greater than 6 mM. Since bovine milk contains a calcium concentration of approximately 30 mM, it would be expected that the caseins would precipitate under the conditions in milk. However, κ-casein, which contains only one to three phosphate groups and binds calcium very weakly, stabilizes them by forming large colloidal micelles when *κ*-casein is mixed with the calcium sensitive caseins. Like other caseins, κ-casein has little defined

secondary or tertiary structure. And κ-casein is classified as an intrinsically disordered or natively unfolded protein. κ-Casein is composed of 169 amino acids which are arranged in an amphiphilic property with very hydrophobic N-terminal domain consisting of residues Glu_1-Phe_{105} and a polar C-terminal domain consisting of Met_{106}-Val_{169}. The flexible hydrophilic C-terminal region of κ-casein is thought to locate on the surface of the casein micelle and stabilizes the micelles through electrostatic and steric interactions.

Previous studies have shown that κ-casein converted into fibril formation at physiological conditions and displayed many of the characteristics of amyloid fibrils including cross-β core structure, Thioflavin-T binding affinity, long, unbranched-threadlike morphologies, and orthogonal to axis of fibrils. However, fibril forming propensity of κ-casein is inhibited when κ-casein is with the other caseins, α_s-casein and β-casein, because the other caseins act as molecular chaperones. Therefore, κ-casein fibrils are not normally formed in the milk that contains 4 different types of caseins at the same time.[8]

In general, fibril formation of amyloid follows sequential procedure that typically includes the unfolding of a protein to partially folded states that subsequently interact and aggregate through the nucleation-dependent mechanism.[9,10] However, unlike fibril formation induced by general nucleation dependent mechanism, the lag-phase of κ-casein fibril formation is independent of protein concentration, and the rate of fibril formation does not increase upon the addition of seeds which are preformed fibrils. And the region from Tyr25 to Lys86, which are included in hydrophobic N-terminal of κ-casein whole amino-acids sequences, is predicted to be incorporated into the core of the fibrils and accounts for the amyloidogenic nature of κ-casein. Also it was proposed that fibril

formation of κ-casein occurs through novel mechanism whereby the rate-limiting step is dissociation of an amyloidogenic precursor from an oligomeric state rather than the formation of stable nucleus.[11] Furthermore, the inherent propensity of κ-casein to form amyloid fibrils could be explained by understanding nature of its monomeric form in solution. A theoretical energy- minimized three-dimensional model suggests that monomeric form of the protein could adopt a "horse-rider" model.[12] In this theoretical model, legs of the horse have two set of antiparallel antiparallel β-sheets, from Lys_{21} to Phe_{55}, they become to core region in fibril formation process.[13] Also it was proposed that fibril formation of κ-casein occurs through novel mechanism whereby the rate-limiting step is dissociation of an amyloidogenic precursor from an oligomeric state rather than the formation of stable nucleus.[11] This feature in fibrillar formation of κ-casein gives advantage to be applied to engineered nano-materials for their rapid formation. Moreover, the protein is disease is good for application in biomedical and food engineering fields since it is not only food grade but also does not have relation with diseases.

In this study, we have investigated the effects of reduction of disulfide bonds within κ-casein and incubating temperature on fibrillation kinetics and fibril morphologies such as contour length and diameter of the fibrils. Also the concentration effects on the contour length of the fibrils was demonstrated, although it had been reported that fibrillation kinetics of κ-casein is independent on the concentration of protein, unlike general fibril formation complied with nucleation dependent fibrillation mechanism.

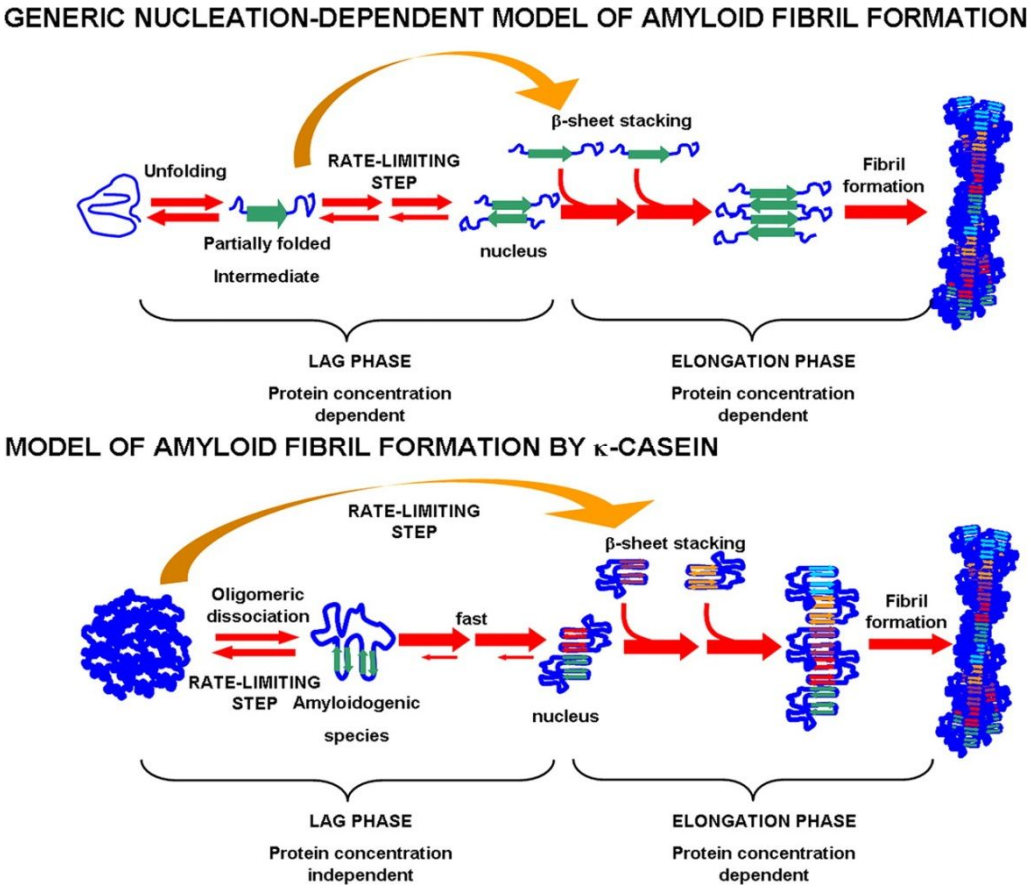

Scheme 2.1. A proposed model to describe differences in the process of fibril formation by proteins that follows a simple nucleation-dependent mechanism compared with fibril formation by κ-casein.[11]

2.2 . Experimental Section

Materials. Bovine milk κ-casein (≥70% κ-casein basis (electrophoresis), lyophilized powder), 1,4-dithiothreitol (DTT), and thioflavin-T (ThT) were purchased from Sigma Aldrich for formation of κ-casein amyloid fibrils. All solutions were prepared with Milli-Q water. For AFM image analysis, mica substrate (Grade V-4 Muscovite, Premium research quality) were purchased from were purchased from SPI and sigma.

Fibril Preparation. κ-Casein was dissolved in phosphate buffer solution (pH 8, 10 mM), with and without DTT (20 mM). The κ-casein solutions were passed through 0.45 μm of nylon syringe filter to remove undissolved precipitates of κ-casein. The concentration of the protein was determined by spectrophotometric methods using a Lamda 35 UV-visible spectrophotometer (Perkin Elmer). Protein solutions were introduced in an oil bath preheated at desired temperature (37, 60, 80, 95 °C). Aliquots were taken at given heating times ranging from 1 hr to 30 days, quenched in ice-cold water and monitored by ThT assay and AFM.

Thioflavin-T Assay. Formation of amyloid fibrils of κ-casein was monitoring using ThT as described previously.[8,14] In brief, aliquots were mixed with 2.5 μM ThT in glycine buffer (50 mM, pH 8.5) and incubated in the dark for 5 min. The fluorescence emission was measured at 485 nm with an excitation at 450 nm using a chemiluminescence spectrophotometer LS-55B (PerkinElmer, U.S.A.). For each assay, samples were prepared in triplicate.

Atomic Force Microscopy (AFM). κ-Casein fibrils were deposited onto freshly cleaved mica substrates. To ensure surface coverage and dispersion of fibrils, each sample was diluted to 1/100 with Milli-Q water immediately before a 30 μL of drop was deposited on to the mica surface. For each sample, the surface was incubated with the diluted fibril solution for 2 min, and then washed with 1 mL of Milli-Q water and dried by a gentle stream of nitrogen gas. The fibrils onto mica substrate were measured at scan rate of 1 Hz using Nanowizard3 (JPK, Germany) with ACTA standard tapping mode cantilever (AppNano). Also the analysis of height and length of fibrils deposited on mica substrate was done with JPK SPM Data Processing for Nanowizard3. The assumption was that fibrils were tubular and the height measurement was considered to be equivalent to diameter.

Transmission Electron Microscopy (TEM). To ensure surface coverage and dispersion of fibrils, each sample was diluted to 1/100 with Milli-Q water. 5 μL of diluted fibril solution was dropped into a carbon coated copper grid (JEOL, Japan) for 10 seconds and the fibril solution was removed by filter paper. Following negative staining with 2% uranyl acetate, the fibrils were examined with TEM of JEM 1010 (JEOL, Japan).

2.3. Results and Discussion

2.3.1. Effects of Reduction of Disulfide Bonds of κ-Casein on Fibril Formation

A monomeric κ-casein contains two cysteines, which have potential to make disulfide bond, within whole 169 amino acids. Therefore the purified κ-casein from whole casein particles are native multimeric (oligomeric) state, from ranging from monomer to decamer, formed by three different types of inter-or inter disulfide bonds which are Cys11-Cys11, Cys11-Cys88, and Cys88-Cys88.[15] According to previous reported mechanism for fibril formation of κ-casein, the propensity toward extensity fibrillation is affected by the degree of dissociation of oligomeric κ-casein by the scission or reduction of disulfide bonds, because amyloidogenic precursor of κ-casein is dissociated forms, only mono-, di-, and trimeric κ-casein. In this study, the fibrillation propensity of κ-casein was compared when κ-casein (80 μM) is thermally incubated in the presence of DTT (20 mM) and without DTT at four different incubation temperatures, 20, 37, 60, and 80 °C for 10 hr. The ability of κ-casein fibrils to bind ThT was used to monitor the formation of fibrils. Figure 2.1 shows ThT fluorescence intensity of fibrils incubated at different temperature. When κ-casein was incubated at 20 °C, fluorescence intensity was almost the same with before incubation and fibril formation was independent on reduction of disulfide bond by DTT. It means κ-casein did not transform into fibril when it is incubated at 20 °C, irrespectively presence of DTT. When the temperature was raised, fluorescence intensity increased by the temperature for both cases of κ-casein incubated with and without DTT. However, fluorescence intensity of κ-casein reduced by DTT showed almost twice higher when compared with fibril incubated in the absence of DTT

at the same incubation temperature. As proposed mechanism of κ-casein fibril formation, the reduction of disulfide bonds within κ-casein, dissociated form of κ-casein, is critical in process of κ-casein fibril formation. Moreover, incubation temperature severely influences conversion of κ-casein into fibril. Also the contour length of fibrils, which were thermally incubated at 80°C in the presence and absence of DTT, was analyzed by AFM measurement (Figure 2.2). Figure 2.2shows morphologies fibrils which were thermally incubated without DTT (a) and with DTT (b), and (c) and (d) are enlarged images of (a) and (b), respectively. As AFM image analysis, the contour length fibril of κ-casein increased when κ-casein was incubated with DTT. According to these result from ThT assay and AFM measurement, we have noticed that fibril is formed at the critical temperature above and the reduction of disulfide bonds within κ-casein not only increases conversion of κ-casein oligomer into fibrils, but also elongate the contour length of fibrils.

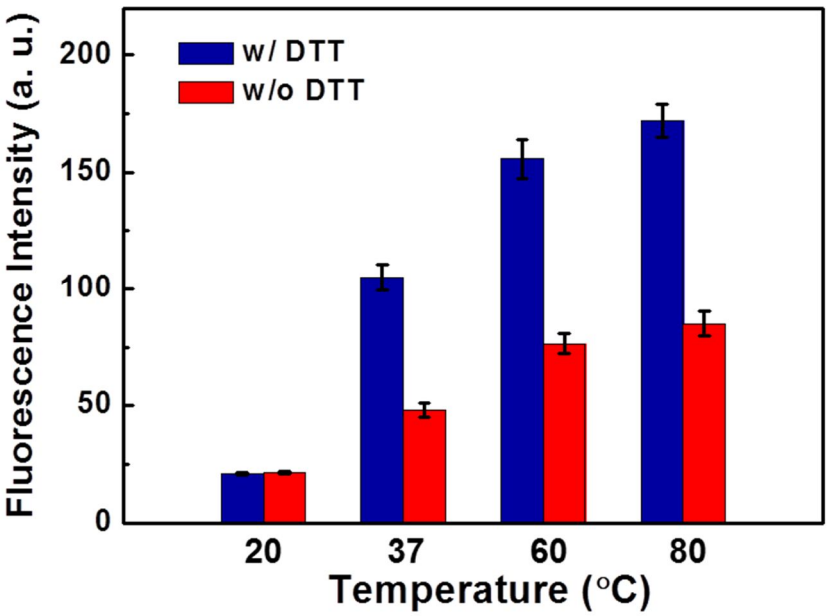

Figure 2.1. ThT fluorescence analysis of fibril formation by reduced and non-reduced κ-casein incubated at four different temperatures for 10 h.

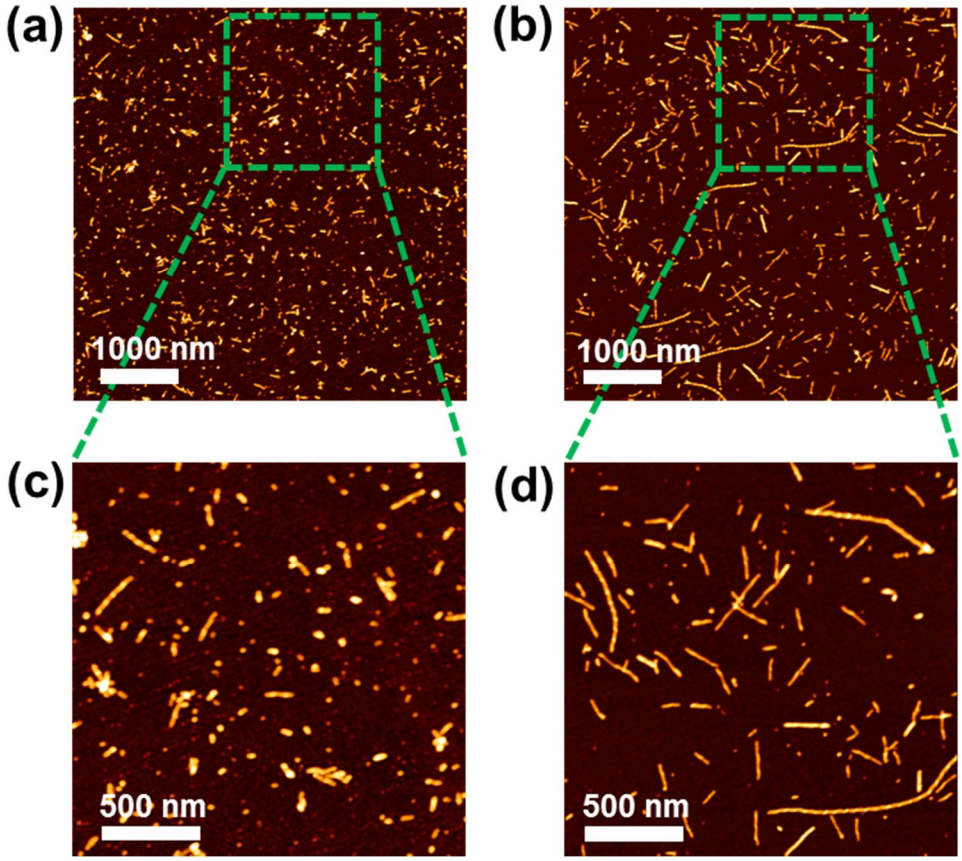

Figure 2.2. AFM images of κ-casein fibrils for 10 h: (a) in the presence of DTT, (b) without DTT, and (c) and (d) are enlarged images of (a) and (b), respectively.

2.3.2. Effect of Incubation Temperature on Fibrillation Kinetics and Morphologies

It is well known that fibrillation kinetics of protein is strongly affected by external conditions such as temperature,[16-18] pH,[19-22] salt,[22-26] solvent,[27-29] and concentration.[10,30-33] Especially, effect of temperature on fibrillation kinetics has been many times reported that the fibrillation kinetics of various amyloidogenic proteins is accelerated by increasing incubation temperature. Here in, we have investigated the effect of temperature on the fibrillation kinetics of κ-casein and also growth of contour length of κ-casein fibrils with ThT assay, and AFM and SEM analysis.

For ThT assay, κ-casein solution (80 μM) in phosphate buffer (pH8, 10 mM) was thermally incubated at four different temperatures (20, 37, 60, and 80 °C) in the presence of DTT (20mM) depended on incubating time. As shown in Figure 2.3, ThT fluorescence intensity was not changed with time, when κ-casein was incubated at 20 °C, suggesting that κ-casein does not form amyloid under this condition. When temperature was raised to 37, 60, and 80 °C, however, the fluorescence intensity increased and higher temperatures promoted further increases in fluorescence intensity. Also the fluorescence intensity increased rapidly and sharply during the early periods of incubation procedure and the lag phase, which represent normally in nucleation depended fibril growth, was not shown. In addition, it is worth noting that the slopes of initial state of thermal treatment were dependent on the temperature, and the maximum fluorescence intensity in saturated region are also strongly depended on the temperature. In other words, fibrillation kinetics of κ-casein is strongly dependent on the incubation temperature and the conversion rate from natively protein to fibrillar structured amyloid also is also affected by temperature.

The reason of temperature dependent fibrillation kinetics can be explained by previous report that temperature of protein solution determines the position of equilibrium between folded and unfolded state of protein structures. In the folded state, there are hydrogen bonds, Van der Waals force and disulfide bonds to stabilize three dimensional protein structures within the protein. Also, in order to minimize unfavorable interactions between hydrophobic residues and aqueous molecules, the most hydrophobic regions are buried in the inner region of the protein.[34,35] However, by heat treatment, the three-dimensional protein structure changes to be unfolded state by breakage of internal bonding, and buried hydrophobic residues are hydrated, which are temperature dependent way to the Gibbs free energy of unfolding. The Gibbs free energy of unfolding for globular proteins has a parabolic dependent on temperature and becomes negative above the thermal denaturation temperature and below the cold denaturation temperature.[35,36] As mentioned above, the Gibbs free energy for unfolding of κ-casein becomes more negative, spontaneous reaction, with increasing temperature, therefore fibril formation is more favorable as temperature increases.

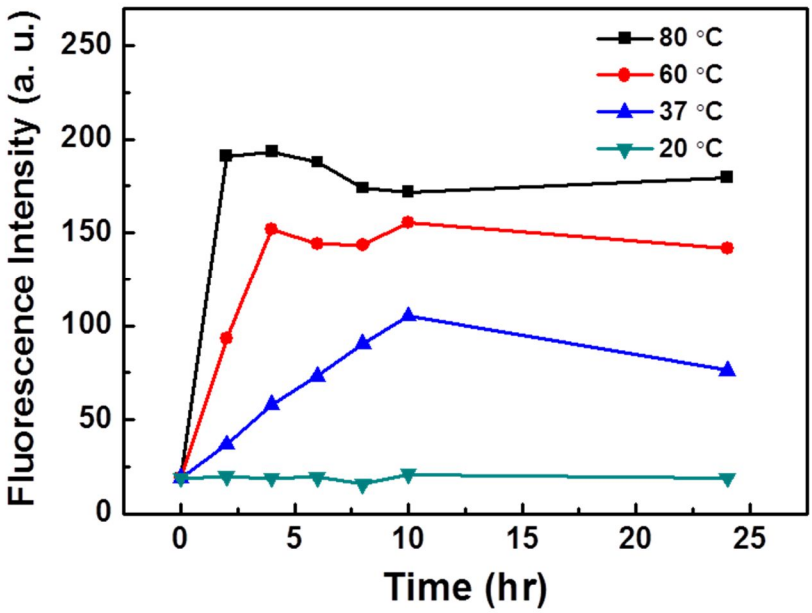

Figure 2.3. Fibril formation kinetics monitoring of κ-casein under four different incubation temperature in the presence of DTT by ThT assay.

In order to investigate the effects of temperature on morphologies of κ-casein fibril, we observed fibrils, which were formed at four different incubation temperatures (37, 60, 80 and 95 °C)in the presence of DTT for 24 hr, with AFM and TEM and Figure 2.4 and Figure 2.5 present the fibril morphologies imaged by AFM and SEM, respectively. As shown in the Figure 2.4 and Figure 2.5, the contour length of the fibrils changed dramatically with incubation temperature and the length was elongated as incubation temperature increases, which suggests that negatively Gibbs free energy for denaturation of κ-casein not only accelerates fibril formation kinetics but also elongates contour length of fibrils between 37 °C and 95 °C. Particularly, the morphologies of fibrils shows distinct changes between 80 °C between 95 °C and we would assume that there is a critical temperature which facilitates beta-sheet stacks to for amyloid fibrils within those ranges of temperature. In addition, we have noticed that the morphologies of each fibril, incubated at different temperature, are different, not only contour lengths. Fibrils incubated at 37 °C show only one type of fibril, rod-like fibril, however the fibrils grown at the other incubation temperature (60, 80 and 95 °C) shows two different types of fibrils, rod-like and twisted fibril. In detail, there are only rod-like fibrils at 37 °C, on the contrary, rod-like fibrils coexist with twisted fibrils at 60, 80 and 95 °C. And the proportion of twisted fibrils increases as incubation temperature increases. The formation of twist fibril are closely related with propensity to fibrillation, therefore it could be explained with degree of κ-casein denaturation by heating accelerates fibrillation and induces twisted fibrils by inter-fibrillar assembly. In other words, the fibrils jointed together to form higher organized fibrils by incubation temperature. Also TEM images of Figure 2.5 show differences in fibril morphologies incubated at two different

temperatures, 60 and 95°C, and the differences in contour length between those fibrils are dramatically. As a result, the contour length and type of fibrils, rod-like and twisted fibril, are determined by incubation temperature. And the detailed analysis of contour lengths and height of fibrils with AFM will be followed.

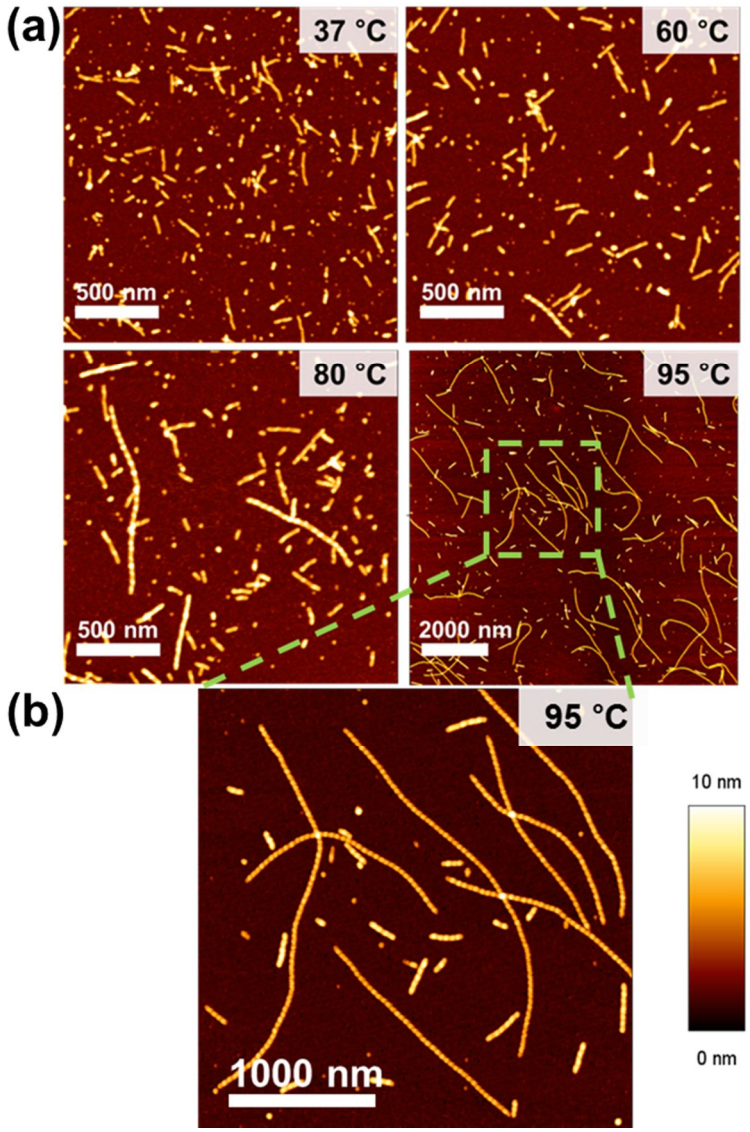

Figure 2.4. AFM images of κ-casein fibrils grown at different incubating temperature to compare contour length for 24 h. (a) shows fibrils grown at 37, 60, 80, and 95 °C and (b) shows the enlarged images of fibrils grown at 95 °C.

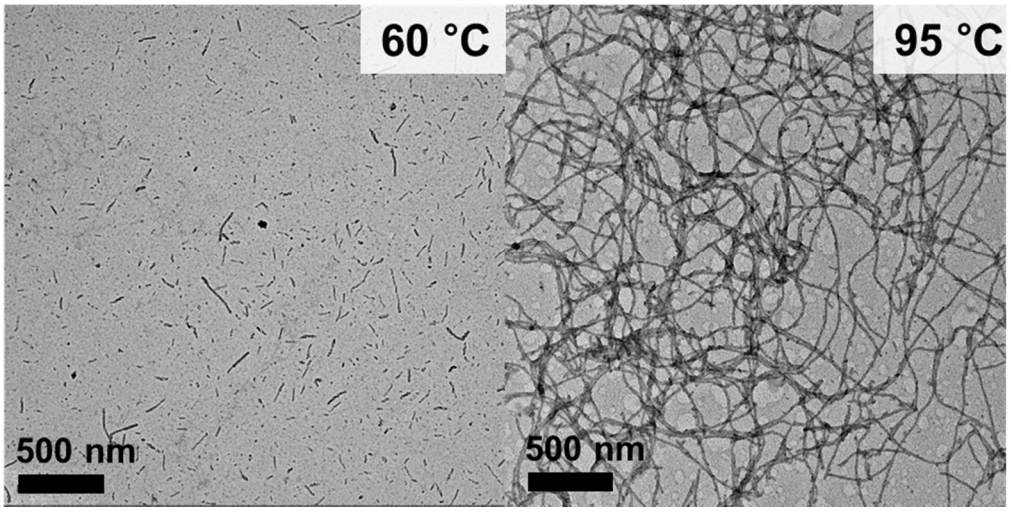

Figure 2.5. TEM images of κ-casein fibrils incubated at different temperature 60 and 95 °C, which show clearly difference contour length of fibrils.

The morphologies including contour length and shapes of κ-casein are dramatically depended on incubation temperature, as described. Thus, we have investigated average contour length and height of each fibrils depended on temperature with Atomic Force Microscopy (AFM) measurement. Originally AFM was developed primarily as surface characterization equipment in solid material science, but today it has become one of the most powerful tools in biology, material science and nanotechnology. As one of the most versatile single molecular technique, AFM have emerged within the last decade as a powerful tool for the study of the structure properties of amyloid fibrils and the fibrillation process.[33,37-41]. This applicability of AFM to study about amyloid fibrils makes to be applied as tool to study the other fibrillar structure system without amyloid signature, such as cellulose[42,43] and collagen.[44,45]

In this study, the contour lengths of the fibrils which were thermally incubated at four different temperatures were analyzed with AFM measurement and analyzed results of contour length were shown in Figure 2.6. To more clear presentation, contour length analysis of fibril incubated at 95 °C was inset. As seen in Figure in 2.6, the contour lengths of fibrils are strongly dependent on the incubating temperature, and fibrils grown at 37 and 60 °C showed maximum contour length within 500 nm. However, when κ-casein was incubated at 95 °C, the contour lengths of the fibrils are broadly distributed from 300 nm to 4 μm regions. Also the fibrils incubated at 80 °C showed the intermediate contour lengths between fibrils incubated at 37 and 60 °C and the other fibrils incubated at 95 °C.

For more detail analysis of contour lengths of fibrils incubated at different temperature, κ-casein solution was incubated for extended period until a month, and the

contour lengths were analyzed as shown in Figure 2.7. In Figure 2.7 (a), the contour length of fibrils grown at 37 °C increases by incubation time, however, maximum length is within 500 nm when incubation time was extended until a month. The contour length distribution of fibrils grown at 60 °C showed similar behavior with when incubated 37 °C, although the in the early stage of fibril formation within 30 min, contour lengths were longer than fibrils incubated at 37 °C. As shown in Figure 2.7 (d), contour length distribution result was completely different with contour length distribution of the other fibrils incubated at 37, 60, and 80 °C. In case of incubating at 95 °C, long fibrils were appeared, which elongated up to 2.5 μm within 30 min as early incubation step.

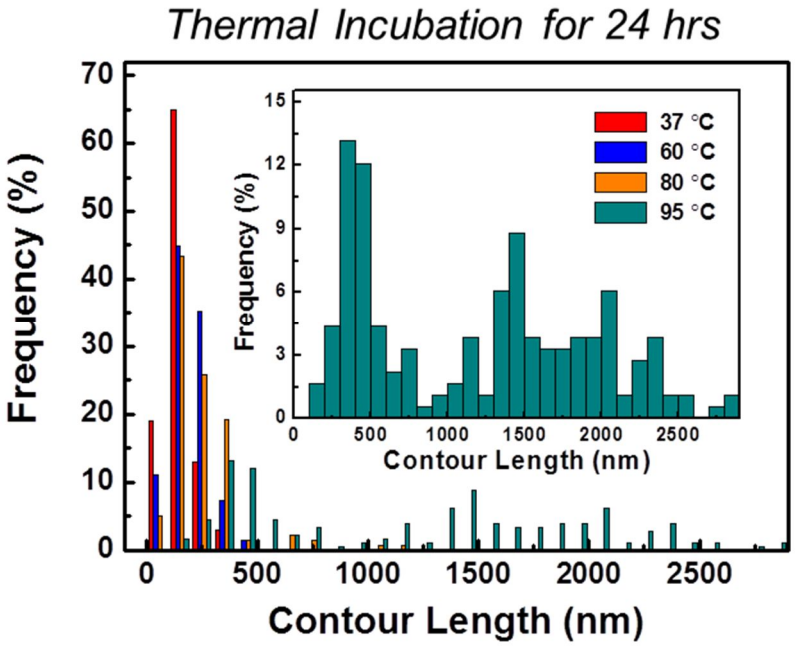

Figure 2.6. Contour length analysis of κ-casein fibrils which grown at four different incubating temperatures: 37, 60, 80, and 95 °C for 24 h.

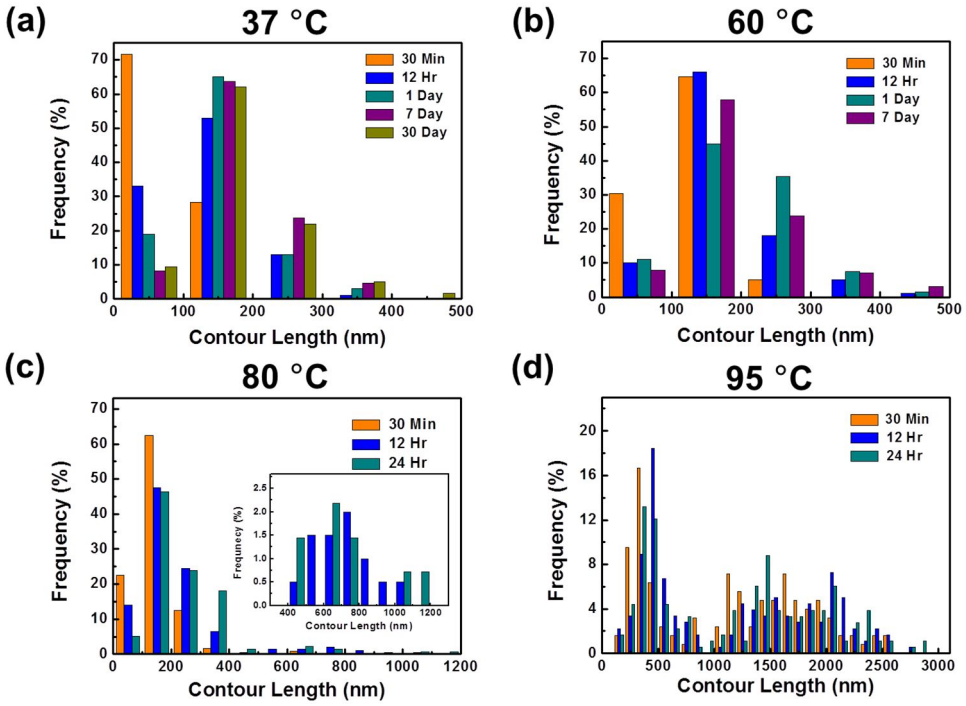

Figure 2.7. Contour length analysis of κ-casein fibrils which grown at four different incubating temperatures: 37, 60, 80, and 95 °C by incubation time.

As the AFM images provide the information on the fibrils in three dimensions, the height information of each fibril was demonstrated by height profile along their contour length. As shown in Figure 2.8, we have noticed that incubation temperature affects not only contour length but also height of fibrils. In case of incubating 37 °C, all of the fibrils have similar height around 4±1 nm, and oligomeric κ-casein presents around 2.5 nm. On the contrary, the thicker fibrils, which have 7±1 nm in height, were appeared from incubating at 60 to 95°C and the proportion of thicker fibrils among the total fibrils increases as incubation temperature increases. And the thicker fibrils show twist-ribbon like structure which indicates thicker fibril is assembled with more than two protofibrils. In previous report, it have been demonstrated that overall morphology of amyloid fibrils depends on the conditions in which fibril formations takes place, and different fibril morphologies are often observed in the same condition for fibrillation. [20,46-48] In the present study, we have demonstrated that the fibril morphologies, contour length and thickness of fibrils, depended on the incubation temperature through AFM analysis, and which is suggested as change of degree of denaturation in protein structure affects the fibrillation propensity of κ-casein.

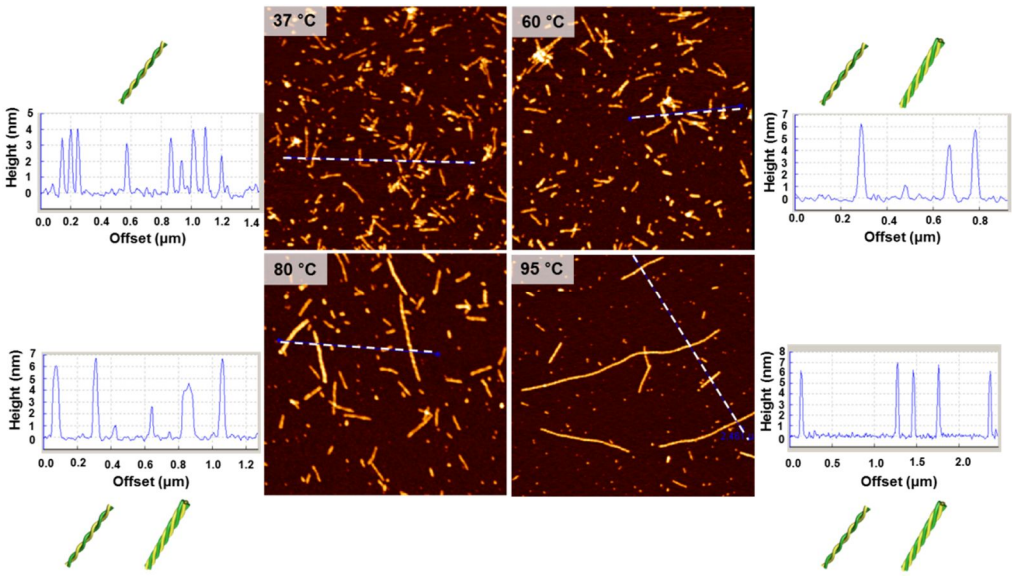

Figure 2.8. Height analysis of κ-casein fibrils incubated at different temperature: 37, 60, 80, and 95 °C for 24 h.

2.3.3. Concentration Effects on Fibrillation of κ-Casein

Formation of amyloid fibrils has been suggested to self-assemble by a nucleated polymerization mechanism, and in case of fibrillation of κ-casein also have been suggested with nucleation-depended model, although the rate-limiting step is dissociation of disulfide bonds within κ-casein not formation of nuclei. Nucleated polymerizations have several well-known features according to the classical model of Oosawa and Asakura including a critical concentration, below which fibrils cannot form, a lag phase before fibril form, and a strong dependence of the fibril formation rate on concentration.[49-51] Fink's group investigated the effect of varying initial concentration (0.2-20 mg/mL) of human recombinant insulin on the fibrillation kinetics, which presented that the higher the initial concentration of insulin, the shorter the lag-time and the steeper the growth curve.[52]

In order to investigate initial concentration effects on the fibril formation of κ-casein, κ-casein solution having ranges from 0.1 mg/ml to 25 mg/ml was thermally incubated at 95 °C in the presence of DTT, and the kinetics of fibril formation and contour length analysis were excuted with ThT-assay and AFM measurement, respectively. As shown in Figure 2.9, fibrillation kinetics is the same under same incubation temperature although the conversion quantity of the fibrils is strongly depended on the initial concentration. The fluorescence intensity increased rapidly and sharply during early periods of incubation process and it showed saturation intensity within 30 min. Moreover, the fluorescence intensity was not changed with prolonged incubation time when concentration of κ-casein solution is 0.1 mg/ml. We noticed that amyloid fibrils were not formed at this concentration, and could be explained this

concentration is below the critical concentration for amyloid fibril formation. The critical concentration for a polymerization is frequently considered to be the concentration monomer in equilibrium with polymer and, as mentioned earlier, is equal to the ratio of rate constants.

$$C_c = k_{off} / K_{on}$$

k_{off} is rate constant for dissociation of the monomer from polymer and k_o is the rate constant for monomer addition to the polymer. In an ideal system, no polymerization occurs below the critical concentration. [53] As seen in Figure 2.9, the native κ-casein has capacity to bind with ThT, prior to incubation, and this feature was previously introduced.[13] The Th-T fluorescence intensity also was dependent on the initial concentration, before thermal incubation.

In order to investigate the effect of temperature on fibril morphology, particularly contour length, the fibrils taken from end of incubation time were measured under dry conditions. As shown in Figure 2.9, contour length of fibrils strongly depended on the initial concentration.

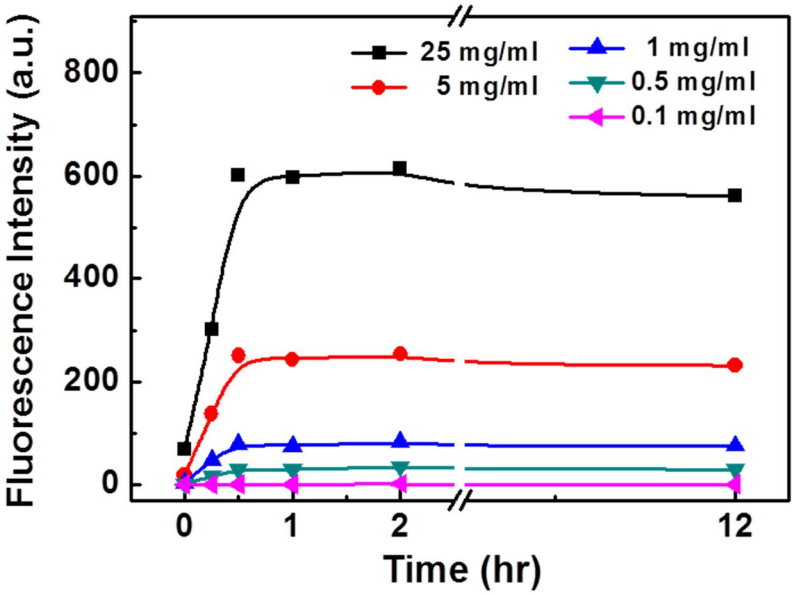

Figure 2.9. ThT assay for fibrillation kinetics of κ-casein depended on the initial concentrations which are incubated at 95 °C for 12 hr in the presence of DTT.

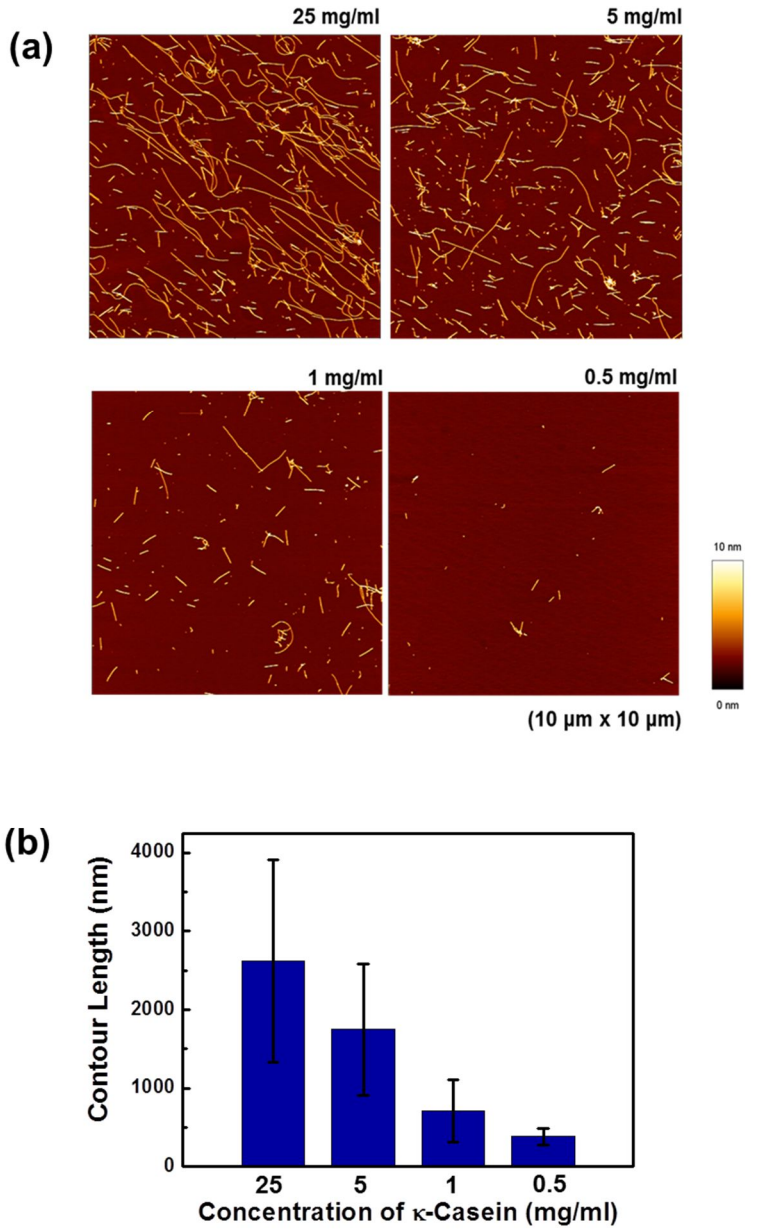

Figure 2.10. Effect of initial concentration of κ-casein on contour length of fibrils incubated at 95 °C for 12 h in the presence of DTT. (a) AFM images of fibrils grown at different initial concentrations, and (b) contour length for fibrils analyzed from AFM images.

2.4. Conclusion

In the present study, we demonstrated fibril formation of κ-casein and some factors to affecting fibrillation kinetics, reduction of disulfide bonds within κ-casein, incubation temperature, and initial concentration. Unlike the fibril formed with nucleation-dependent mechanism, the rate-limiting step for fibrillation of κ-casein is dissociating multimeric κ-casein into monomeric, dimeric and trimeric κ-casein. Therefore the reduction of disulfide bonds is critical to induce fibrillation and the contour length of fibrils also elongated by reduction of disulfide bonds. Incubation temperature is, also, one of the most critical factors to change the fibrillation kinetics and fibril morphologies. In the initial step of fibrillation, the kinetics increases rapidly and sharply, and then the kinetics set as saturated at different values depended on the temperature. The slope of kinetics during early stage is dependent on the temperature. Therefore, incubation temperature affected on not only conversion rates into fibrils, but also kinetics (slopes of fluorescence intensity graph) of fibrillation of κ-casein. Also the morphologies was affected by the temperature, thus contour length and height increases as temperature increases due to degree of protein denaturation to have propensity to fibril forming by heating. As similar with fibril formed through nucleation depended mechanism, κ-casein showed that the degree of conversion from native protein to fibrillar structures increases by initial concentration increases. Also the contour length of the fibrils was elongated with increase of initial concentration. Fibrillation kinetics and morphology of κ-casein fibrils, induced by nucleation-depended mechanism, is controlled by reduction of disulfide bonds, temperature, and initial concentration.

2.5 References

(1) Knowles, T. P.; Fitzpatrick, A. W.; Meehan, S.; Mott, H. R.; Vendruscolo, M.; Dobson, C. M.; Welland, M. E. *Science* **2007**, *318*, 1900.

(2) Selkoe, D. J. *Nature* **2003**, *426*, 900.

(3) Sunde, M.; Blake, C. C. F. *Q Rev Biophys* **1998**, *31*, 1.

(4) Knowles, T. P. J.; Buehler, M. J. *Nat Nanotechnol* **2011**, *6*, 469.

(5) Mezzenga, R.; Schurtenberger, P.; Burbidge, A.; Michel, M. *Nat Mater* **2005**, *4*, 729.

(6) Mine, Y. *Trends Food Sci Tech* **1995**, *6*, 225.

(7) Swaisgood, H. E. *Chemistry of caseins.* **1992**, 139.

(8) Thorn, D. C.; Meehan, S.; Sunde, M.; Rekas, A.; Gras, S. L.; MacPhee, C. E.; Dobson, C. M.; Wilson, M. R.; Carver, J. A. *Biochemistry-Us* **2005**, *44*, 17027.

(9) Bhak, G.; Choe, Y. J.; Paik, S. R. *Bmb Rep* **2009**, *42*, 541.

(10) Xue, W. F.; Homans, S. W.; Radford, S. E. *P Natl Acad Sci USA* **2008**, *105*, 8926.

(11) Ecroyd, H.; Koudelka, T.; Thorn, D. C.; Williams, D. M.; Devlin, G.; Hoffmann, P.; Carver, J.A. *J Biol Chem* **2008**, *283*, 9012.

(12) Kumosinski, T. F.; Brown, E. M.; Farrell, H. M. *Journal of dairy science* **1993**, *76*, 2507.

(13) Farrell, H. M., Jr.; Cooke, P. H.; Wickham, E. D.; Piotrowski, E. G.; Hoagland, P. D. *J Protein Chem* **2003**, *22*, 259.

(14) Thorn, D. C.; Ecroyd, H.; Sunde, M.; Poon, S.; Carver, J. A. *Biochemistry-Us*

2008, *47*, 3926.

(15) Rasmussen, L. K.; Hojrup, P.; Petersen, T. E. *European journal of biochemistry / FEBS* **1992**, *207*, 215.

(16) Gursky, O.; Aleshkov, S. *Bba-Protein Struct M* **2000**, *1476*, 93.

(17) Kusumoto, Y.; Lomakin, A.; Teplow, D. B.; Benedek, G. B. *P Natl Acad Sci USA* **1998**, *95*, 12277.

(18) McKnight, R. E.; Jackson, D. R.; Yokoyama, K. *Eur Biophys J Biophy* **2013**, *42*, 495.

(19) Abe, H.; Kawasaki, K.; Nakanishi, H. *J Biochem-Tokyo* **2002**, *132*, 863.

(20) Fraser, P. E.; Nguyen, J. T.; Surewicz, W. K.; Kirschner, D. A. *Biophys J* **1991**, *60*, 1190.

(21) Srinivasan, R.; Jones, E. M.; Liu, K.; Ghiso, J.; Marchant, R. E.; Zagorski, M. G. *J Mol Biol* **2003**, *333*, 1003.

(22) Rao, V. M.; Pham, H. L.; Shaw, P. N.; McGeary, R. P.; Ross, B. P. *Abstr Pap Am Chem S* **2011**, *241*.

(23) Campioni, S.; Mannini, B.; Lopez-Alonso, J. P.; Shalova, I. N.; Penco, A.; Mulvihill, E.; Laurents, D. V.; Relini, A.; Chiti, F. *J Mol Biol* **2012**, *424*, 132.

(24) Dai, B.; Kang, S. G.; Huynh, T.; Lei, H. Z.; Castelli, M.; Hu, J.; Zhang, Y.; Zhou, R. H. *P Natl Acad Sci USA* **2013**, *110*, 8543.

(25) Fujiwara, S.; Matsumoto, F.; Yonezawa, Y. *J Mol Biol* **2003**, *331*, 21.

(26) Klement, K.; Wieligmann, K.; Meinhardt, J.; Hortschansky, P.; Richter, W.; Fandrich, M. *J Mol Biol* **2007**, *373*, 1321.

(27) Chaudhary, N.; Singh, S.; Nagaraj, R. *Biopolymers* **2008**, *90*, 783.

(28) Shen, C. L.; Murphy, R. M. *Biophys J* **1995**, *69*, 640.

(29) Wei, G. H.; Shea, J. E. *Biophys J* **2006**, *91*, 1638.

(30) Ow, S. Y.; Dunstan, D. E. *Soft Matter* **2013**, *9*, 9692.

(31) Kroes-Nijboer, A.; Venema, P.; Bouman, J.; van der Linden, E. *Food Biophys* **2009**, *4*, 59.

(32) Skerget, K.; Vilfan, A.; Pompe-Novak, M.; Turk, V.; Waltho, J. P.; Turk, D.; Zerovnik, E. *Proteins* **2009**, *74*, 425.

(33) van Raaij, M. E.; van Gestel, J.; Segers-Nolten, I. M. J.; de Leeuw, S. W.; Subramaniam, V. *Biophys J* **2008**, *95*, 4871.

(34) Makhatadze, G. I.; Privalov, P. L. *J Mol Biol* **1993**, *232*, 639.

(35) Privalov, P. L.; Makhatadze, G. I. *J Mol Biol* **1993**, *232*, 660.

(36) Franks, F. *Biophysical chemistry* **2002**, *96*, 117.

(37) Anderson, M.; Bocharova, O. V.; Makarava, N.; Breydo, L.; Salnikov, V. V.; Baskakov, I. V. *J Mol Biol* **2006**, *358*, 580.

(38) De Jong, K. L.; Incledon, B.; Yip, C. M.; DeFelippis, M. R. *Biophys J* **2006**, *91*, 1905.

(39) Maurstad, G.; Prass, M.; Serpell, L. C.; Sikorski, P. *Eur Biophys J Biophy* **2009**, *38*, 1135.

(40) Wegmann, S.; Jung, Y. J.; Chinnathambi, S.; Mandelkow, E. M.; Mandelkow, E.; Muller, D. J. *J Biol Chem* **2010**, *285*, 27302.

(41) Zhou, X. F.; Liu, J. S.; Li, B.; Pillai, S.; Lin, D. D.; Liu, J. H.; Zhang, Y. *Nanoscale* **2011**, *3*, 3049.

(42) Chinga-Carrasco, G. *Nanoscale Res Lett* **2011**, *6*.

(43) Cheng, Q. Z.; Wang, S. Q.; Harper, D. P. *Compos Part a-Appl S* **2009**, *40*, 583.

(44) Habelitz, S.; Balooch, M.; Marshall, S. J.; Balooch, G.; Marshall, G. W. *J Struct Biol* **2002**, *138*, 227.

(45) Strasser, S.; Zink, A.; Janko, M.; Heckl, W. M.; Thalhammer, S. *Biochem Bioph Res Co* **2007**, *354*, 27.

(46) Jimenez, J. L.; Guijarro, J. L.; Orlova, E.; Zurdo, J.; Dobson, C. M.; Sunde, M.; Saibil, H. R. *Embo J* **1999**, *18*, 815.

(47) Bauer, H. H.; Aebi, U.; Haner, M.; Hermann, R.; Muller, M.; Arvinte, T.; Merkle, H. P. *J Struct Biol* **1995**, *115*, 1.

(48) Goldsbury, C. S.; Cooper, G. J. S.; Goldie, K. N.; Muller, S. A.; Saafi, E. L.; Gruijters, W. T. M.; Misur, M. P. *J Struct Biol* **1997**, *119*, 17.

(49) Ferrone, F. *Method Enzymol* **1999**, *309*, 256.

(50) Goldstein, R. F.; Stryer, L. *Biophys J* **1986**, *50*, 583.

(51) Oosawa, F., and S. Asakura. *Academic Press, London.* **1975**.

(52) Nielsen, L.; Khurana, R.; Coats, A.; Frokjaer, S.; Brange, J.; Vyas, S.; Uversky, V. N.; Fink, A. L. *Biochemistry-Us* **2001**, *40*, 6036.

(53) Frieden, C. *Protein Sci* **2007**, *16*, 2334.

Chapter 3. Polymeric Nanocomposites Containing κ-Casein Amyloid Fibrils by Layer-by-Layer deposition

3.1. Introduction

Protein aggregates involving amyloid fibrils have recently received much attention in a variety of research areas such as medicine,[1-4] nanotechnology,[5,6] food,[7,8] and soft matter science.[9,10] One most widely known role of amyloid fibrils, induced by hydrogen bonds between parallel or anti-parallel beta sheets, is its close connection to neurodegenerative diseases such as Alzheimer's and Parkinson's diseases.[11-13] However, not all amyloid fibrils are disease-related and amyloid fibrils from non-disease related proteins have great potentials for functional nanobio-materials due to their highly ordered structure, robust mechanical properties, and elasticity.[14-16] Furthermore, those amyloid fibrils could be easily modified to generate specific anchoring sites for inorganic materials or biomolecules.[17,18] These merits make the amyloid fibrils very attractive and promising candidates for the development of advanced nanobio-materials. Among the numerous applications of amyloid fibrils, it would be good for use as reinforcement within polymer-matrix nanocomposites thin film.

The use of organic filler has become ubiquitous in polymeric systems and the polymer nanocomposites are manufactured for diverse applications including aerospace component and automobiles, and so on. Among various ways for fabrication of nanocoposite, layer-by-layer is one of the prominent methods to build ultrathin polymer

which contains functional materials such as carbon nanotubes, grapheme sheets,[19-25] gold nanoparticles,[26-29] quantum dots,[30-32] and drugs and controls over nanometer resolution in thickness. Furthermore, functional nanomaterials could be inserted at desired position as nanometer resolution within multilayer thin films. It is worth noting that the properties of assembled film vary depended on the assembly environment and conditions, thus properties of nanocomposite thin film based on LbL deposition can be well controlled by changing various parameters including pH, ionic strength, salt concentration, temperature, light, and magnetic field. Therefore, understanding the factors, which influence nanocomposite properties such as growth behavior, surface roughness, and porosity, is very critical to develop functional nanocomposite thin film.

Herein, the nanocomposite thin film incorporating amyloid fibril, which is food grade, biocompatible, and have highly ordered structure, has been investigated by LbL deposition technique. The amyloid fibrils are positively and negatively charged under acidic and basic conditions, and the fibrils could be assembled with oppositely charged PEs. Depended on the type of PEs, the nanocomposite films were assembled with electrostatic interactions or hydrogen bonds by adjusting pH values. Based on the understanding to fibril/PEs multilayered nanocomposite, we have investigated a method producing fiber-reinforced nanocomposite capsules with LbL assembly onto silica colloid cores. Alternating layers positively charged protein fibrils and negatively charged polyelectrolytes were adsorbed onto silica microparticles. Alternating layers of κ-casein fibrils and PEs forms a shell with a structure of a fiber-reinforced nanocomposite, and removal of silica particles makes fibril-reinforced nanocomposite capsules.

3.2. Experimental Section

Materials. Bovine milk κ-casein (≥70% κ-casein basis (electrophoresis), lyophilized powder), 1,4-dithiothreitol (DTT), poly(acrylic acid) (PAA, Mw = 90,000 g/mol), Poly(sodium 4-styrenesulfonate) (PSS, Mw = 70,000 g/mol), and poly(diallyldimethyl ammonium chloride) (PDAC, Mw = 100,000 ~ 200,000) were obtained from Sigma Aldrich. All materials were used as received and all solutions were prepared with Milli-Q water and the concentration of polyelectrolyte solution was fixed at 1 mg/ml. Silicon wafers and silica particles (Microparticles GmbH, Diameter = 3 μm) were used as substrates for two dimensional LbL film and three dimensional capsule with LbL film, respectively.

Fibril Preparation. κ-Casein was dissolved in phosphate buffer solution (pH 8, 10 mM), with and without DTT (20 mM). The κ-casein solutions were passed through 0.45 μm of nylon syringe filter to remove undissolved precipitates of κ-casein. The concentration of the protein was determined by spectrophotometric methods using a Lamda 35 UV-visible spectrophotometer (Perkin Elmer). 80 μM (5 mg/ml) of κ-casein solution was thermally treated in the presence of DTT (20 mM) with an oil bath preheated at 80 °C for 24 hr. Prior to use κ-casein fibril to build up LbL film, fibrils were dialyzed against to Milli-Q water under 4 °C in order to remove DTT and salts included in phosphate buffer solution, and the Milli-Q water was replaced every 6 hr for 3 days.

Multilayer Film Assembly. All LbL films were assembled with dip-assisted LbL

deposition method and assembled at two different pH conditions, pH 3, and 8. Prior to LbL assembly, silicon water was treated with RCA solution (NH_3OH : H_2O_2 : H_2O = 1: 1: 5) for 10 min at 70 °C, to be negatively charged. When multilayer film was assembled at pH 3, silicon substrate was dipped into κ-casein fibril solution at the first and then dipped into the negatively charged PEs solution, PAA and PSS. On the contrary, when the multilayer fibril was assembled at pH 8, silicon substrate was dipped into positively charged PEs solution, PDAC at the first and the dipped into fibril solution. The adsorption time in each κ-casein fibril solutions and PEs solution was 10 min followed by three rinse baths of distilled water adjusted at the same pH with PEs and fibrils solutions for 1, 1, and 1 min each, respectively. No drying step was used in the deposition procedure until it was in the last layer. The cycle was repeated to reach the desired number of bilayers of (κ-casein/PEs) and (PEs/κ-casein) multilayered films.

Formation of LbL Capsules Incorporating κ-Casein Fibrils. 100 μL of 5 wt% silica particles was washed with Milli-Q water by vortex mixing and centrifugation (1000 rpm for 2 min), and then silica particles were treated with RCA solution (NH_3OH : H_2O_2 : H_2O = 1: 1: 5) for 10 min and washed with Milli-Q water to completely remove the RCA solution. Negatively charged silica particles were diluted to 0.5 mL with Milli-Q water. Subsequently, 0.5 mL of κ-casein fibril solution (pH 3) was added. After deposition for 10 min with a gentle vortex, unbound fibrils were removed by three times of centrifugation (1000 rpm, 2 min). The negatively charged PEs solution, PAA and PSS, was then added to deposit on the fibril coated silica particles under same experimental

conditions. This assembly step was done until the film have desired number of the layers. In order to form a capsule, the silica core was removed through HF treated (5 v/v %) for 1 hr.

Zeta-Potential Measurement. The zeta-potential of κ-casein fibrils depended on the pH and multilayer film coated silica particles were measured by electrophoretic light scattering spectrophotometer (ELS-8000). The periodic changes in the zeta-potentials were measured upon the alternate deposition of cationic κ-casein fibrils and anionic PAA and PSS onto colloidal silica particles and the fibrils were

Characterization. The thickness of prepared LbL film were measured by surface profilometer (Alpha Step IQ, KLA Tenco) and the surface morphology of the film was examined by atomic force microscopy (Nanowizard3 JPK, Germany) with ACTA standard tapping mode cantilever (AppNano) in the tapping mode in air. The cross-sectional view of the multilayer film and morphologies of capsules were investigated by (SEM, JEOL-6701F) at an operating voltage of 20 kV. The samples were prepared for cross-sectional SEM images by cooling them in liquid nitrogen and cleaving the cold substrate to obtain a clear cress-section.

3.3. Results and Discussions

3.3.1. Surface Charge of κ-Casein Fibrils Depended on pH

The surface charge densities of κ-casein fibrils which were thermally incubated at 80 °C for 24 hours in phosphate buffer (pH 8, 10 mM) were characterized by zeta-potential measurement. As seen in Figure 3.1.(a), the surface charge densities are strongly dependent on the environmental pH conditions, which indicating that type of charges and density of charge on κ-casein fibrils are easily controlled by external pH adjustment. And the isoelectric point of fibrils was shown within the ranges from pH 4 to 5, which is similar with isoelectric point of native *κ*-casein (pI: 4.5~5.8).[33] It is suspected that hydrophilic amino acids of κ-casein have propensity to exposure toward to aqueous environment, which property continues when κ-casein is transformed into amyloid fibrils due to consisting of the same amino-acids residues. And they are induced as positive charged fibrils when pH value is below 4 and the value of positive charge increases as pH decreases due to pronation within amino acids. On the contrary, they are induced as negative charged fibrils when pH value is above 5, but the charged density was consistent by the increases pH.

In order to confirm the surface charge density of κ-casein fibrils, fibrils dialyzed in Milli-Q water was dropped onto the three different types of surfaces, RCA treated silicon wafer, negatively charged $(PDAC/PSS)_3$, and positively charged $(PDAC/PSS)_{3.5}$ LbL films. As shown in Figure 3.1.(b), the negatively charged κ-casein fibril in Milli-Q water were only adsorbed vigorously onto positively charged $(PDAC/PSS)_{3.5}$ surface and a negligible quantity of the fibrils were adsorbed on to $(PDAC/PSS)_3$ surface, which

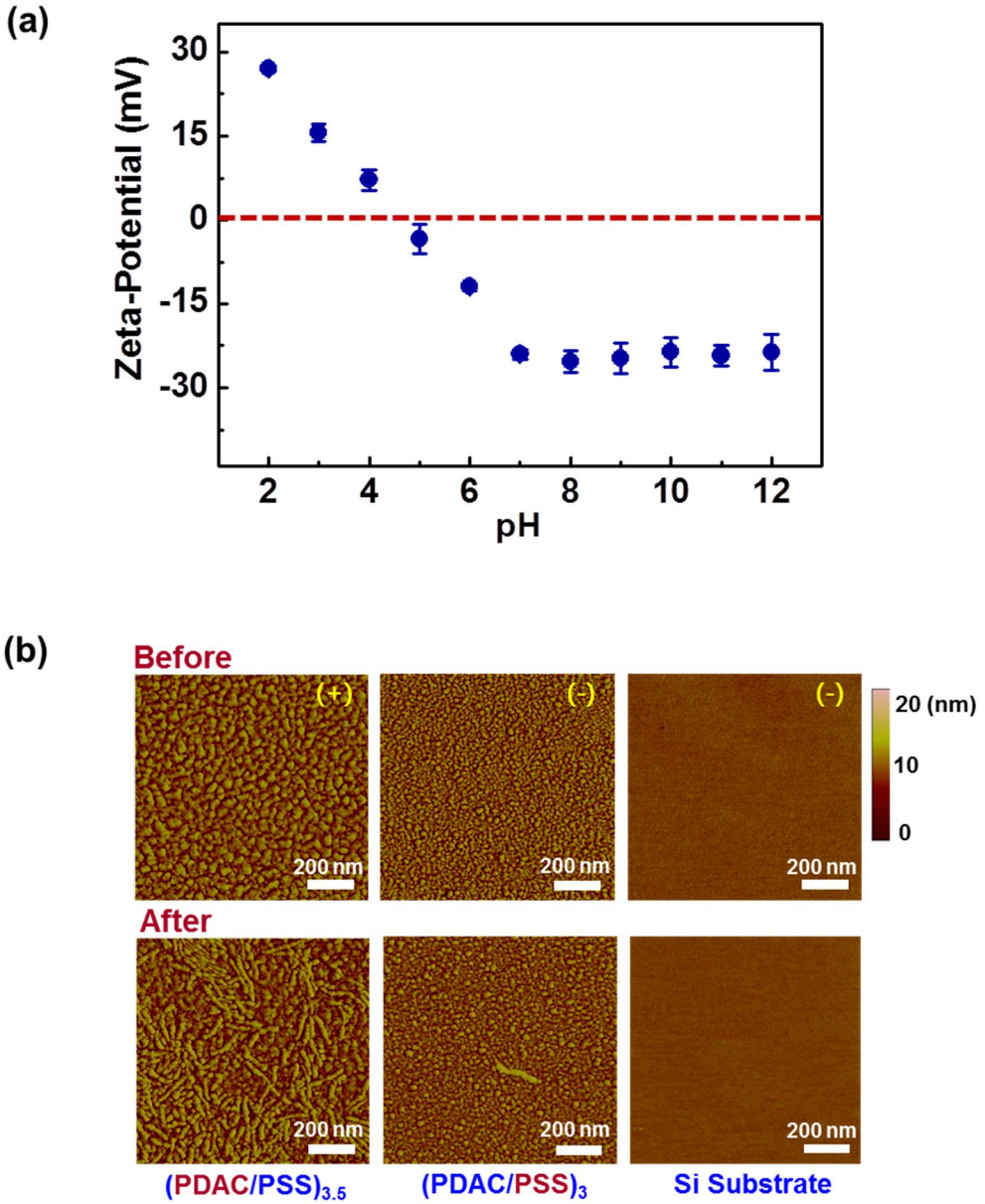

Figure 3.1. Characterization of surface charge density of κ-casein fibrils (a) zeta potential measurement by pH values, (b) adsorption of negatively charged fibrils onto charged surfaces.

indicating that the surface charge density of κ-casein fibrils are affected by pH condition and fibrils are bound on the substrate by electrostatic interactions.

Furthermore, we have investigated charge reversibility of κ-casein fibrils depended on external pH values as shown in Figure 3.2 (a). The transparent fibril solution of pH 6 was changed to turbid when pH value increased to pH 4.5, indicating that the repulsive forces between negatively charged fibrils prohibit aggregation at pH 6, however the fibrils were aggregated due to lack of repulsive force near isoelectric point, pH 4.5. At the lower pH than the isoelectric point, the solution became transparent, again, because fibrils, which are positively charged at lower pH than isoelectric point, are repulsive each other. This change of solution turbidity depended on external pH was reversible. In addition, both of positively charged fibrils at pH 3 and negatively charged fibrils at pH 6 are mixed with PDAC and PSS solutions, the pH of the PDAC and PSS solutions are the same with pH of fibril solution, as shown in Figure 3.2. (b). At pH 3, the solution became turbid when fibril solution was mixed with PSS, whereas the solution was changed to turbid when fibril solution was mixed with PDAC at pH 6. This result shows the charge density of κ-casein fibrils is determined by external pH and the induced charge density is reversible by pH adjustment, which makes that the fibrils are electrostatically assembled within the multilayer film by layer-by-layer deposition method.

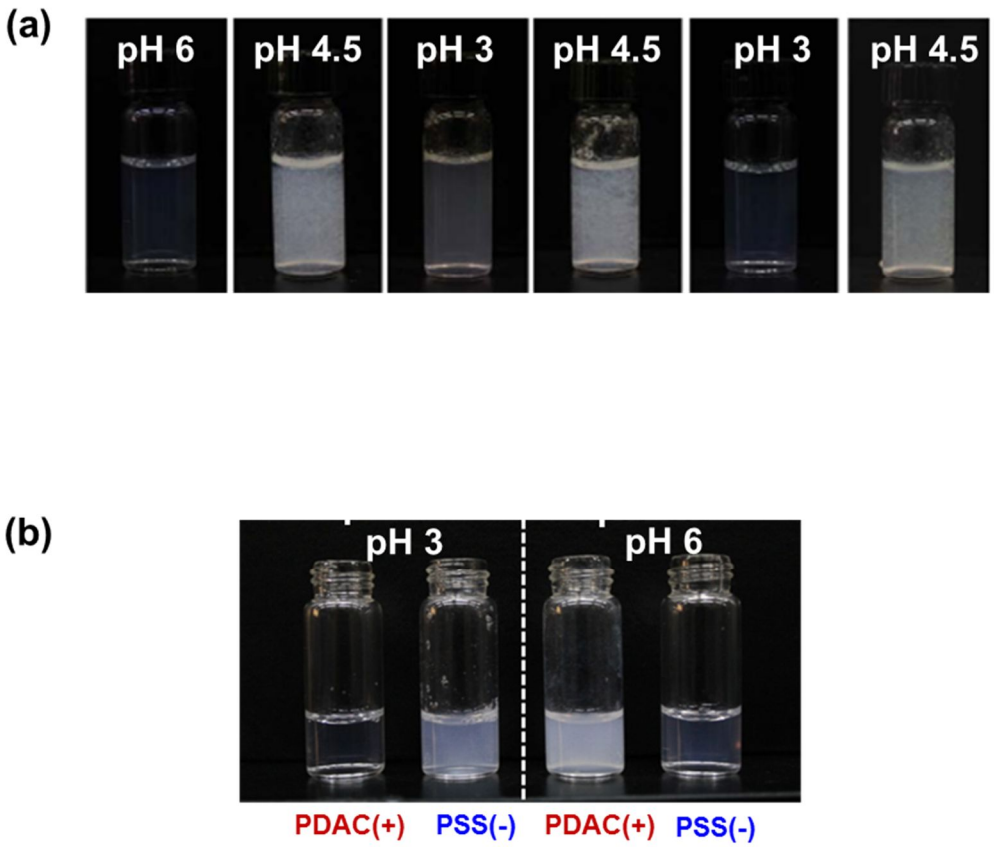

Figure 3.2.(a) Reversible surface charge of κ-casein fibrils depended on pH and (b) complex with oppositely charged PEs at pH 3 and 6.

3.3.2. Nanocomposite Thin Film Incorporating Amyloid Fibrils by Dip-Assisted LbL deposition.

The multilayered thin film incorporating κ-casein fibrils was prepared with oppositely charged PEs by dip-assisted LbL deposition method, as demonstrated in Scheme 3.1. The property, charge density of fibrils is determined by external pH, makes the multilayer film could be assembled with negatively and positively charged PEs upon pH values. In the present study, PSS and PAA were applied as pair PEs to positively charged fibrils at pH 3 while PDAC was applied as a pair PEs to negatively charged fibrils at pH 8.

Two kinds of the multilayer films, (κ-casein fibrils/PSS) and (κ-casein fibrils/PAA), were assembled at pH 3, successfully and the thickness growth curves and cross-sectional views are presented in Figure 3.3.(a) and (b), respectively. Two different types of the multilayer films showed very different film growth behaviors. In case of (κ-casein fibrils/PAA) film, it exhibits a typical exponential growth behavior within 9 deposition cycles and thereafter a rapid linear growth with an increment of 128 nm per deposition cycles. The rapid linear growth following the exponential grow was also observed in other exponential assembled LBL film.[34,35] On the other hands, the (κ-casein fibrils/PSS) film shows typical linear growth with an increment of 14.4 nm per deposition cycles. This clear distinction between growth behaviors of two different types of the films is attributed to different intermolecular interactions between κ-casein fibrils and PEs within the multilayer films. PAA is one of the most representative weak PEs, which will be partially dissociated at intermediate pH, on the contrary PSS is strong PEs, which is dissociated completely in solution for most reasonable pH values. It has been investigated that the degree of ionization of PAA is controlled by pH, and the ionized carboxylic group are

below 10% among total carboxylic groups of PAA. Therefore the major intermolecular interaction between κ-casein fibrils and PAA is not electrostatic interactions, but rather hydrogen bonds acts as binding force between PAA and κ-casein fibrils. Most of the carboxylic groups are pronated and bound with amino acids including F, O, and N by hydrogen bond, and a small number of ionized carboxylic groups are bound to fibrils with electrostatic interactions. On the other hands, PSS and κ-casein fibrils are assembled with electrostatic interaction due to fully charged PSS at reasonable pH range. The difference in building mechanism gives rise to totally different film growth behavior as shown in Figure 3.3. In addition, the surface roughness and its changes were analyzed by AFM measurement. In case of (κ-casein fibrils/PAA) film, the surface roughness is below 5 nm and is not changed with increases layer of the film, while the surface roughness increases until 12 bilayer then is saturated in case of (κ-casein fibrils and PSS) films. This similar surface roughness behavior was reported.[36] We have assumed that the different surface morphology behaviors are due to type of PEs not different intermolecular interactions. PAA is hydrophilic charged polymer, thus PAA builds smooth surfaces including rearrangement of PAA to compensate the rough surfaces, while PSS has hydrophobic part within the molecule. The hydrophobic parts lead the aggregation of PSS and it has impacts on creating rough surfaces.

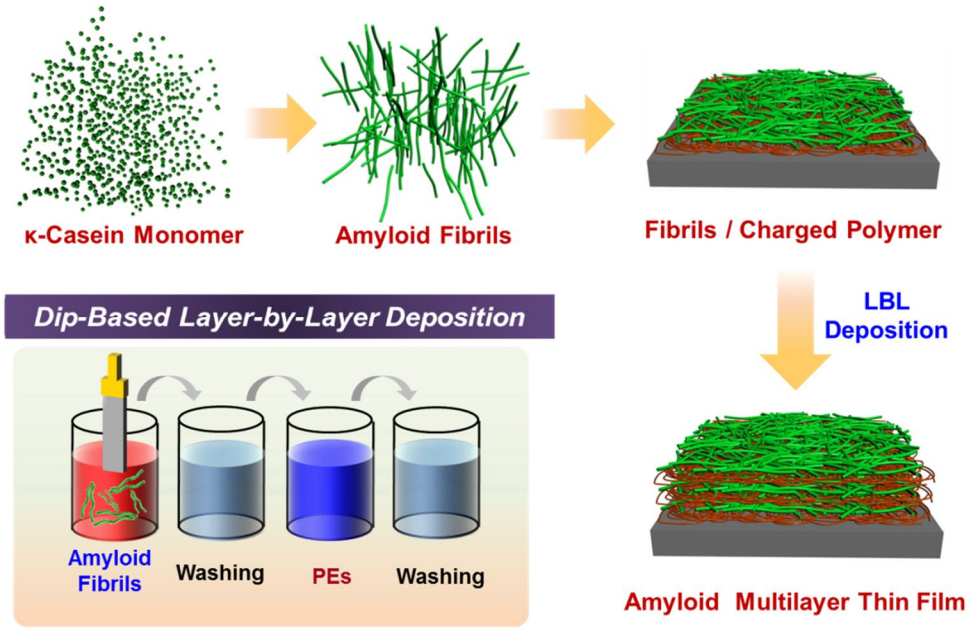

Scheme 3.1. Fabrication of nanocomposite thin films incorporating amyloid fibrils by dip-assisted LbL deposition method.

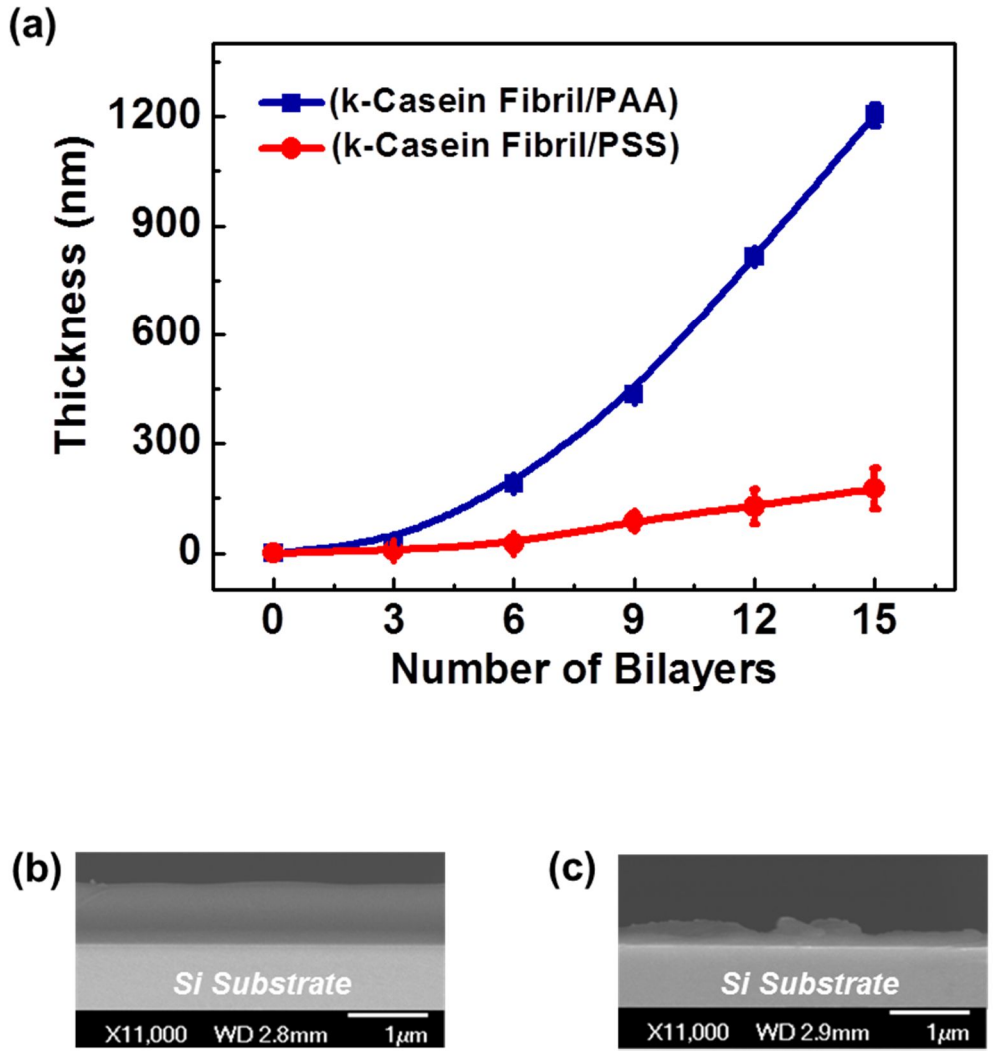

Figure 3.3. Multilayer film growth behavior when κ-casein fibril was assembled with negatively charged PEs at pH 3.

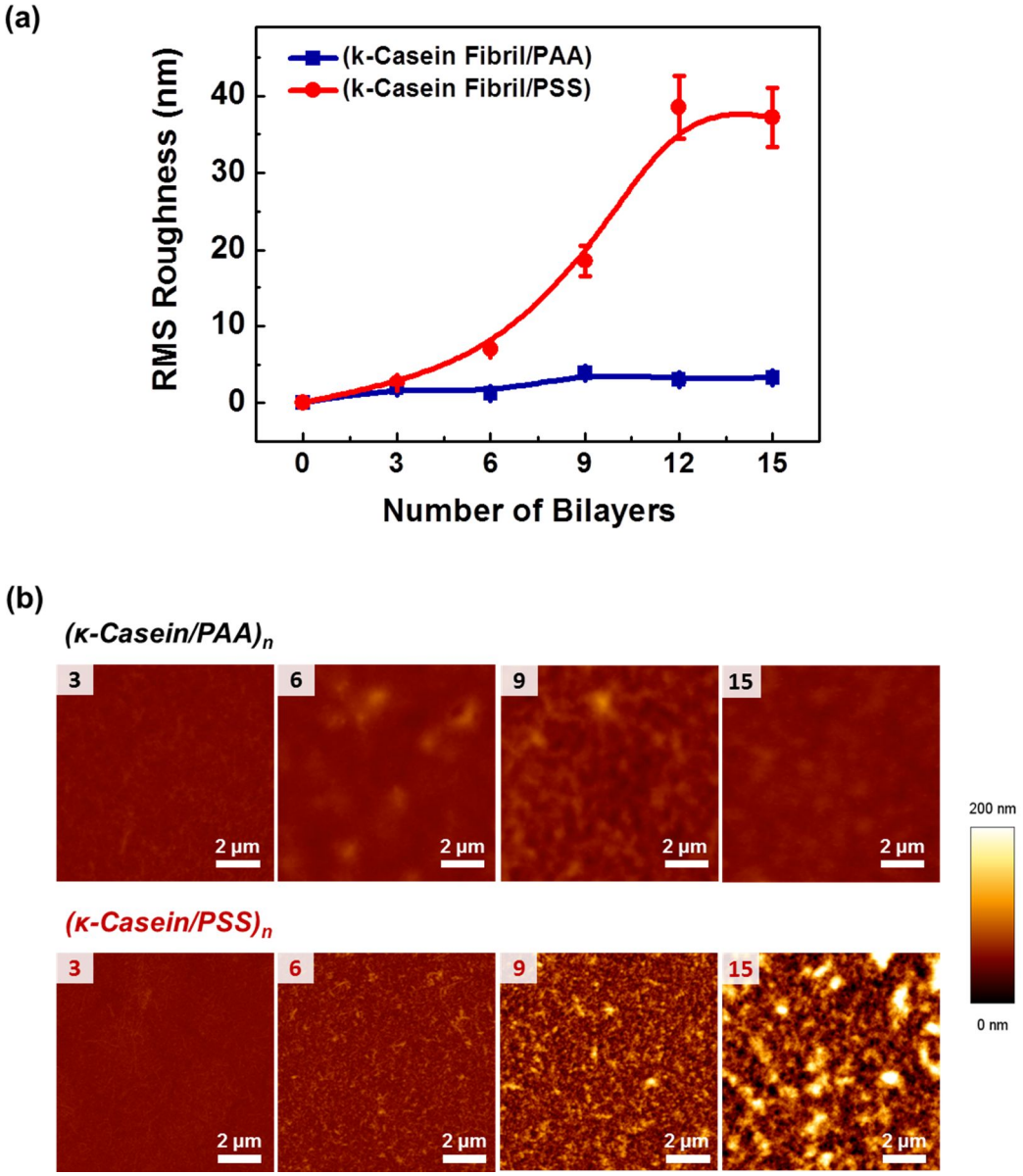

Figure 3.4. Surface roughness analysis with number of bilayers.

The negatively charged κ-casein fibrils were assembled with PDAC at pH 8 and the film growth was plotted and cross-sectional view of the films were shown in Figure 3.5.(a) and (b), respectively. The PDAC is also strong PEs, which is the same with PSS in the multilayer film assembled at pH 3, therefore the charge density is not changed by pH condition. In the case of (PDAC/ κ-casein fibrils) film assembly, the electrostatic interaction is major force between PDAC and κ-casein fibrils and the film growth behavior is very similar with the film (κ-casein fibrils/PSS) as a linear growth with an increment of 29.5 nm per deposition cycles. Although the increment value is a little bigger than the (κ-casein fibrils/PSS) film, the growth behavior is the similar as linear growth curve. Furthermore, the surface roughness of the (PDAC/ κ-casein fibril) film also was analyzed by AFM measurement, shown in Figure 3.6. and the roughness behavior is also similar with roughness of (κ-casein fibrils/PSS) film. The surface roughness increases as number of bilayers increase until 12 bilayer and then was saturated. We have notice that growth behavior and surface roughness of the films were affected by building mechanism of the film such as electrostatic interaction and hydrogen bonds.

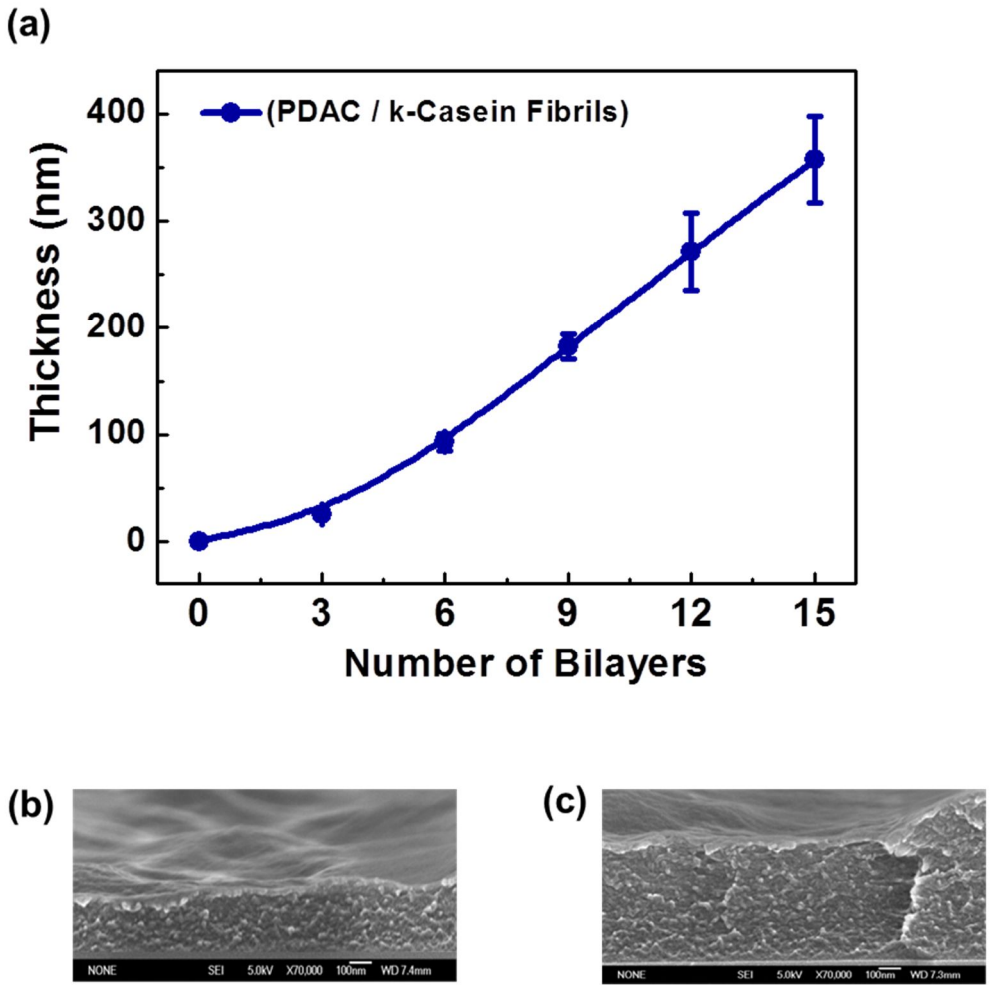

Figure 3.5. Multilayer film growth behavior when κ-casein fibril was assembled with positively charged PEs at pH.

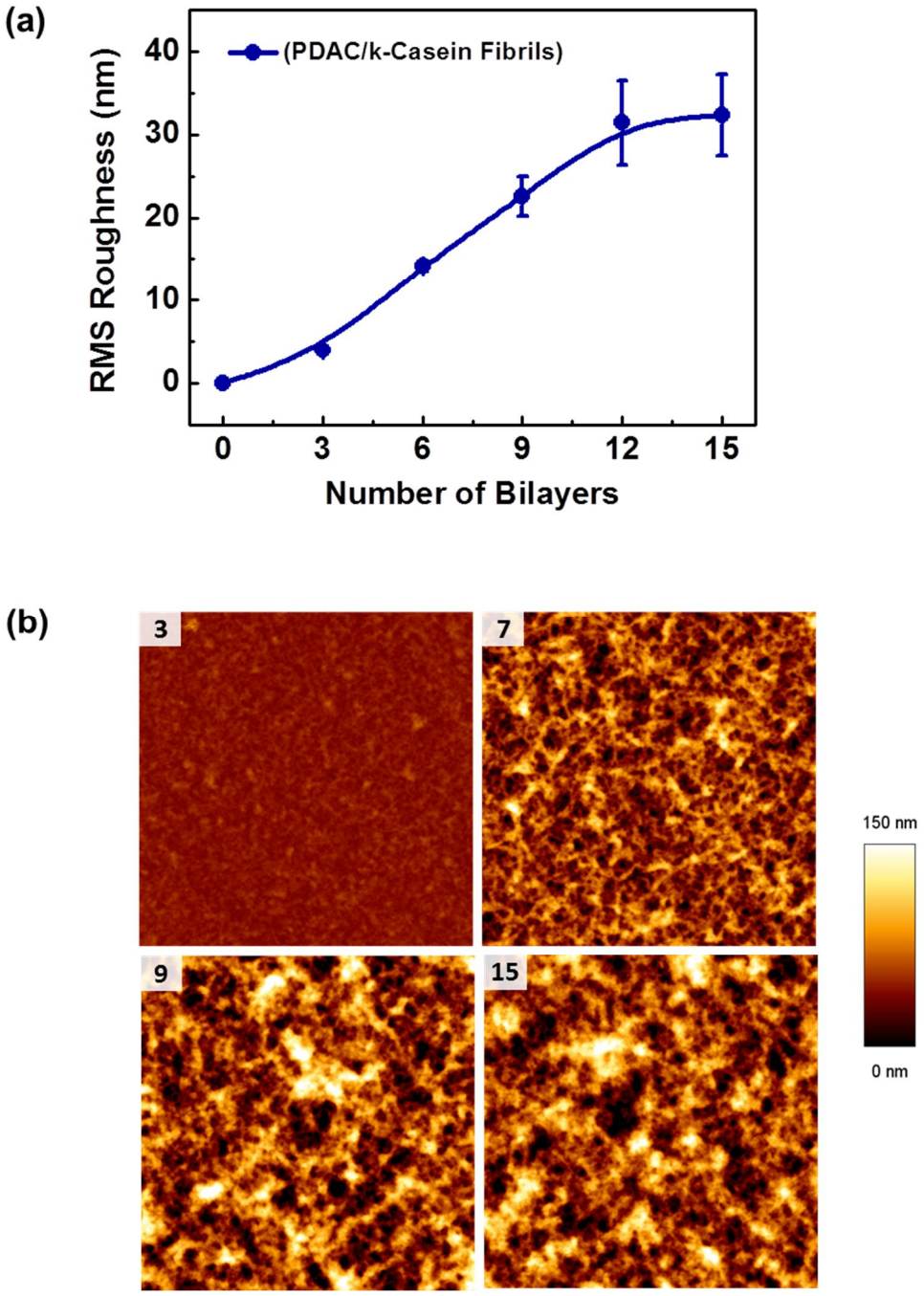

Figure 3.6. Surface roughness analysis with number of bilayers.

3.3.3. Hollow Amyloid Capsules Prepared by LbL Deposition.

The hollow capsules were assembled based on layer-by-layer deposition method. In order to preparation of two different types of capsules, (κ-casein fibrils/PAA) and (κ-casein fibrils/PSS), fibrils and PEs were deposited on silica colloidal particles at pH 3 and schematic illustration is shown in Scheme 3.2. After LbL deposition, as similar demonstrated with other previous reports of using a sacrificial template to create the hollow structure,[25,37-40] hollow capsules incorporating κ-casein fibrils were obtained by removal of silica template with HF (5 %) for 1 hour.

To assure deposition of PEs and fibrils, zeta-potential was measured as a function of the number of deposited layers for both (κ-casein fibrils/PAA) and (κ-casein fibrils/PSS) films, as shown in Figure 3.7.(a). As confirmed by these measurements, zeta potential of silica colloids treated with RCA are slightly negatively charged (-1.73 mV) at acidic condition (pH 3), and zeta-potential value of silica particles coated with fibrils increased to + 14.4 mV. Then the two different types of LbL films assembled on the silica colloids particles show different zeta-potential oscillating behaviors and the gap of the zeta-potential values between fibril coated surfaces and PEs coated surfaces is bigger in (κ-casein fibrils/PSS) films than (κ-casein fibrils/PAA) films. We assume that this difference in periodic oscillation behaviors is attributed to intermolecular interactions between κ-casein fibrils and PEs to be assembled into the LbL film. The (κ-casein fibrils/PSS) films are assembled by electrostatic interactions at pH 3 while the (κ-casein fibrils/PAA) films are formed by combined force of hydrogen bonds and electrostatic interactions. The oscillation behavior of (κ-casein fibrils/PSS) film with surface charge reversal is typically observed in electrostatic LbL assembly of oppositely charged

polymers at surfaces. However, in contrast to the regular LbL assembly of conventional PEs, the LbL films assembled by hydrogen bonds were characterized by the overall negative zeta-potential throughout the entire multilayer formation.[41,42] In the present study, although (κ-casein fibrils/PAA) film assembled on silica colloids shows periodic oscillation in zeta-potential values, zeta-potential values for odd number of layers are around +10mV and even number of layers are almost zero. The reason for the small differences of zeta-potential values within (κ-casein fibrils/PAA) films is attributed to the intermolecular interaction when films are assembled. Most of carboxylic groups in PAA are protonated at pH 3 and the protonated PAA is bound with fibril by hydrogen bonds and a few deprotonated carboxylic groups within PAA is bound with fibrils by electrostatic interactions. Therefore the combined forces of hydrogen bonds and electrostatic interactions are driving force to assemble the LbL film and induced the small changes of zeta-potential values, and also especially the silica colloids coated with fibrils as a top surface have propensity to be aggregated each other, due to lack of repulsive force between silica colloids.

On the basis of stable film growth of (κ-casein fibrils/PAA) and (κ-casein fibrils/PSS) multilayers on silica colloids, we investigated the morphologies of silica particles coated with κ-casein fibrils and PEs with scanning electron microscopy (SEM), as shown in Figure 3.7.(b). The surface morphologies of the films on silica particles were different. More smooth surface was shown in (κ-casein fibrils/PAA)$_{6.5}$ and rough surface was shown in (κ-casein fibrils/PSS)$_{6.5}$, indicating that the surface morphologies are correlated with films assembled on Si substrate by dip-assisted LbL deposition.

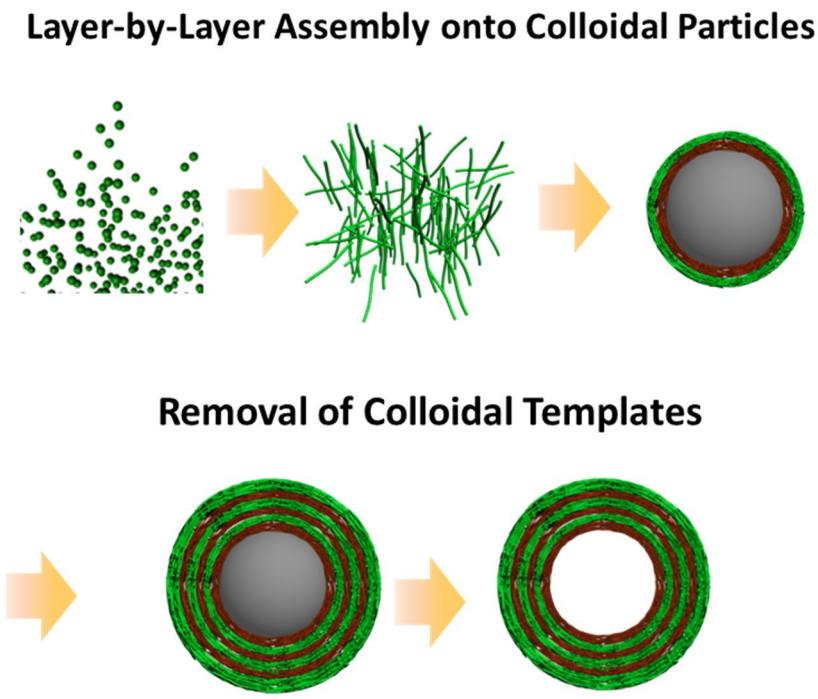

Scheme 3.2. Schematic illustration of LbL assembly of κ-casein fibril and PEs onto silica colloidal particles and the preparation of multilayer hollow capsules with removal of the sacrificial template.

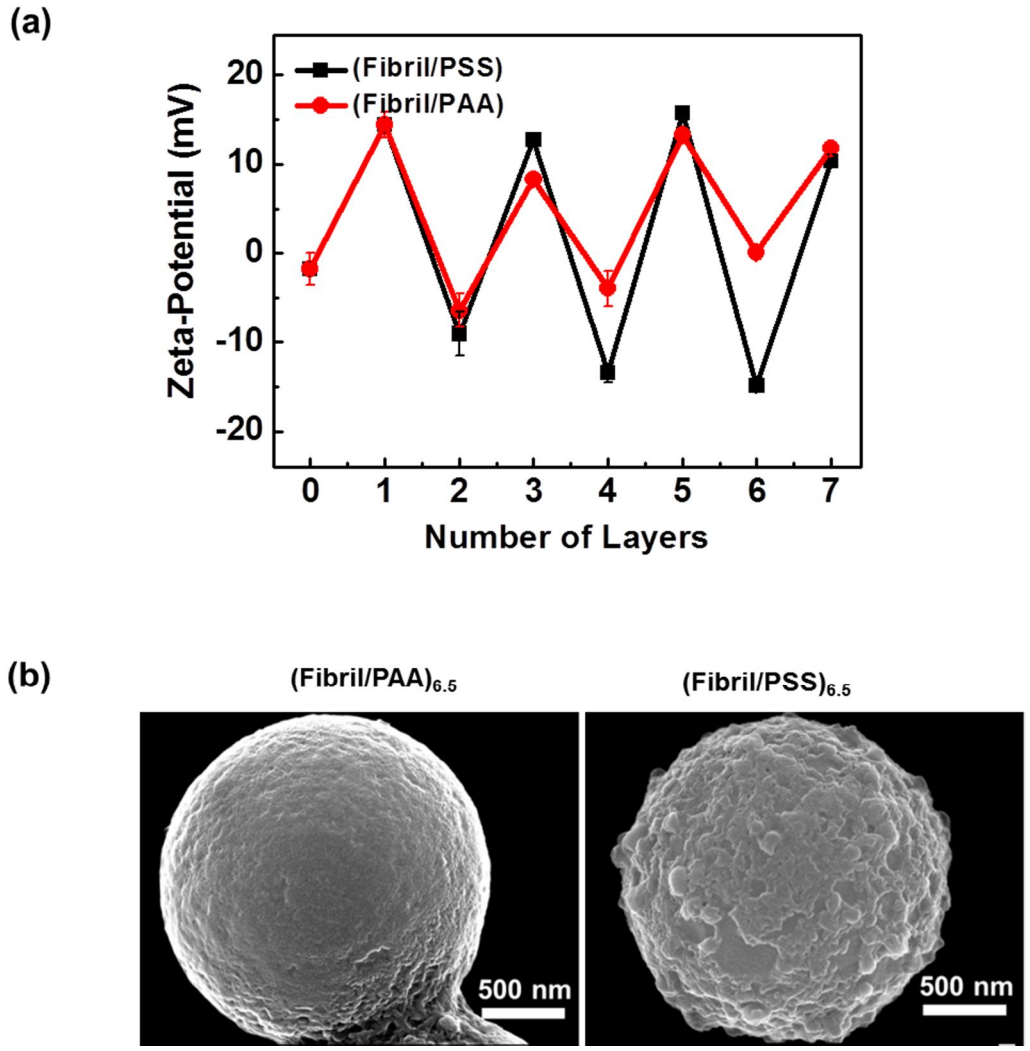

Figure 3.7. (a) Zeta-potentials of silica particles alternatively assembled with κ-casein fibrils and PEs (b) SEM images of (κ-casein fibrils/PEs)$_{6.5}$ multilayer films on a colloidal silica particle.

In order to obtain hollow capsule of fibril incorporating LbL film, silica colloids coated with (κ-casein fibril/PEs) films were exposed to HF (5 %) solution of 1 hour. As shown in Figure 3.8, two different kinds of capsules were obtained from two kinds of LbL films on silica colloids. As mentioned above, (κ-casein fibril/PAA) film assembled by combination of hydrogen bonds and electrostatic interaction are unstable when the film are exposed in changed pH value from deposition pH condition. Therefore (κ-casein fibril/PAA)$_{6.5}$ could be affected by pH change in HF solution and the capsules obtained from the film shows porous capsule morphologies, while the (κ-casein fibril/PSS)$_{6.5}$ capsules show no changes in their morphologies by change in pH of solution, because the film was assembled by electrostatic interaction. The capsules obtained from two different types of LbL films have shown different morphologies not only porosity but also their thickness of the shells. As mentioned previous, the film thickness growth behaviors of both of the film attributed to building mechanisms. Like the thickness of the films assembled on silicon substrate, the thickness of films assembled on silica particles have similar trend, which (κ-casein fibril/PAA)$_{6.5}$ shell was thicker than shell of (κ-casein fibril/PSS)$_{6.5.}$ It is evidence about different thickness between the films that (κ-casein fibril/PAA)$_{6.5}$ shell was not collapsed when it was dried on the silicon substrate with many random folds caused by local instabilities and wrinkling as a result of capillary forces acting on microcapsules, on the contrary,[25] (κ-casein fibril/PSS)$_{6.5}$ shell was collapsed, completely.

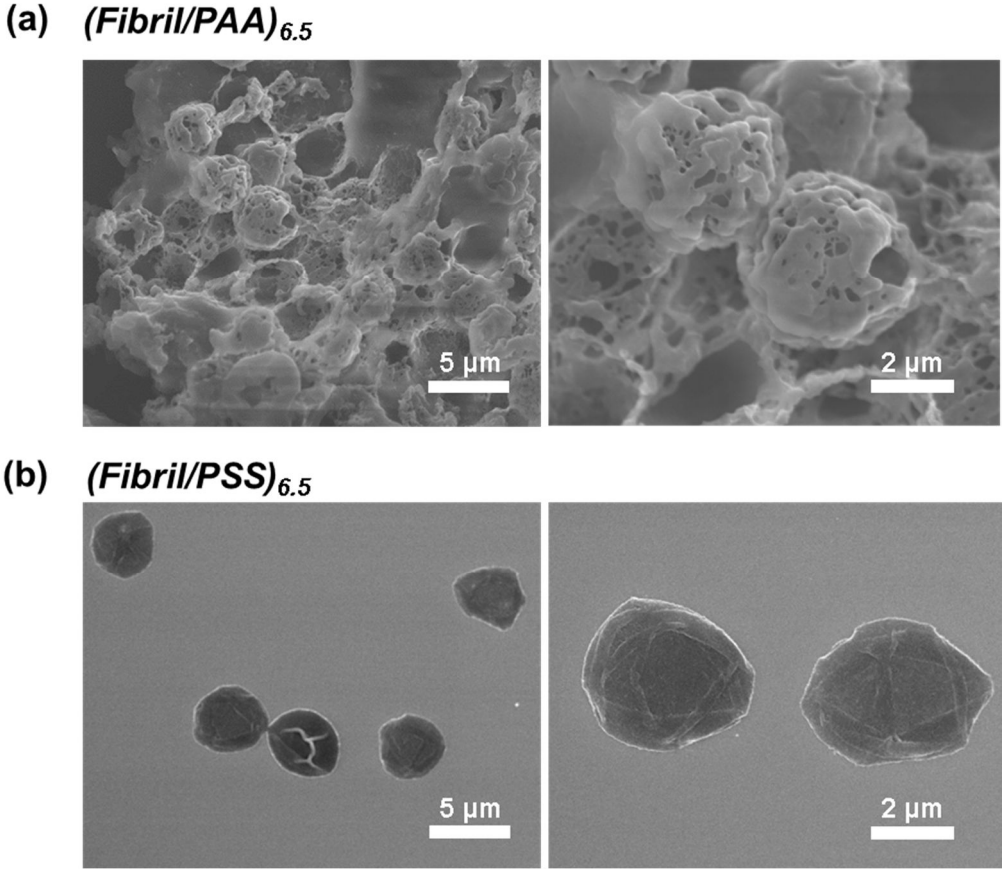

Figure 3.8. SEM images of dried hollow (a) (κ-casein fibrils/PAA)$_{6.5}$ and (b) (κ-casein fibrils/PSS)$_{6.5}$ capsules on silicon wafer.

Moreover, we measured morphologies of **(**κ-casein fibrils/PSS)$_{6.5}$ capsules after removal of silica templates with HF. As seen in Figure 3.9., each capsule was separately and was very uniform in size with an average diameter of 4 $\pm$ 0.1 μm as defined by the original core. The shell thickness of the **(**κ-casein fibrils/PSS)$_{6.5}$ capsules can be determined from atomic force microscopy (AFM) cross-sections and was about 50 nm as shown in Figure 3.10. The region, where cross-sectional height was measured, consisting of double layers of the capsules. Therefore the thickness of the shell is assumed about 25 nm, which have correlation with thickness of the **(**κ-casein fibrils/PSS)$_{6.5}$ film deposited on silicon substrate.

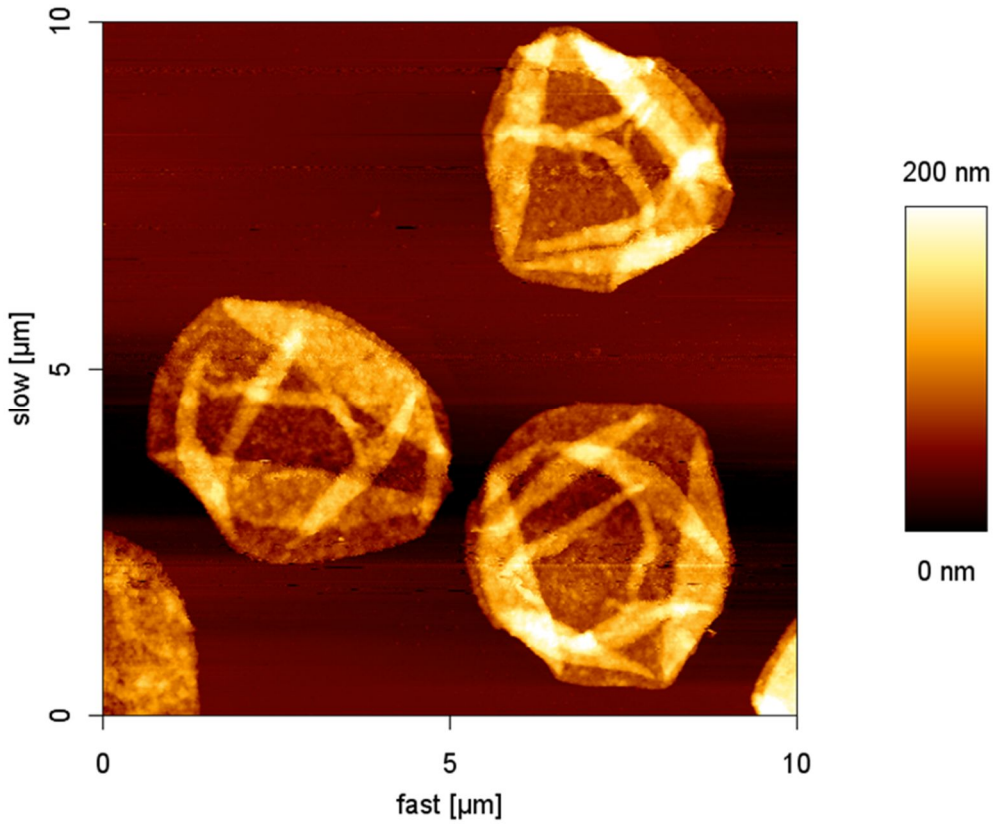

Figure 3.9. AFM images of dried (κ-casein fibrils/PSS)$_{6.5}$ capsules.

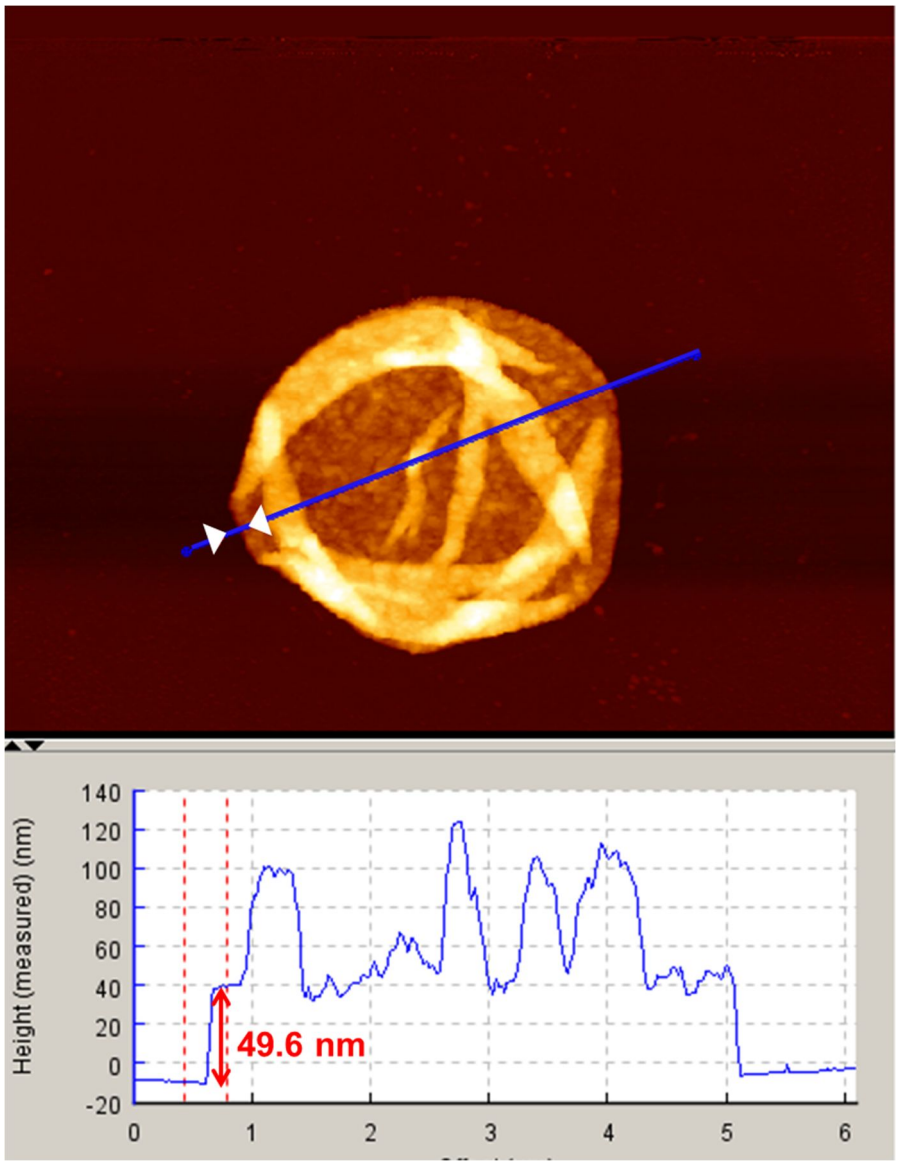

Figure 3.10. Height analysis of (κ-casein fibrils/PSS)$_{6.5}$ capsules with AFM.

3.4. Conclusion

Amyloid fibril is one of the most attractive nanomaterials based on amino acids and has numerous merits including biocompatibility, highly ordered structures, robust mechanical properties, and resistance to harsh environment. In present study, we have demonstrated that nanocomposite film incorporating amyloid fibrils induced from a kind of milk protein, κ-casein, with dip-based layer-by-layer deposition. The matured fibrils of κ-casein were assembled with polyelectrolyte to fabricate nanocomposite films by attractive intermolecular interactions. The charge density of κ-casein fibrils is affected by pH value and it is negatively and positively charged when the fibrils are in acid and basic environmental condition, respectively. The charge density can be adjusted by changing the pH of the solvent which makes them excellent candidates for thin films or capsules by electrostatic interaction driven LbL film. Three different types of nanocomposite films were fabricated with negatively charged PSS and PAA at pH 3, and with positively charged PDAC at pH 8. (κ-casein fibril/PAA) film was assembled by combined force of hydrogen bonds and electrostatic interaction because more than 90% of carboxylic groups in PAA is protonated at pH 3, and the (κ-casein fibril/PSS) and (κ-casein fibril/PDAC) film were assembled by electrostatic interaction at pH 3 and 8, respectively. The film based on electrostatic interaction showed linear film growth and increased surface roughness with the number of layer, while the film based on combined force of electrostatic interaction and hydrogen bonds showed exponential film growth and the consistent surface roughness with the number of the film layers. Also microcapsules were formed successfully with (κ-casein fibril/PEs)$_{6.5}$ assembled at pH 3 and the thickness of

the shell is correlated with film thickness assembled on silicon substrate. Our results suggest that all the film characteristics strongly depend on the method of its preparation. It is anticipated that nanocomposite film and capsule incorporated with amyloid could be applied to biomedical tissue engineering, drug, and food engineering.

3.5. References

(1) Bracalello, A.; Santopietro, V.; Vassalli, M.; Marletta, G.; Del Gaudio, R.; Bochicchio, B.; Pepe, A. *Biomacromolecules* **2011**, *12*, 2957.

(2) Kasai, S.; Ohga, Y.; Mochizuki, M.; Nishi, N.; Kadoya, Y.; Nomizu, M. *Biopolymers***2004**, *76*, 27.

(3) Bogush, V. G.; Sokolova, O. S.; Davydova, L. I.; Klinov, D. V.; Sidoruk, K. V.; Esipova, N. G.; Neretina, T. V.; Orchanskyi, I. A.; Makeev, V. Y.; Tumanyan, V. G.; Shaitan, K. V.; Debabov, V. G.; Kirpichnikov, M. P. *Journal of neuroimmune pharmacology : the official journal of the Society on NeuroImmune Pharmacology* **2009**, *4*, 17.

(4) Woolfson, D. N.; Ryadnov, M. G. *Current opinion in chemical biology* **2006**, *10*, 559.

(5) Zhang, L.; Li, N.; Gao, F.; Hou, L.; Xu, Z. *Journal of the American Chemical Society* **2012**, *134*, 11326.

(6) Gazit, E. *Chemical Society reviews* **2007**, *36*, 1263.

(7) Pearce, F. G.; Mackintosh, S. H.; Gerrard, J. A. *Journal of agricultural and food chemistry* **2007**, *55*, 318.

(8) Foegeding, E. A. *Food Biophysics* **2006**, *1*, 41.

(9) Krysmann, M. J.; Castelletto, V.; Kelarakis, A.; Hamley, I. W.; Hule, R. A.; Pochan, D. J. *Biochemistry* **2008**, *47*, 4597.

(10) Yan, H.; Frielinghaus, H.; Nykanen, A.; Ruokolainen, J.; Saiani, A.; Miller, A. F. *Soft Matter* **2008**, *4*, 1313.

(11) Hardy, J.; Selkoe, D. J. *Science* **2002**, *297*, 353.

(12) Masters, C. L.; Simms, G.; Weinman, N. A.; Multhaup, G.; McDonald, B. L.; Beyreuther, K. *Proc. Natl. Acad. Sci. U. S. A.* **1985**, *82*, 4245.

(13) Chiti, F.; Dobson, C. M. In *Annual Review of Biochemistry*; Annual Reviews: Palo Alto, 2006; Vol. 75, p 333.

(14) Knowles, T. P.; Fitzpatrick, A. W.; Meehan, S.; Mott, H. R.; Vendruscolo, M.; Dobson, C. M.; Welland, M. E. *Science* **2007**, *318*, 1900.

(15) Meersman, F.; Cabrera, R. Q.; McMillan, P. F.; Dmitriev, V. *Biophys. J.* **2011**, *100*, 193.

(16) Adamcik, J.; Berquand, A.; Mezzenga, R. *Appl Phys Lett* **2011**, *98*.

(17) Ostrov, N.; Gazit, E. *Angew Chem Int Edit* **2010**, *49*, 3018.

(18) Kasotakis, E.; Mossou, E.; Adler-Abramovich, L.; Mitchell, E. P.; Forsyth, V. T.; Gazit, E.; Mitraki, A. *Biopolymers* **2009**, *92*, 164.

(19) Choi, Y.; Gu, M.; Park, J.; Song, H. K.; Kim, B. S. *Adv Energy Mater* **2012**, *2*, 1510.

(20) Dong, X. Y.; Wang, L.; Wang, D.; Li, C.; Jin, J. *Langmuir* **2012**, *28*, 293.

(21) Yang, M.; Hou, Y.; Kotov, N. A. *Nano Today* **2012**, *7*, 430.

(22) Zhu, J. Y.; He, J. H. *Nanoscale* **2012**, *4*, 3558.

(23) Lee, S. W.; Kim, J.; Chen, S.; Hammond, P. T.; Shao-Horn, Y. *Acs Nano* **2010**, *4*, 3889.

(24) Shim, B. S.; Zhu, J. A.; Jan, E.; Critchley, K.; Kotov, N. A. *Acs Nano* **2010**, *4*, 3725.

(25) Kozlovskaya, V.; Kharlampieva, E.; Drachuk, I.; Cheng, D.; Tsukruk, V. V. *Soft*

Matter **2010**, *6*, 3596.

(26) Lee, H.; Jang, Y.; Seo, J.; Nam, J. M.; Char, K. *Acs Nano* **2011**, *5*, 5444.

(27) Poon, Z.; Lee, J. B.; Morton, S. W.; Hammond, P. T. *Nano Lett* **2011**, *11*, 2096.

(28) Combs, Z. A.; Chang, S. H.; Clark, T.; Singamaneni, S.; Anderson, K. D.; Tsukruk, V. V. *Langmuir : the ACS journal of surfaces and colloids* **2011**, *27*, 3198.

(29) Gromova, M. S.; Sigolaeva, L. V.; Fastovets, M. A.; Evtushenko, E. G.; Babin, I. A.; Pergushov, D. V.; Amitonov, S. V.; Eremenko, A. V.; Kurochkin, I. N. *Soft Matter* **2011**, *7*, 7404.

(30) Nagaraja, A. T.; Sooresh, A.; Meissner, K. E.; McShane, M. J. *Acs Nano* **2013**, *7*, 6194.

(31) Yoon, M.; Kim, Y.; Cho, J. *Acs Nano* **2011**, *5*, 5417.

(32) Zheng, Z. Z.; Zhou, Y. L.; Li, X. Y.; Liu, S. Q.; Tang, Z. Y. *Biosens Bioelectron* **2011**, *26*, 3081.

(33) Holland, J. W.; Deeth, H. C.; Alewood, P. F. *Proteomics* **2004**, *4*, 743.

(34) Podsiadlo, P.; Michel, M.; Lee, J.; Verploegen, E.; Kam, N. W. S.; Ball, V.; Lee, J.; Qi, Y.; Hart, A. J.; Hammond, P. T.; Kotov, N. A. *Nano Lett* **2008**, *8*, 1762.

(35) Porcel, C.; Lavalle, P.; Decher, G.; Senger, B.; Voegel, J. C.; Schaaf, P. *Langmuir* **2007**, *23*, 1898.

(36) Lee, D.; Rubner, M. F.; Cohen, R. E. *Nano Lett* **2006**, *6*, 2305.

(37) Kida, T.; Mouri, M.; Kondo, K.; Akashi, M. *Langmuir* **2012**, *28*, 15378.

(38) Johnston, A. P. R.; Kamphuis, M. M. J.; Such, G. K.; Scott, A. M.; Nice, E. C.; Heath, J. K.; Caruso, F. *Acs Nano* **2012**, *6*, 6667.

(39) Ochs, C. J.; Such, G. K.; Caruso, F. *Langmuir* **2011**, *27*, 1275.

(40) Krzyzanek, V.; Sporenberg, N.; Keller, U.; Guddorf, J.; Reichelt, R.; Schonhoff, M. *Soft Matter* **2011**, *7*, 7034.

(41) Kozlovskaya, V.; Yakovlev, S.; Libera, M.; Sukhishvili, S. A. *Macromolecules* **2005**, *38*, 4828.

(42) Yang, S. Y.; Lee, D.; Cohen, R. E.; Rubner, M. F. *Langmuir : the ACS journal of surfaces and colloids* **2004**, *20*, 5978.

Chapter 4.

In-Situ Fibrillation of κ-Casein within LbL Film by External Stimuli

4.1. Introduction

In the last decade, numerous studies have reported on not only assembly not also mechanical characteristics of amyloid fibrils. As previous reports, amyloid is stiffer than cytoskeleton components such as actin filament, microtubules and intermediate filaments.[1-5] In order to utilize robust mechanical properties of amyloid fibrils, researchers have previously constructed protein fibril-based nanocomposites by adding fully matured protein fibrils into different bulk matrices such as silicon elastomer (poly(dimethylsiloxane)),[6] poly(L-lactic acid), poly(ethylene glycol)[7] and epoxy resin.[8] These new types of nanocomposites, filled with optimal content of protein fibrils, possess tuned and balanced physical and mechanical properties such as stiffness and Young's modulus without sacrificing their thermal and elongation properties. More recently, nanocomposites containing protein fibrils and graphene sheets have been demonstrated to be biodegradable and highly conductive.[7]

The layer-by-layer (LbL) deposition has frequently been applied, due to its versatility, to develop functional multilayered thin films in various fields such as energy, environmental, and biomedical applications since its inception in the early 1990s.[9-11] The film thickness of the LbL films can easily be tuned with nanometer-scale resolution and a

wide variety of materials such as polymers, metals, ceramics, and biological molecules in different forms could be incorporated into the films at desired location. Also, the LbL deposition is possible with all kinds of intermolecular interactions such as electrostatic interactions, hydrogen bonds, and hydrophobic interactions. The intensity of these intermolecular interactions between paring molecules could also be tuned by external stimuli such as pH or salts, resulting in the release or disintegration of the molecules as well as the swelling of the multilayer film.[12-14]

In the present study, we explored the *in-situ* fibrillation of κ-casein within multilayer films consisting of κ-casein and PAA by the LbL deposition.

4.2. Experimental Section

Materials. Bovine milk κ-casein, poly(acrylic acid) (PAA, M_w = 100 000 g mol^{-1}), poly(sodium 4-styrene sulfonate) (PSS, M_w = 70 000 g mol^{-1}) and 1,4-dithiothreitol (DTT), thioflavin-T (Th-T) were purchased from Sigma-Aldrich and used as received without further purification. Silicon wafers were used as substrates to build multilayer thin films.

Preparation of LbL Multilayered Film With κ-Casein/PEs. κ-Casein from bovine milk (10 mg/ml) was dissolved in 18MΩ Milli-Q water (pH 3) and negatively charged PEs, PAA (1 mg/ml) and PSS (1mg/ml), was dissolved in 18MΩ Milli-Q and then the polymer solutions were adjusted to pH3 by adding diluted HCl and NaOH solutions. Only PSS solution contained salt (NaCl 0.1 M) to build up successfully by charge screening of PSS chain. The κ-casein solution was filtered by nylon syringe filter (0.45 μm) to remove undissolved precipitates and the concentration of κ-casein was adjusted to 5 mg/ml and then κ-casein solution was additionally adjusted at pH3. (κ-Casein/PAA) and (κ-casein /PSS) films were assembled by dip-based LbL depostion on silicon wafer treated with RCA solution (NH_3OH : H_2O_2 : H_2O = 1: 1: 5) for 10 min at 70 °C . The dipping time in each κ-casein and PEs solutions was 10 min followed by three rinse baths of distilled water adjusted at pH 3 for 1, 1, and 1min each, respectively. No drying step was used in the deposition procedure until it was in the last layer. The cycle was repeated to reach the desired number of bilayers of (κ-casein/PAA) and (κ-casein/PSS) multilayered films.

Fibrillation of κ-Casein within LbL Film. The prepared multilayered films were dipped in DTT solution (20 μM) and thermally treated at 80°C for desired incubation time. To control of intermolecular interaction between κ-casein and its pair PEs, PAA and PSS, the pH of DTT solution was varied: pH 3, 5, and 8.

Fibrillation of κ-Casein/PEs Mixtures in Bulk Solution. The concentration ratio of κ-casein and PAA or PSS for complex formation was fixed at 5 : 1 (in mg/ml), which is the same as the experimental conditions for the LbL multilayer film assembly. The solutions were initially mixed at pH 3 and pH of the solutions was then adjusted to pH 5 and 8. These mixed solutions, adjusted to pH 3, 5, and 8, were then thermally incubated for 12 hr at 80 °C in the presence of DTT, which is again the same condition for the film experiments.

Characterization. The thickness of prepared LbL film were measured by surface profilometer (Alpha Step IQ, KLA Tenco) and the surface morphology of the *in-situ* nanocomposite was examined by atomic force microscopy (AFM, Veeco Dimension 3100) with super sharp tip (SSS-NCHR, NANOSENSORS) in the tapping mode in air. The interior morphology of nanocomposite was investigated by scanning electron microscopy (SEM, JEOL-6701F) at an operating voltage of 20 kV. The samples were prepared for cross-sectional SEM images by cooling them in liquid nitrogen and cleaving the cold substrate to obtain a clear cress-section. Zeta-potential value of κ-casein as a

function of pH was measured by electrophoretic mobility measurement (Otsuka Electronics, ELS-8000).

Monitoring of Swelling Behavior of the Multilayer Films with QCM-D. The swelling behavior of the multilayer films was monitored by QCM-D and Q-Tools analysis. The pH-triggered changes in the frequency (Δf_3) of the multilayer film deposited on an Au sensor crystal (QSX301) were monitored by QCM-D (Q-Sense D300, Q-Sense AB). Two different types of the multilayer films were stabilized at pH3 water, which is the same pH for the initial film deposition and then pH 5 water was injected to the sample chamber.

4.3. Results and Discussion

4.3.1 Growth Behaviors of κ-Casein Containing LbL Films

The charge density of the κ-casein (pI: 4.5 ~ 5.8)[15] is affected by pH of their surrounding environment due to the gain or loss of protons and the pH dependence on the charge density of κ-casein is demonstrated in Figure 4.1. Since the κ-casein is positively charged at pH 3 as confirmed by zeta potential measurements, two kinds of negatively charged PEs, poly(acrylic acid) (PAA) (Mw = 100 000) and poly(4-styrene sulfonic acid) (PSS) (Mw = 70 000), were employed as oppositely polymers to construct multilayer films to verify the effect of controlled intermolecular interactions between *κ*-casein and oppositely charged PEs on the fibrillation of κ-casein within the multilayer films. Figure 4.2. shows the film thickness growth curves of two different types of the LbL films, indicating that the film growth behavior is significantly dependent on the type of polyanions used. The growth of (κ-casein/PAA) films exhibits an exponential-like growth behavior for the first few bilayers, followed by a linear growth from 6 bilayers showing the large increment in film thickness with each bilayer deposition. On the contrary, the growth of (κ-casein/PSS) bilayers is essentially linear with a very small thickness increment per each bilayer deposition. The average thickness per bilayer in linear growth regime is 261 $\pm$ 2 and 7 $\pm$ 0.5 nm for the (κ-casein/PAA) and (κ-casein/PSS) films, respectively. This tremendous difference is caused by the different building mechanisms of the LbL films. The degree of ionization of PSS, fully charged, is independent on the pH values and the (κ-casein/PSS) films were constructed by electrostatic interactions at pH 3. On the other hand, the degree of ionization of PAA is strongly dependent on the pH values. The pKa of PAA has been reported as

range of 5.5~6.5 and the degree of ionization is about 5 % at pH 3 in bulk solution. However the charge density of an absorbing PAA would increase substantially from its soluble-state value when it is incorporated into a multilayer film. The degree of ionization of PAA increases about 20-40 % (pKa value: 3.5~5.5) at pH 3 when PAA assemble with oppositely charged linear polymer, poly(allylamine hydrochloride) (PAH) and poly(diallydimethylammonium chloride) (PDAC).[16] Thus, we expect that the degree of ionization of PAA within the (κ-casein/PAA) multilayer film would increase when PAA is adsorbing on the positively charged κ-casein at pH 3. However the degree of such increased ionization of PAA is insignificant when compared with PAA assembled with fully charged linear polymer PDAC and PAH since the zeta-potential of κ-casein (+13 mV) at pH 3 is low compared with the value of synthetic PEs.[17] Also Cuisinier et al.[18] and Izumrudov et al.[17] have reported that protonated polycarboxylic acids of PAA and poly(methacrylic acid) and amide bonds of proteins are associated by hydrogen bonding. Thus, the amide bonds in κ-casein and protonated carboxylic acid should also form the hydrogen bonding. In addition, the amino acids such as Gln (Q), Asn (N), Asp (D), and Glu (E) in the κ-casein are also associated with protonated carboxylic groups in PAA at pH 3 by hydrogen bonding and the number of the four different types of amino acids is 36 among 169 whole amino acids sequence in the κ-casein.

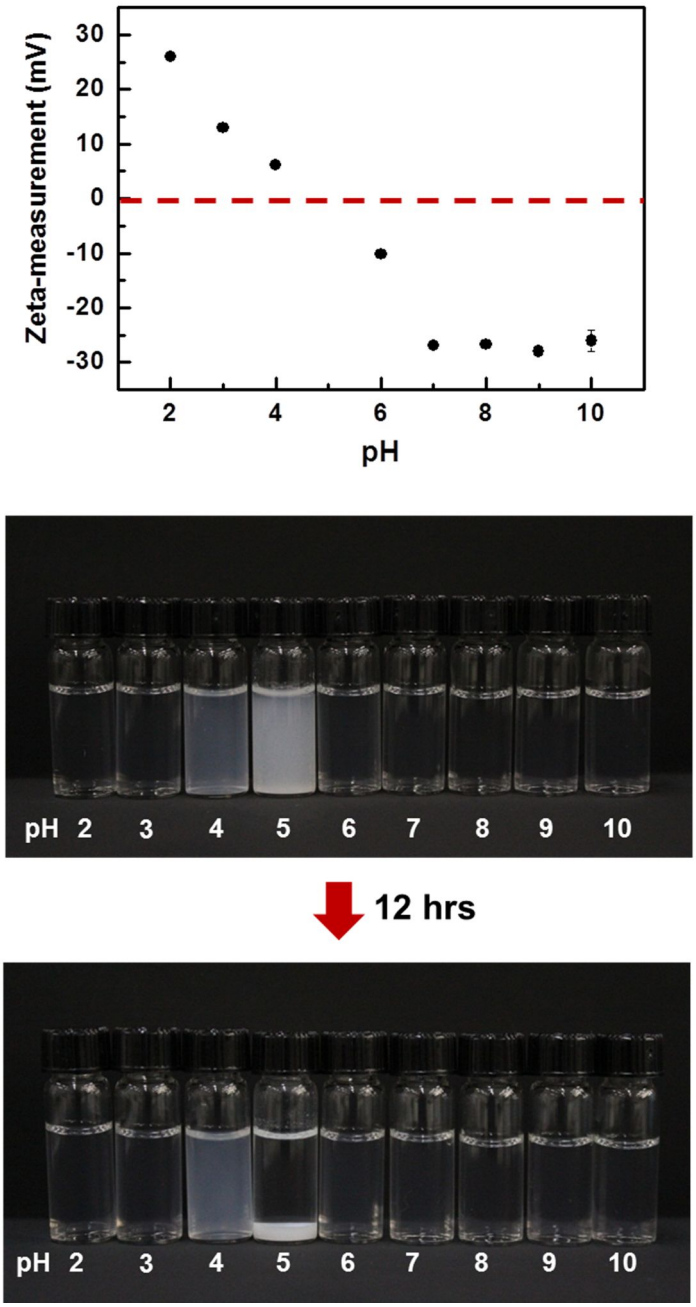

Figure 4.1. Zeta-potential and turbidity measurements of κ-casein as a function of pH.

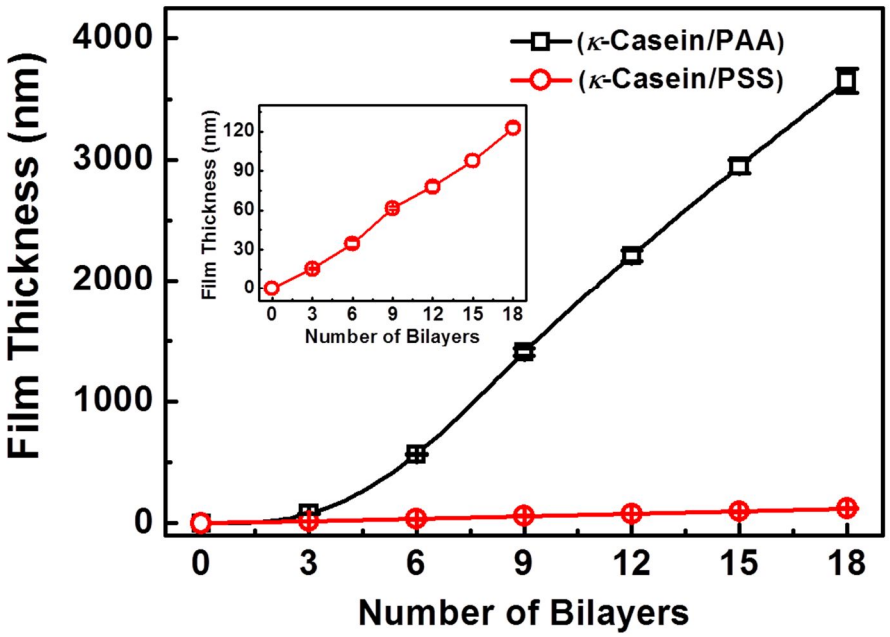

Figure 4.2. The film growth behavior of (κ-casein/PAA) and (κ-casein/PSS) multilayered films assembled at pH 3 on silicon substrates by the dip-based LbL deposition. An inset shows the magnified film thickness growth of (κ-casein/PSS) multilayers showing the linear growth.

4.3.2 pH Dependent on the Film Growth Behavior

To ascertain the driving forces for the film construction, the (κ-casein/PAA) multilayer films were constructed in different deposition conditions: κ-casein (pH 3) with PAA at three different pH values (2, 3 and 4). The film growth curves (in Figure S2) show the fastest growth of a multilayer film when assembled at pH 3/3 (denoting the pH of κ-casein/pH of PAA) when compared with other deposition conditions pH 3/4 and pH 3/2. The electrostatic interactions are believed to increase in the film assembled at pH 3/4 while the hydrogen bonding is more likely for the film assembled at pH 3/2. We believe that the deposition of a multilayer film with the highest bilayer thickness, assembled at pH 3/3, is mainly driven by the combined interactions of both hydrogen bonding and electrostatic interactions. The experimental data showing the different film growth behavior is given in Figure 4.3.

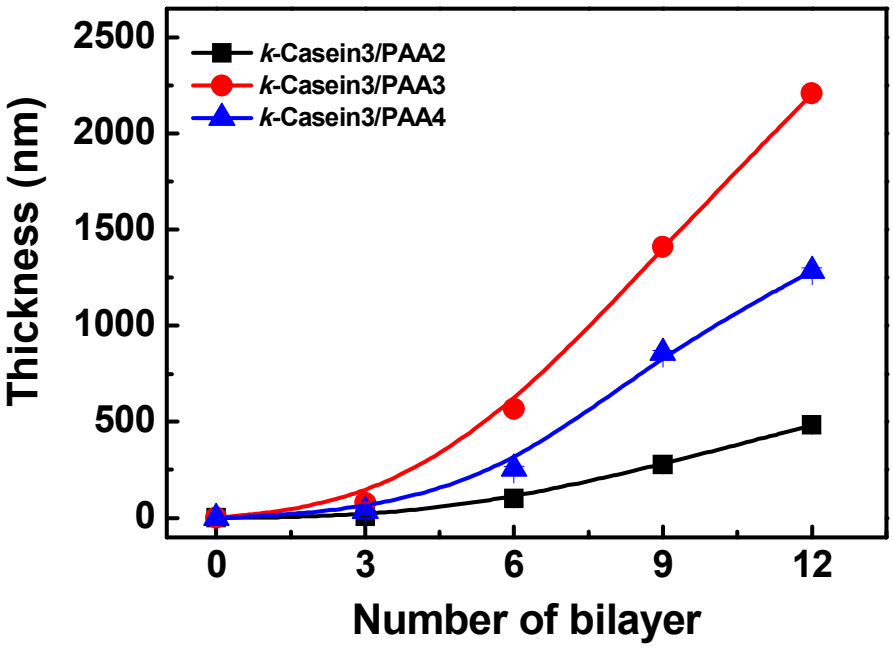

Figure 4.3. The film growth behavior of (κ-casein/PAA) multilayer films assembled with κ-casein (pH 3) and PAA at different pH values (pH 2, 3, and 4).

4.3.3. κ-Casein Fibril Formation within LbL Films by External Stimuli

Figure 4.4 is the AFM phase images of two different types of LbL films: the (κ-casein/PAA)$_{6.5}$ films on the left column and the (κ-casein/PSS)$_{6.5}$ films on the right column. The images of (a) and (b) are the surface morphologies of each film assembled at room temperature and pH 3. The images of (c, d), (e, f), and (g, h) are the surface morphologies of the films thermally treated for 6 hr at pH 3, 5, and 8, respectively. The films thermally treated at pH 3, the same pH value in which the multilayer films were initially deposited, do not show the formation of amyloid fibrils because of strong intermolecular interactions between κ-casein and pairing PEs (PAA) maintained, hindering the mobility of κ-casein to form fibrils. When these films were thermally incubated at pH 5, the κ-casein was successfully fibrillated within the (κ-casein/PAA) multilayer films but not within the (κ-casein/PSS) multilayer films. We believe that the decrease in the number of hydrogen bonds between κ-casein and PAA by the deprotonation of carboxylic acid groups in PAA and the reduced electrostatic attractions due to the change in zeta potential of κ-casein from positive to neutral values when pH changes from 3 to 5 (Figure 4.1) all contributed to gain the mobility of κ-casein within the film to form fibrils. We also note that the fibril morphology within the film is quite different from the fibrils formed with the treatment at pH 5 in the bulk solution shown in Figure 4.5.well-distributed fibrils within the film without massive κ-casein aggregates. This is due to the fact that well-dispersed κ-casein were uniformly deposited when the initial deposition condition is pH 3 and were transformed into fibrils when thermally treated in pH 5 of DTT solution without massive aggregation of κ-casein owing to intermolecular interactions between κ-casein and pairing PEs within the multilayered

films. Although the degree of charge density of κ-casein varies by changing pH so much like weak PEs, the fibril formation was not achieved when the κ-casein was initially strongly bound to PSS, presumably due to the negligible change in the intermolecular interactions between κ-casein and PSS, because the degree of ionization of a weak PEs is strongly dependent on the type of oppositely charged PEs within the LbL films.[19] We also note that when the multilayer films were thermally incubated at pH 8, (κ-casein/PAA) film was completely dissociated while the (κ-casein/PSS) film maintained over 90% of its original film thickness. In addition, the $(\kappa\text{-casein/PAA})_{6.5}$ film was thermally incubated at pH 4, a midway between pH 3 and 5, in the presence of DTT in order to clarify how sensitively the fibrillation of κ-casein within LbL films is affected by pH stimuli. The fibrils formed at pH 4 show the morphology similar to the fibrils formed at pH 5 except the fact that the number density of fibrils within the film is lower than the number density of fibrils formed at pH 5, as shown in Figure 4.6. These results demonstrate that the sensitive control of intermolecular interactions between κ-casein and pairing PEs within multilayered films is crucial in transforming κ-casein into fibrils within the multilayer films.

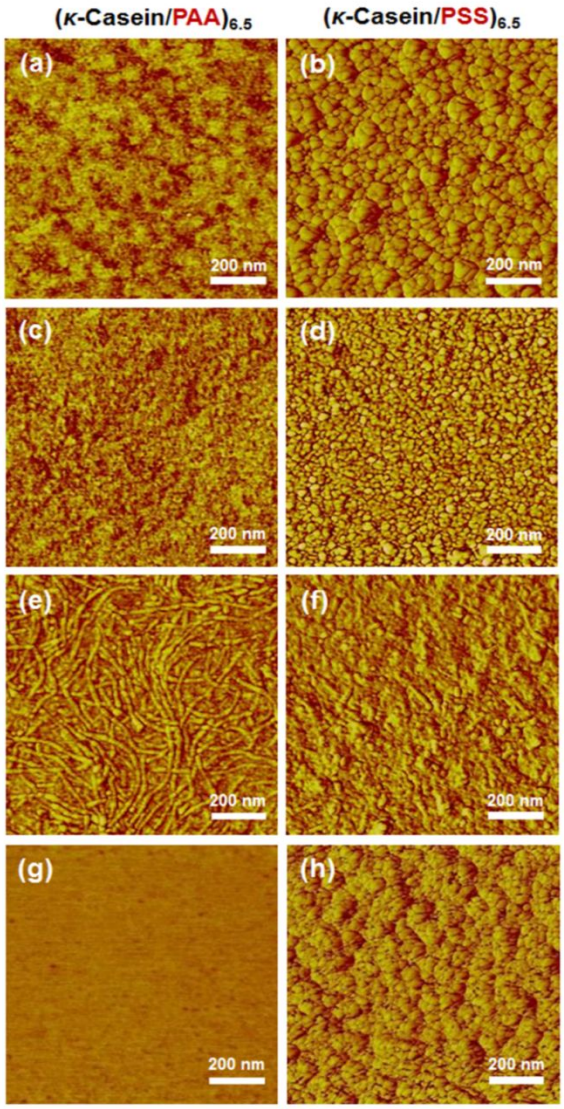

Figure 4.4. AFM phase images of the surface morphologies of (κ-casein/PAA)$_{6.5}$ (left column) and (κ-casein/PSS)$_{6.5}$ (right column) multilayer films. (a) and (b): the surface morphologies of films assembled at room temperature and pH 3; (c) and (d), (e) and (f), and (g) and (h): the surface morphologies of films thermally incubated in DTT solutions (20 mM) in pH 3, 5 and 8.

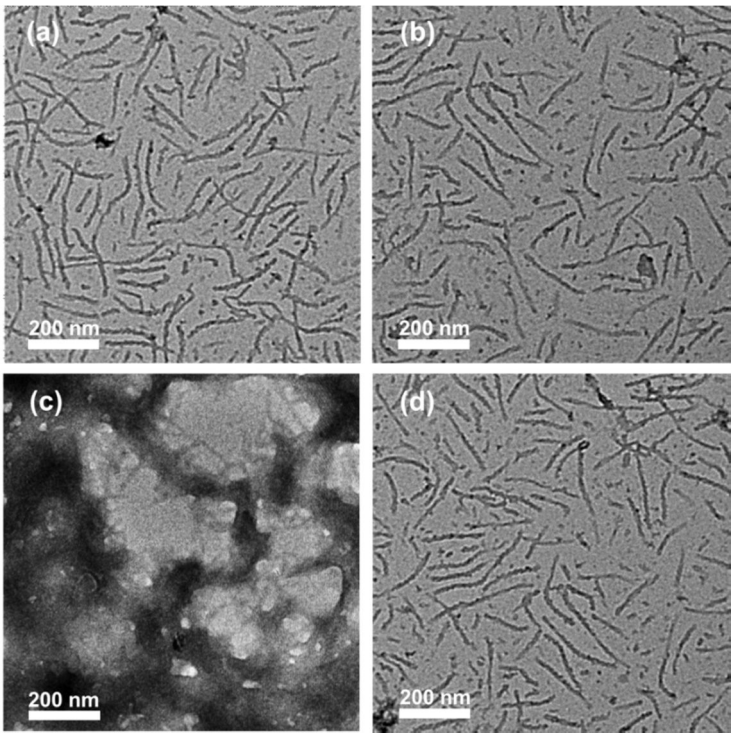

Figure 4.5. TEM images of κ-casein fibrils or aggregates formed in bulk solution treated in different pH values ((a) pH 3, (b) pH 4, (c) pH 5, and (d) pH 8) at 80 °C for 12 h in the presence of DTT.

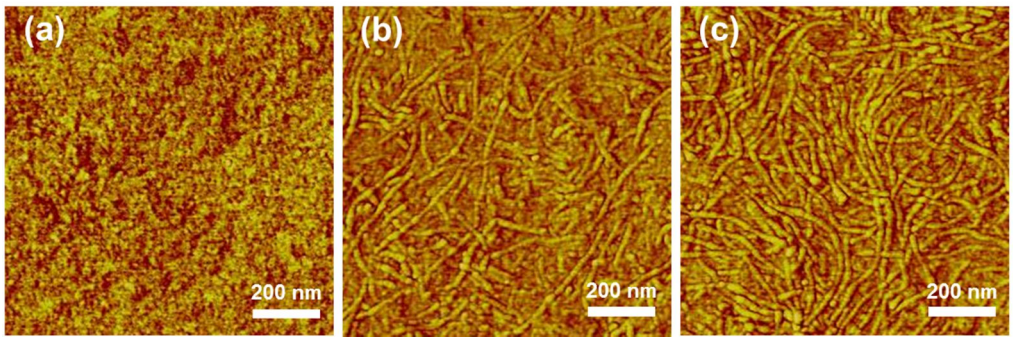

Figure 4.6. AFM phase images of (κ-casein /PAA)$_{6.5}$ which were thermally treated at 80°C in DTT solution for 6 hr with three different pH conditions: (a) pH 3, (b) pH 4, and (c) pH 5.

4.3.4. Different Response of Complex consisting of κ-Casein Micelles and Polyelectrolyte to pH conditions

In order to confirm the pH sensitivity of intermolecular interactions between κ-casein and charged polyelectrolytes for the formation of fibrils in bulk solutions, κ-casein solutions were mixed with two types of polyelectrolytes (i.e., PAA and PSS) at pH3 and thermally incubated for 12 hr at pH 3, 5 and 8 in the presence of DTT, which are the same conditions for the film experiment. At pH 3, the both mixtures showed big aggregates of clusters consisting of κ-casein and PAA or PSS. However, in the case of κ-casein/PAA mixtures, the massive aggregates, initially formed by the complexation at pH 3, were gradually dissociated by the increase in pH with κ-casein fibrils formed at pH 5 and 8 by thermal incubation. In contrast, the κ-casein/PSS mixtures were found to be less influenced by pH adjustment without forming fibrils, although the size of clusters somewhat decreased at pH 8 (Figure 4.7). Although there have been several reports on the kinetics of fibril formation of proteins affected by charged macromolecules,[20,21] the type of pairing PEs, such as weak and strong PEs, mainly determines the fibril formation of κ-casein within LbL films.

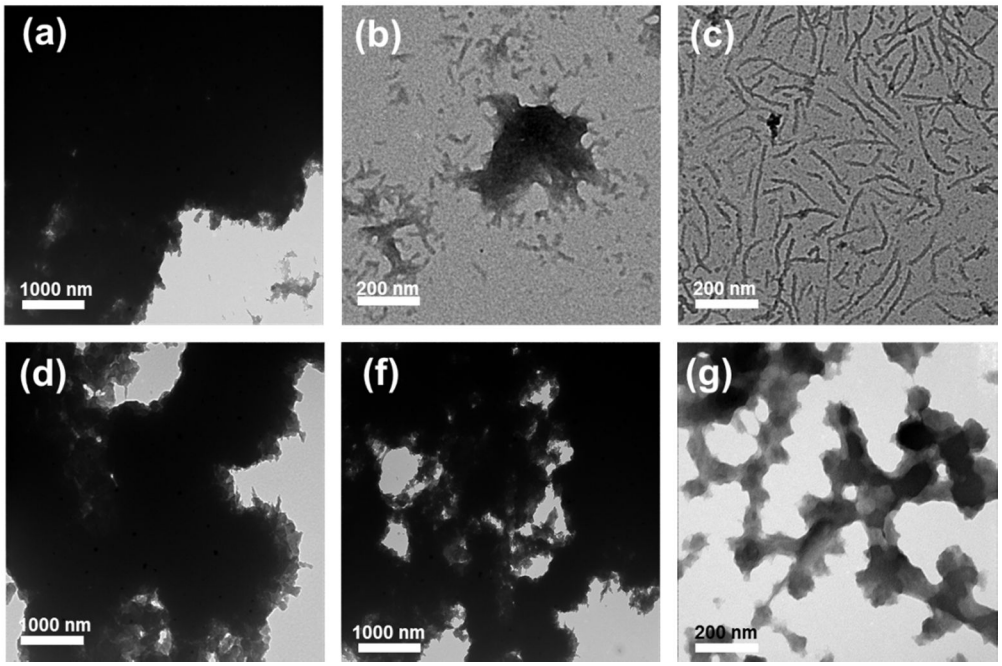

Figure 4.7. TEM images of (κ-casein/PAA) mixtures as well as (κ-casein/PSS) mixtures after thermal incubation at different pH in the presence of DTT. The three images (a, b, c) of in the first row show the (κ-casein/PAA) mixtures while the three images (d, f, g) in the second row show the (κ-casein/PSS) mixtures at different final pH. Note that first, second, and third columns are the final pH values of 3, 5, and 8, respectively during the thermal incubation.

4.3.5. Swelling Behavior Monitored by Quartz Crystal Microbalance with Dissipation(QCM-D)

The swelling behavior of two different types of the films, (κ-casein/PAA) and (κ-casein /PSS) films, are monitored with quartz crystal microbalance with dissipation monitoring (QCM-D), which were both subject to post-treatment at pH 5 of water, as seen in figure 4.8. We set the bilayer number at 3.5 for both film systems such that the film swelling could be monitored by QCM-D. We noted the significant decrease in the frequency ($\Delta f_3/3$ = -110 (Hz)) when the $(\kappa\text{-casein/PAA})_{3.5}$ film was post-treated at pH 5, indicating that the film was gradually swollen up to 12 hr by the pH change. On the other hand, there is no such changes in the frequency for the $(\kappa\text{-casein/PSS})_{3.5}$ film. We believe that the swelling of weak PE-based $(\kappa\text{-casein/PAA})_{3.5}$ film is induced by the charge imbalance (i.e., deprotonation of carboxylic acids in PAA) within the film, originating from the pH change. This film swelling is believed to assist the increase in the mobility of κ-casein within the multilayer film to form fibrils.

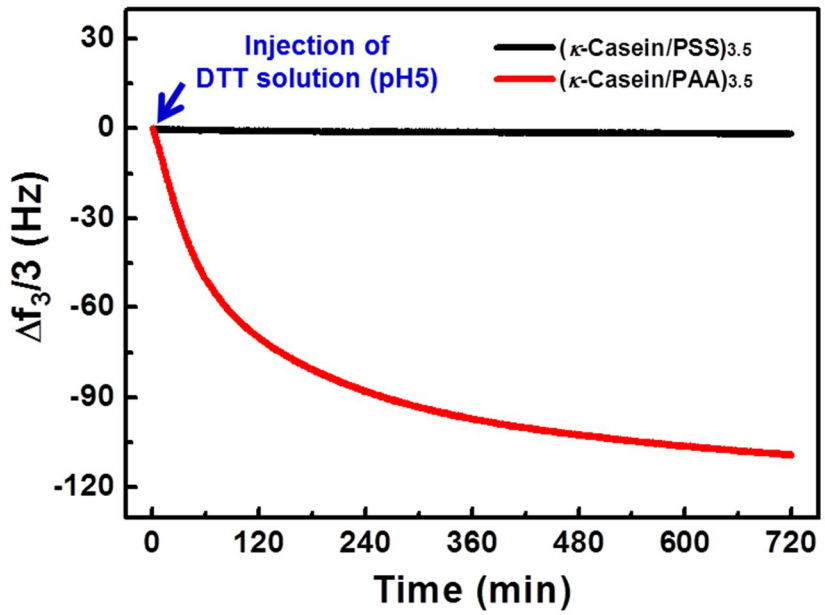

Figure 4.8. QCM-D responses showing the difference in frequency change between (κ-casein/PAA)$_{3.5}$ and (κ-casein/PSS)$_{3.5}$ multilayer films upon treatment at pH 5.

4.3.6. Inner structure of the Film

The AFM image shown in Figure 4.10.(a) presents the bottom side of the film which was thermally treated for 12 hr. at 80 °C in the presence of DTT at pH 5. As seen in Figure 4.10.(a), the fibrils were formed even in bottom of the film which contacted on the silicon substrate. In addition, the SEM image shown in Figure 4.10.(b) is the cross-sectional image of a (κ-casein/PAA)$_{6.5}$ film, which are the same film with AFM measured in Figure 4.10.(b). It is interesting to note that the κ-casein were not only fibrillated on the surface of the (κ-casein/PAA) LbL film but was also fibrillated throughout the film and the fibrils were also fully entangled together. This fibrillation within all over the thin film matrix including surface, interior and bottom of the film and entanglement between fibrils would be anticipated that plays a role as reinforcement in the nanocomposite thin film.

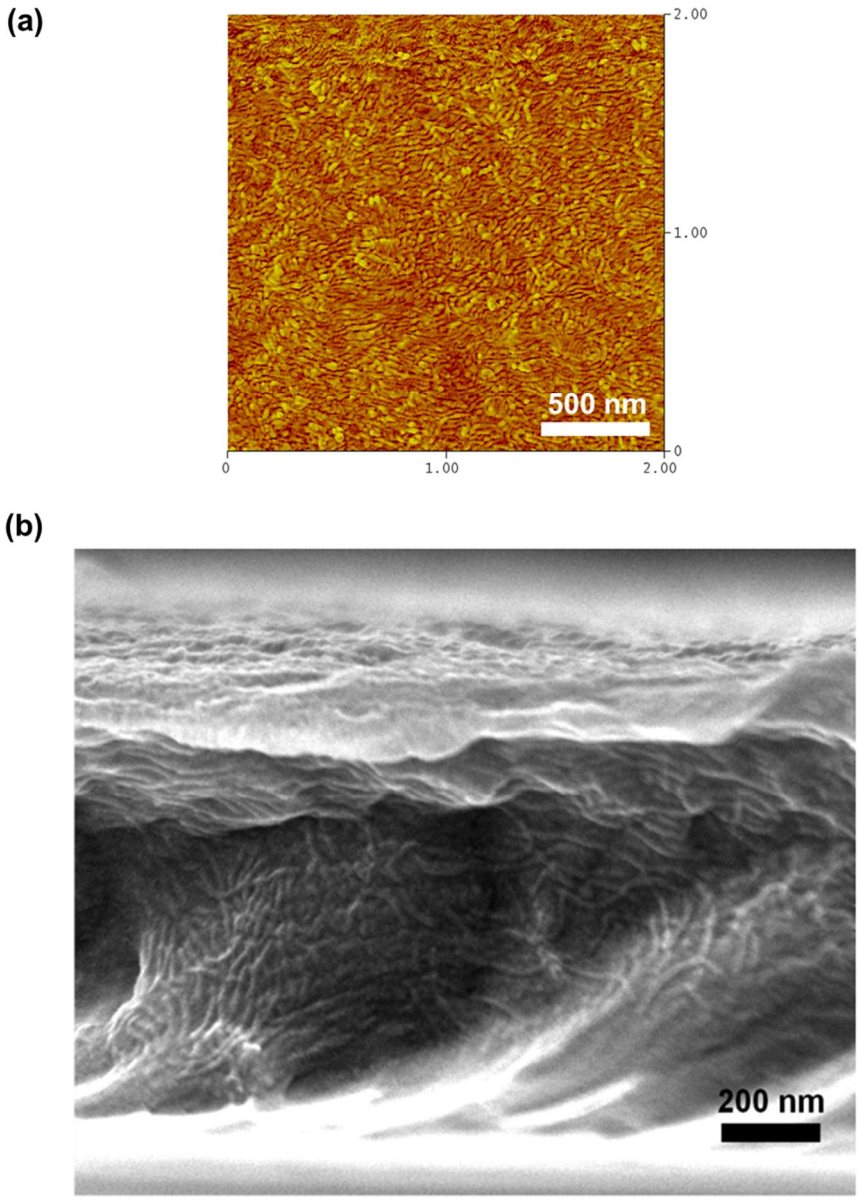

Figure 4.9. (a) AFM images of bottom of (κ-casein/PAA)$_{6.5}$ multilayer films thermally treated at pH 5 in DTT solution (20 mM). (b) A SEM cross-sectional image of a (κ-casein /PAA)$_{6.5}$ multilayer film thermally treated for 12 hr in DTT solution (pH 5, 20 mM).

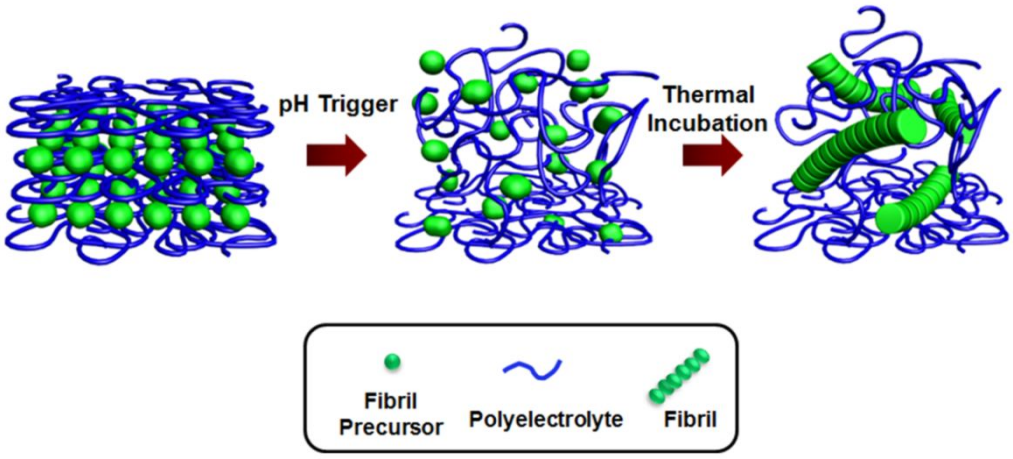

Scheme 4.1. A schematic on the formation of in-situ nanocomposite films by pH change and thermal incubation of multilayer films consisting of κ-casein and an oppositely charged PEs.

4.4. Conclusion

We have explored the formation of *in-situ* nanocomposite films consisting of a weak PEs (PAA) and κ-casein, employed as biocompatible amyloid fibril precursors, constructed by the dip-based LbL deposition. The κ-casein was transformed into amyloid fibrils without film delamination by combined external stimuli such as pH, reductant, and heat. The aspect ratio as well as the fibril density of such amyloid fibrils within the multilayer films was controlled by incubation time. The formation of *in-situ* nanocomposite films, triggered by external stimuli, could open up new types of nanocomposite platforms suitable for a wide range of advanced materials and biomedical applications.

4.5. References

(1) Kojima, H.; Ishijima, A.; Yanagida, T. *P Natl Acad Sci USA* **1994**, *91*, 12962.

(2) Claessens, M. M. A. E.; Bathe, M.; Frey, E.; Bausch, A. R. *Nat Mater* **2006**, *5*, 748.

(3) VanBuren, V.; Cassimeris, L.; Odde, D. J. *Biophys J* **2005**, *89*, 2911.

(4) Schaap, I. A. T.; Carrasco, C.; de Pablo, P. J.; MacKintosh, F. C.; Schmidt, C. F. *Biophys J* **2006**, *91*, 1521.

(5) Fudge, D. S.; Gardner, K. H.; Forsyth, V. T.; Riekel, C.; Gosline, J. M. *Biophys J* **2003**, *85*, 2015.

(6) Oppenheim, T.; Knowles, T. P. J.; Lacour, S. P.; Welland, M. E. *Acta Biomater* **2010**, *6*, 1337.

(7) Li, C. X.; Adamcik, J.; Mezzenga, R. *Nature nanotechnology* **2012**, *7*, 421.

(8) Even, N.; Adler-Abramovich, L.; Buzhansky, L.; Dodiuk, H.; Gazit, E. *Small* **2011**, *7*, 1007.

(9) Decher, G.; Hong, J. D. *Makromol Chem-M Symp* **1991**, *46*, 321.

(10) Tang, Z. Y.; Wang, Y.; Podsiadlo, P.; Kotov, N. A. *Adv Mater* **2006**, *18*, 3203.

(11) Ji, L. W.; Tan, Z. K.; Kuykendall, T.; An, E. J.; Fu, Y. B.; Battaglia, V.; Zhang, Y. G. *Energ Environ Sci* **2011**, *4*, 3611.

(12) Kharlampieva, E.; Ankner, J. F.; Rubinstein, M.; Sukhishvili, S. A. *Phys Rev Lett* **2008**, *100*.

(13) Mauser, T.; Dejugnat, C.; Sukhorukov, G. B. *Journal of Physical Chemistry B* **2006**, *110*, 20246.

(14) Zhuk, A.; Mirza, R.; Sukhishvili, S. *Acs Nano* **2011**, *5*, 8790.

(15) Holland, J. W.; Deeth, H. C.; Alewood, P. F. *Proteomics* **2004**, *4*, 743.

(16) Choi, J.; Rubner, M. F. *Macromolecules* **2005**, *38*, 116.

(17) Izumrudov, V. A.; Kharlampieva, E.; Sukhishvili, S. A. *Biomacromolecules* **2005**, *6*, 1782.

(18) Gergely, C.; Bahi, S.; Szalontai, B.; Flores, H.; Schaaf, P.; Voegel, J. C.; Cuisinier, F. J. G. *Langmuir : the ACS journal of surfaces and colloids* **2004**, *20*, 5575.

(19) Sukhishvili, S. A.; Kharlampieva, E.; Izumrudov, V. *Macromolecules* **2006**, *39*, 8873.

(20) Goers, J.; Uversky, V. N.; Fink, A. L. *Protein science : a publication of the Protein Society* **2003**, *12*, 702.

(21) Jones, O. G.; Adamcik, J.; Handschin, S.; Bolisetty, S.; Mezzenga, R. *Langmuir* **2010**, *26*, 17449.

Chapter 5.

Fibrillation of κ-Casein through Thickening and Branching of Fibrils on the LbL Film

5.1. Introduction

Protein aggregation of soluble peptides/proteins into highly ordered fibrils has received considerable attention because of their association with many neurodegenerative diseases[1-3] As well-known examples of disease related amyloid, plaques of β-amyloid peptide and α-synuclein are discovered in Alzheimer's and Parkinson's patients, respectively.[4-7] Therefore the short chains of peptides such as GAV-9 (NH_2-VGGAVVAGVOCONH$_2$), a conversed consensus of α-synuclein, β-amyloid, and prion protein, widely applied as a biological model system to study protein folding and aggregation.[8-11] Although differences in the native structures and functions of the amyloid forming proteins, they form similar fibrillar structures irrespective of the types of proteins and they have certain interaction with lipid membrane surfaces.[12,13] Therefore, the investigation about formation of amyloid fibrils on the surface of lipid membrane is excessively important and may provide an insight into understanding the mechanism of amyloid fibril formation which has relations with diseases.

Beyond aspect of medical research field, the study of protein aggregation has recently attracted a lot of attention because self-assembly of peptides into nanostructure with desired shapes and functionalities provides a route to fabricate new materials and

functional devices.[14,15] Furthermore, the study of protein aggregation on the surfaces has also recently attracted a lot of attention and grown even more important due to the increased use of inorganic and synthetic surfaces as interfaces in bio/nanotechnology. Due to self-assembly of peptides/proteins is usually sensitively affected by many weak interactions, non-covalent interactions, including hydrogen bonding, hydrophobic interactions, van der Waals forces, electrostatic interactions, and π-π stacking[16-19] and is occur under certain conditions,[20-22] affective factors for assembly from soluble protein into amyloid fibrils strongly depends on the types of proteins. Also, in a physically confined environment, it has been shown that confinement effects can play dominant roles on self-assembly of block copolymers to generate critical structures which are not accessible in bulk, thus providing opportunities to engineer new structure with potential novel applications. Recently Hu and coworkers demonstrated that self-assembly behavior of peptide in the water nanofilm on mica, as a model system, showing different epitaxial self-assemble behaviors at relative humidity.[23] In this case, water film has a role as confined region because the water nanofilm contact with air, which are interface between water and air.

In previous study, we have developed nanocomposite induced by in-situ assemble of κ-casein oligomers into amyloid fibrils within LbL multilayer film consisting of κ-casein oligomers and weak polyelectrolyte, PAA, by external stimuli including heat, and pH changes. In this study, we investigated that fibrillation kinetics depended on incubation time and how the factors which influence to fibrillation kinetics in bulk, such as temperature, reduction of disulfide bonding, and quantity of κ-casein oligomers, affect on the fibril formation and kinetics on the LbL film.

5.2. Experimental Section

Materials. Bovine milk κ-casein, poly(acrylic acid) (PAA, M_w = 100 000 g mol^{-1}) and 1,4-dithiothreitol (DTT) were obtained from Sigma-Aldrich and used as received without further purification. Silicon wafers were used as substrates to build multilayer thin films.

Preparation of LbL Multilayered Film With Up-Casein/PEs. κ-Casein from bovine milk (10 mg/ml) was dissolved in 18MΩ Milli-Q water (pH 3) and negatively charged PEs, PAA (1 mg/ml), was dissolved in 18MΩ Milli-Q and then the polymer solutions were adjusted to pH3 by adding diluted HCl and NaOH solutions. The κ-casein solution was filtered by nylon syringe filter (0.45 μm) to remove undissolved precipitates and the concentration of κ-casein was adjusted to 5 mg/ml and then κ-casein solution was additionally adjusted at pH3. (κ-Casein/ PAA) films were assembled by dip-based LbL depostion on silicon wafer treated with RCA solution (NH_3OH : H_2O_2 : H_2O = 1: 1: 5) for 10 min at 70 °C . The dipping time in each κ-casein and PEs solutions was 10 min followed by three rinse baths of distilled water adjusted at pH 3 for 1, 1, and 1min each, respectively. No drying step was used in the deposition procedure until it was in the last layer. The cycle was repeated to reach the desired number of bilayers of (κ-casein/PAA) multilayered films.

Fibrillation of κ-Casein within LbL Film. The prepared multilayered films were dipped in DTT solution (20 μM, pH 5) or Milli-Q water (pH 5) and thermally treated at 40°C or 80°C for desired incubation time.

Characterization of Film Thickness and Surface Morphologies. The thickness of prepared LbL film were measured by surface profilometer (Alpha Step IQ, KLA Tenco) and the surface morphology of the *in-situ* nanocomposite was examined by atomic force microscopy (JPK, Nanowizard 3) with super sharp tip (SSS-NCHR, NANOSENSORS) in the tapping mode in air.

Monitoring of Adsorption Behavior of κ-casein and PAA with QCM-D. The adsorption behavior of κ-casein and PAA to build up the multilayer films was monitored by QCM-D and Q-Tools analysis. The changes in the frequency (Δf_3) of the multilayer film deposited on an Au sensor crystal (QSX301) were monitored by QCM-D (Q-Sense D300, Q-Sense AB). The concentration of κ-casein and PAA was diluted as 10 times compared (κ-casein: 0.5 mg/ml, PAA: 0.1 mg/ml) when the LbL film are assembled because adsorption with same concentration of κ-casein and PAA solution reaches the detection limit of QCM equipment within 3 bilyaers.

5.3. Results and Discussion

5.3.1. Monitoring of κ-Casein Fibrillation with incubation Time

Figure 5.1. shows the AFM images of the surface morphologies of the (κ-casein/PAA)$_{6.5}$ multilayer films thermally incubated at 80 °C in a DTT solution of pH 5, as a function of incubation time. We have noticed that length as well as the packing density of fibrils increases with the incubation time. For the first 2 hr of thermal incubation, there was no transformation of κ-casein into fibrils observed. The kinetics of fibril formation on the LbL film surface is slower when it compared with fibrillation kinetics under same incubating temperature in bulk solution. Small fraction of fibrils started to appear from 4 hr of thermal incubation and the fibrillation persisted and became more pronounced up to 12 hr of incubation. The kinetics of fibril formation of κ-casein on the LbL film was totally slower when compared with fibrillation kinetics of κ-casein in bulk solution. It is thought that mobility of bound κ-casein oligomers on the surface of the LbL film is restricted, thus it need to extended time to assemble into amyloid fibrils. Interestingly, the morphology of κ-casein fibrils was different with fibril grown in bulk solution, indicating that assembly of protein into fibrils affected by environmental conditions such as pH value and dimensional differences in space. The aspect ratio of fibrils grown on the LbL film was three times bigger than fibrils grown in bulk solution, which were induced by two kinds of factors: pH and space. When the fibrils are assembled in bulk solution, the κ-casein is thermally incubated within broad ranges of pH value, except for pH 5. If κ-casein is thermally incubated at pH 5, κ-casein aggregates into randomly amorphous aggregates due to lack of electro-repulsive forces between κ-casein molecules at near

isoelectric points. Therefore the fibrils assembled are not branched for extended thermal incubation in bulk solution, except pH 5. Also the surface plays a role as the catalyst to assemble fibrils extended.

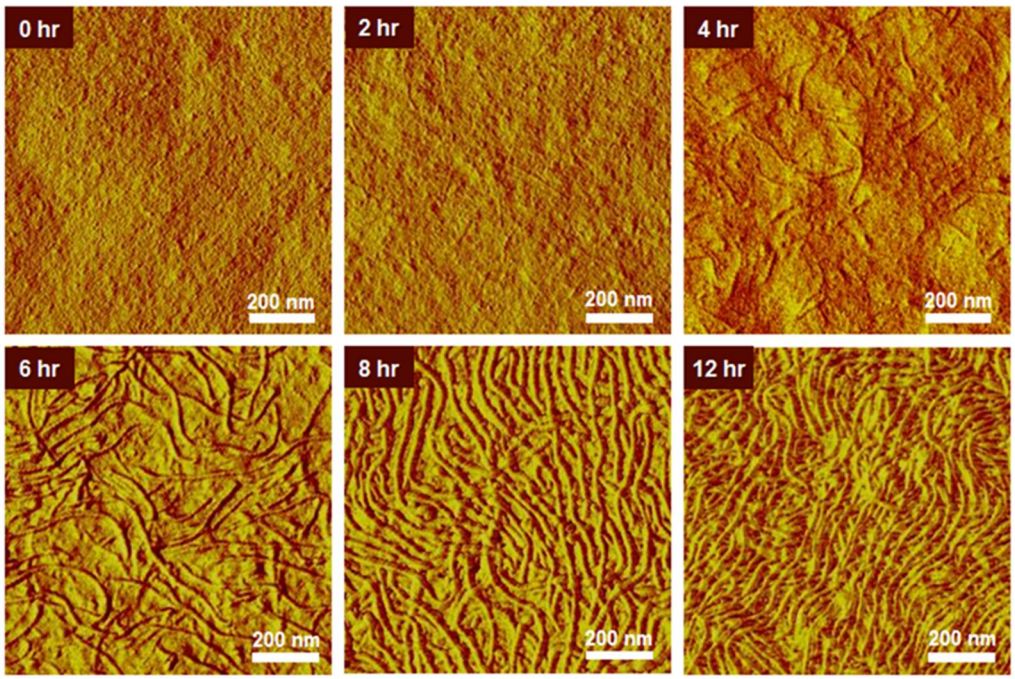

Figure 5.1. Surface morphologies of the (κ-casein/PAA)$_{6.5}$ multilayer films thermally treated at pH 5 in DTT solution (20 mM) as a function of incubation time.

Furthermore, the LbL film including κ-casein oligomer and PAA was thermally treated under same incubation environment, at 80 °C and in the presence of DTT, to monitor the change of fibrils on the LbL film with prolonged incubation until 36 hr. As shown in Figure 5.2.(a), the κ-casein fibrils have under gone substantial changes in their morphologies, which presenting increased thickness of fibrils and branching structure among the fibrils. In order to monitoring of morphological changes of the fibrils in more detail, the surfaces of the LbL film were analyzed with AFM after 12, 18, 24, and 36 hr, and the images are in Figure 5.3.(b). It presented that thickness of the fibrils was 6~8 nm and they was not branched or linked each other when the LbL film thermally incubated for 12 hr. However, the thickness of fibrils increased until 100 nm. And the number of thickened fibrils increased, on contrary the number of fibrils having thickness in 6~8 nm decreased with incubation time until 36 hr. This increase of fibril thickness and branching among fibrils were not seen in the bulk experiment, and this phenomenon is closely relative with fibrillation environment, especially on the LbL film. As we thought the extended contour length of fibrils assembled on the LbL film were affected by pH value and dimensions of space for fibril formation, it is suggested that the thickening and branching of the fibrils have close relations with intermolecular interactions between fibrils and difference in dimension of space for fibril formation. Matured or assembled κ-casein fibrils which appear 6-8 nm in thickness are secondary assembled with fibrils each other resulted in thickening of the fibril and branching each other with extended thermal incubation, as mentioned previous, because the isoelectric point of fibrils are close to pH 5.

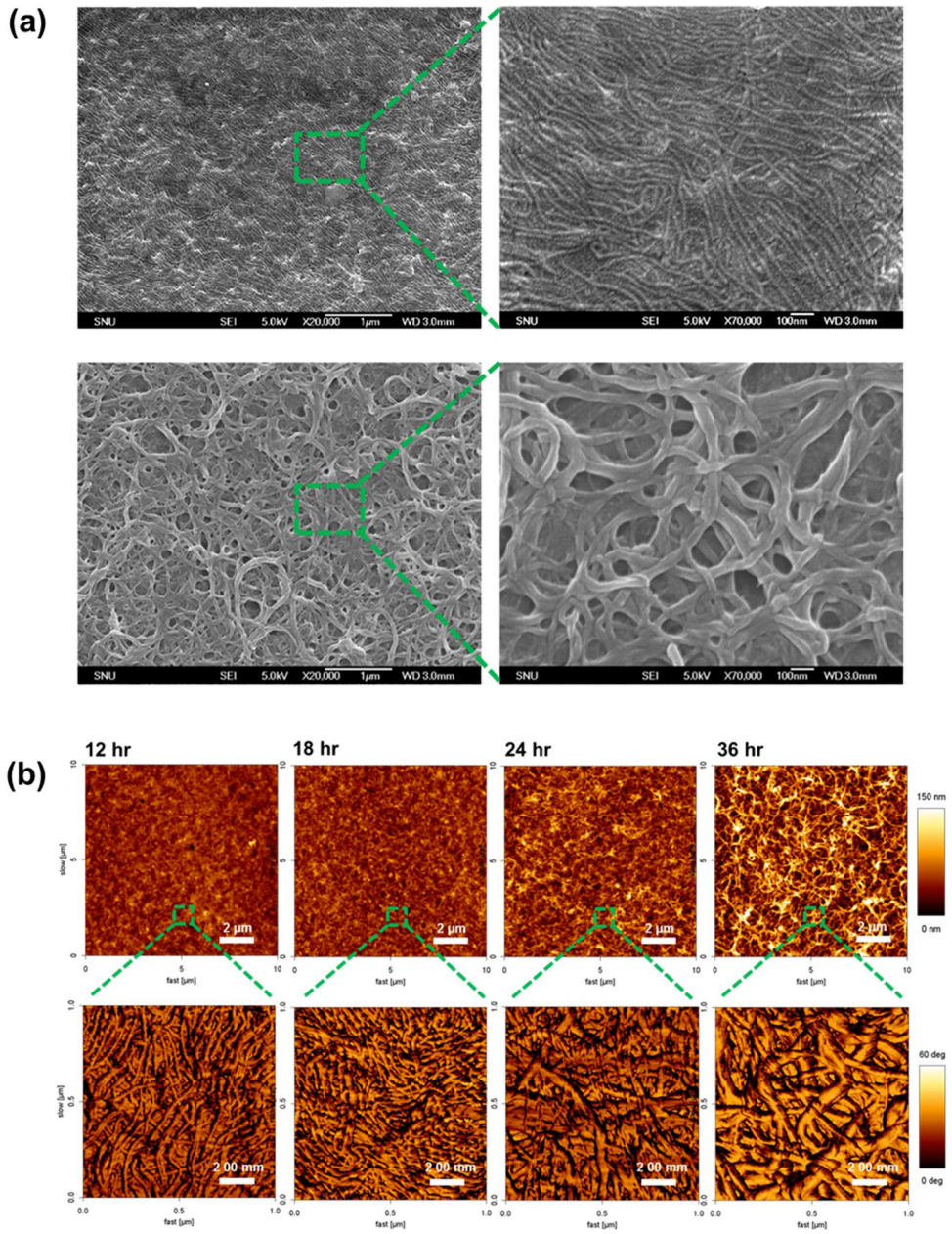

Figure 5.2. Surface morphologies of (κ-casein/PAA)$_{6.5}$ Film after thermally incubated at 80 °C in the presence of DTT. (a) SEM images of the film after incubated for 12 and 36 h, and (b) AFM images of the film after thermally incubated for 12, 18, 24, 36 h.

5.3.2. Factors Affecting Fibrillation of κ-Casein on the LbL Films

We investigated that incubation temperature, degree of reduction of disulfide bonds as well as concentration of κ-casein influence on the kinetics of κ-casein fibrillation when κ-caseins are incubated in bulk solution. Although the fibrils formed on the LbL film show different morphology as extended thermal incubation, we demonstrated that the effects of factors including quantity of κ-casein, reduction of disulfide bonds, and heat, on the fibrillation as well as thickening and branching of the fibrils on the LbL film. To elucidate the effect of quantity of κ-casein within LbL film, the films containing different amount of κ-casein were thermally incubated at 80 °C in the presence of DTT until 36 hr. The varying amount of κ-caseins on the surface of LbL film was easily obtained by courtesy of the film growth behavior. Figure 5.3.(a) and (b) demonstrates the film growth behavior analyzed by profilermeter and QCM-D, respectively. As shown in Figure 5.3., the LbL film are grown appearing exponential, non-linear growth behavior in not only film thickness bur also mass of the film until 6 bilayers by combined force with hydrogen bonds and electrostatic interactions between κ-casein and PAA. Therefore the varying quantity of κ-casein adsorbed on the LbL film was easy with merely varying in the number of layers of the LbL film. Also we have noticed that the mass of κ-casein adsorbed on the LbL film are much huge than PAA adsorbed on the LbL film. We assume that this difference was induced by oligomeric state of κ-casein. Although the molecular weight of κ-casein (18.8 kDa) is smaller than PAA (100kDa), κ-casein form from monomer to decamer due to disulfide bonds by cysteine within κ-casein.

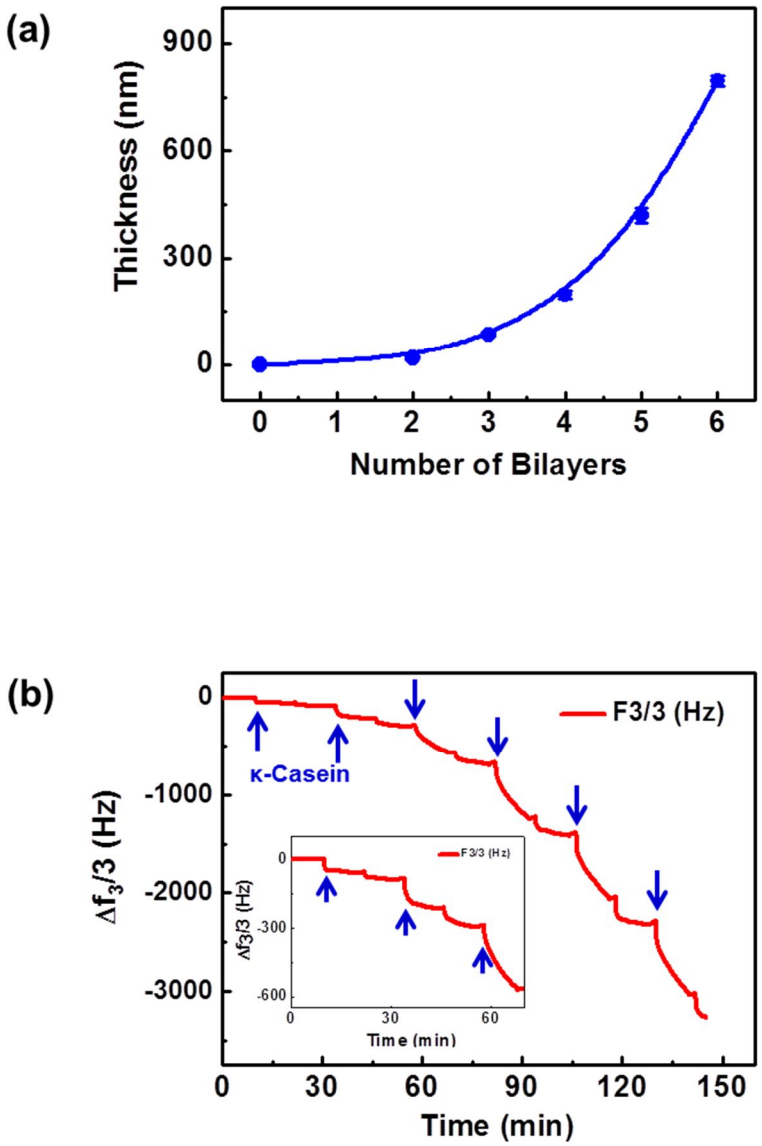

Figure 5.3. Characterization of the film growth behaviors (a): film thickness growth curve measured by surface profiler, and (b): Mass growth of the film monitored by QCM-D.

In order to investigate the effect of quantity of κ-casein on the fibrillation process, the six different (κ-casein /PAA) multilayer film, which were varied on the number of bilayer, were thermally incubated at 80 °C in the presence of DTT until 36 hr and the surface morphologies were analyzed by AFM measuring, as shown in Figure 5.4. In the figure, (a) column presents phase images of film incubated for 12 hr, and (b) and (c) columns present phase and height images of the film incubated 36 hr, respectively. As seen in the figure, the fibrils were not formed on the monolayer of κ-casein until 36 hr and the number of thick fibrils increased as increase in number of bilayer, indicating that the increasing quantity of κ-casein on the LbL film induces the thickening of the fibrils. This behavior of fibrillation and additional assembly are strongly affected by quantity of κ-casein on the LbL film, and the quantity dependent fibrillation mechanism of κ-casein fibrils on the LbL film is correlated with fibrillation mechanism in bulk solution which is based on nucleation dependent amyloid assembly mechanism.

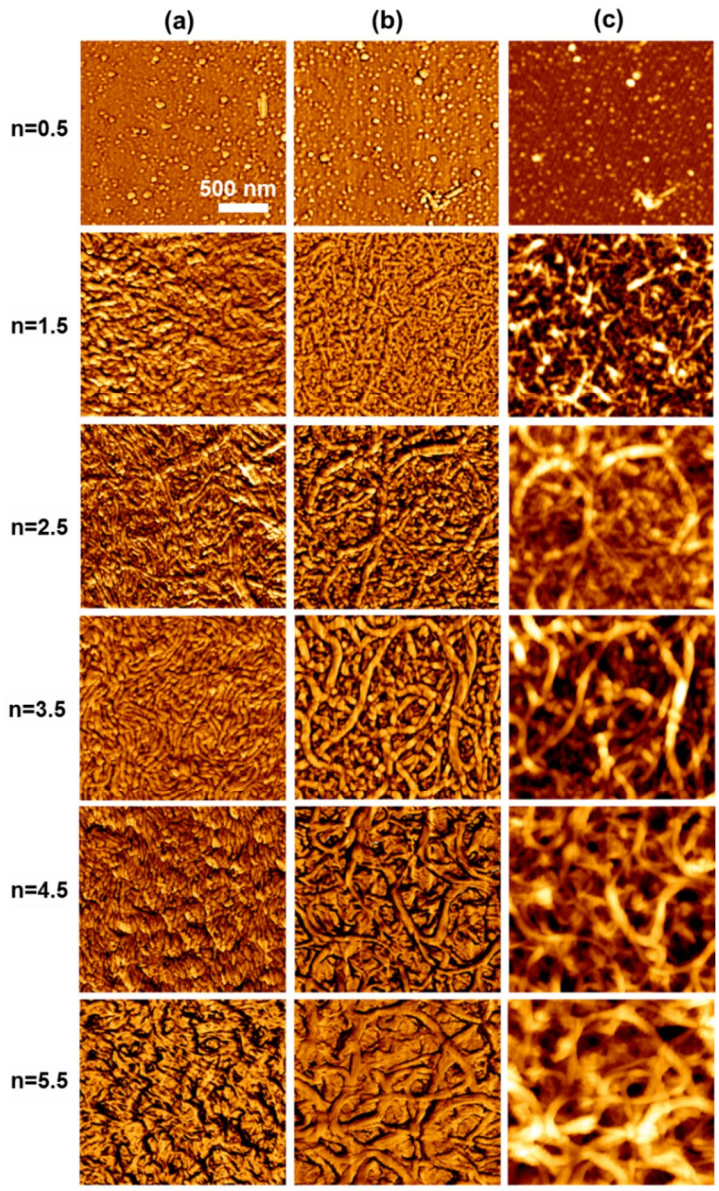

Figure 5.4. AFM images of the surfaces of (κ-casein//PAA)$_n$ film varying number of layer of deposition after thermally incubated for 12 and 36 h. (a) Phase images of 12 h incubated films, (b) phase images of 36 h incubated films and (c) height images of 36 h incubated films.

Also we demonstrated that the effects of two kinds of affecting factors including temperature and reduction of disulfide bonds on the fibrillation of κ-casein on the LbL films. The number of the bilayer was fixed at 6.5 bilayers in order to maintain same quantity of κ-casein on the LbL films. The AFM images shown in Figure 5.5 demonstrate effects of temperature on the fibril formation on the LbL film, as a control experiment shown in (a) which the LbL films were thermally treated at 80 °C in the presence of DTT. In case of (b), the LbL films were thermally treated at 40 °C in the presence of DTT. The fibrillation rate including normal fibril formation and both of thickening and branching of the fibrils was delayed at low incubation temperature. In point of thickening of the fibrils, the thickness of the fibrils did not increase until 10 day at 40 °C, which are extremely slower fibrillation rate when it compared with fibrillation of κ-casein on the LbL films at 80 °C. Moreover the number of thicken fibrils are also less than the number of thicken fibrils incubated at 80 °C. The fibrillation kinetics of κ-casein on the LbL film is strongly depended on the incubation temperature, which are correlated with fibrillation kinetics in the bulk solution.

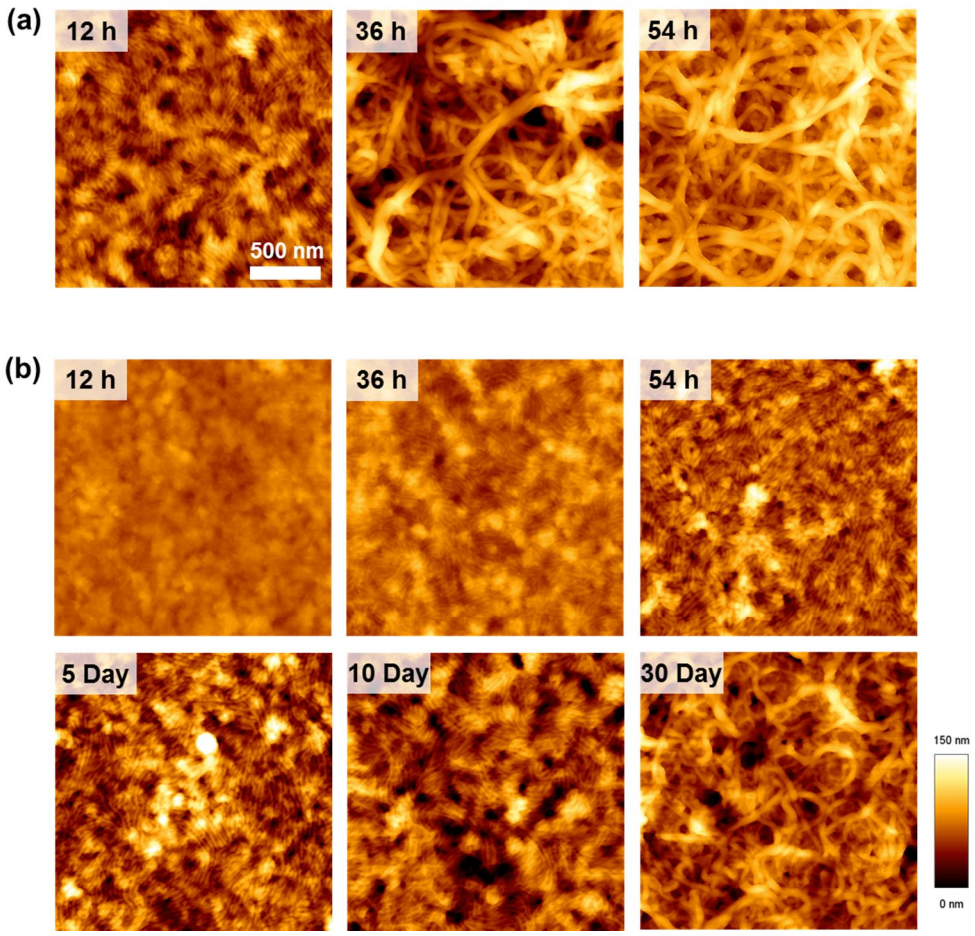

Figure 5.5. AFM images of the surfaces of (κ-casein/PAA)$_{6.5}$ film thermally incubated at different temperature in the presence of DTT. (a) Surface morphologies of the film thermally incubated at 80 °C, as control experiment. (b) Surface morphologies of the film thermally incubated at 40 °C

In addition, the reduction effect of disulfide bonds within κ-casein on fibrillation rates within the LbL film was also demonstrated, as shown in Figure 5.6. The (κ-casein/PAA)$_{6.5}$ films were thermally incubated at 80 °C in the presence of DTT as a control experiment (a), and the LbL films were incubated in the absence of DTT (b), in order to compare the fibrillation rate and fibril morphologies. When the both of the films were thermally incubated for 12 hr, the fibrils appeared only in the films incubated in the presence of DTT and density of fibrils are much less in the film incubated in the absence of DTT. Finally the fibril grown in the absence of DTT also was thickened by thermal incubation for 7 days, and the number of fibrils was much less than fibrils grown in the presence of DTT. Even though time to need to be thickened fibrils is shorter than fibrils incubated at 40 °C in the presence of DTT, the absence of DTT also not only delay the fibrillation kinetics, but also decrease the number of fibrils. Because the only dissociated κ-casein such as monomer, dimer, and trimmer are assembled into fibril, the dissociated κ-casein is very small without DTT and the lack of dissociated κ-casein decreases number of fibrils.

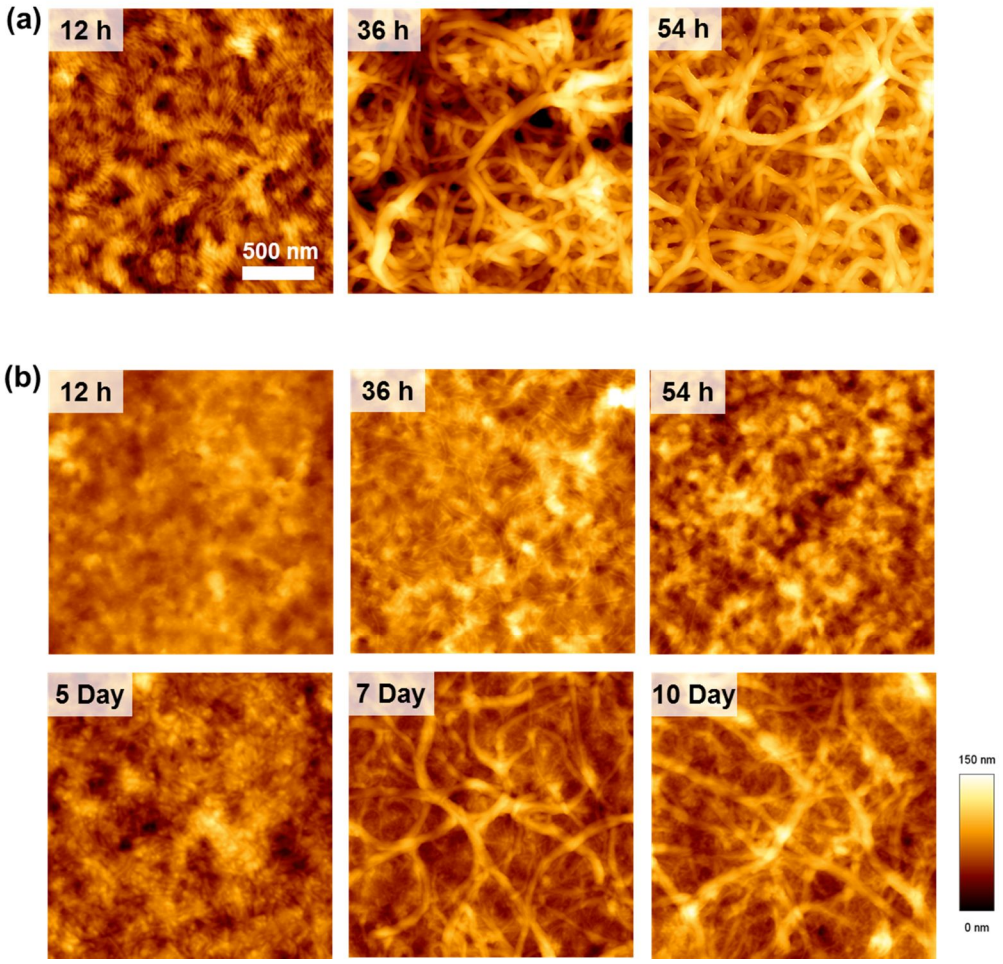

Figure 5.6. AFM images of the surfaces of (κ-casein/PAA)$_{6.5}$ film thermally incubated at 80 °C (a) in the presence of DTT, as a control experiment and (b) in the absence of DTT.

Based on analysis of AFM measurement of (κ-casein/PAA) multilayer films incubated in various environments, the fibrillation mechanism including thickening and branching of fibrils on the LbL film was assumed and shown in Scheme 5.1. The oligomeric κ-casein ranged from monomer to decamer is dissociated by reduction agent such as DTT. Monomeric κ-casein forms nuclei, followed by protofibrils and fibrils with intertwining of protofibrils by extended thermal incubation. The fibrils grown on the LbL film are intertwined each other, which resulted in thickening and branching of fibrils.

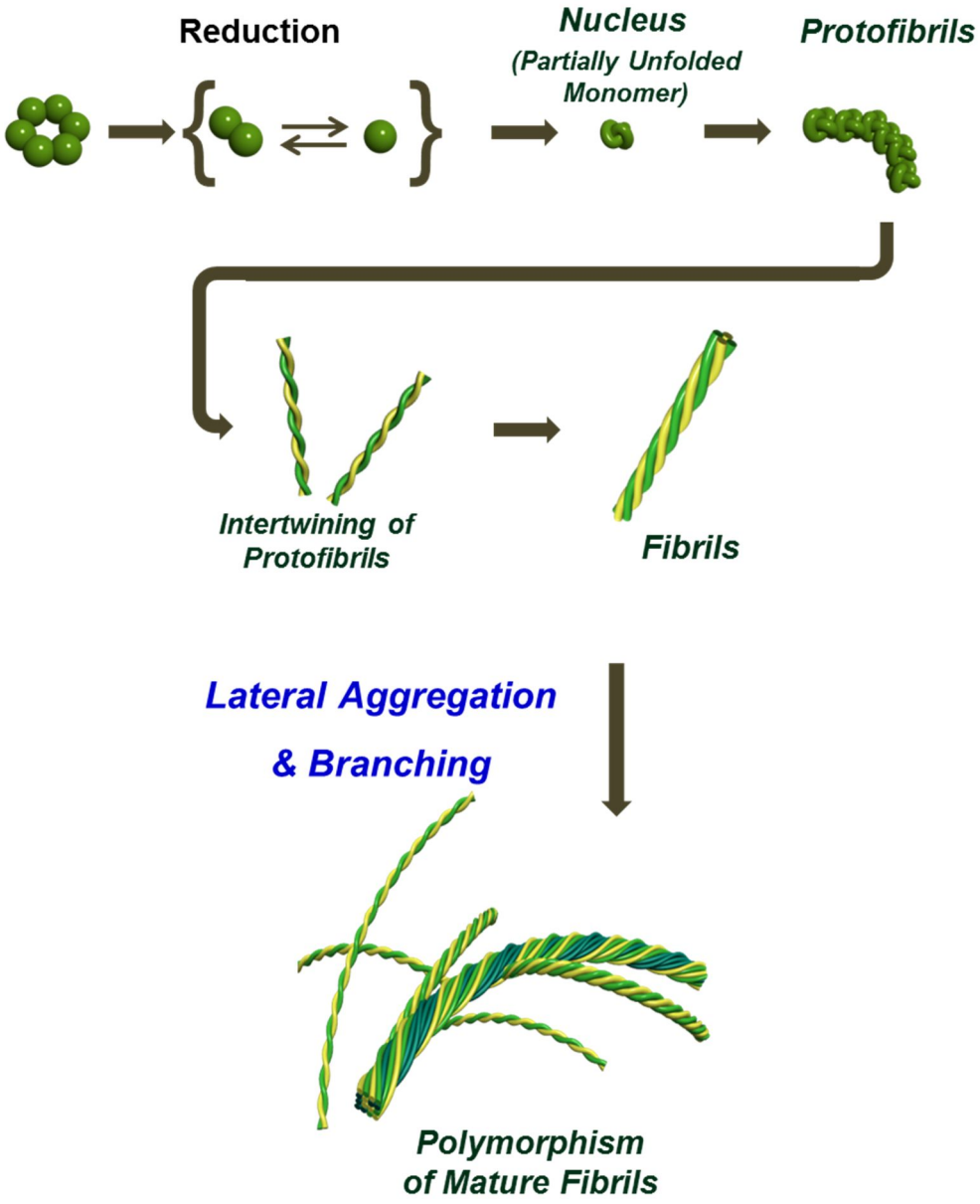

Scheme 5.1. A schematic diagram of fibril formation of κ-casein on the LbL film

5.4. Conclusion

Fibrillation kinetics of κ-casein is affected by environmental condition such as temperature and concentration as well as reduction of disulfide bonds within κ-caseins in bulk solution. Moreover these factors which influence on the fibrillation kinetics, control also contour length of fibrils as well as diameter of fibrils by intertwining of fibrils. In this study, we demonstrated the fibrillation of κ-casein within LbL film and the kinetics. Although fibrillation kinetics of κ-casein within LbL film is delayed when compared to fibrillation kinetics of κ-casein in solution, the contour length of fibrils increased more than three times. And also the fibrils were thickened and twined each other by extended thermal incubation, which were depended on the incubation temperature and reduction of disulfide bonds. In addition, this study provides a potential platform for fabricating structure controlled nanomaterials by self-assembly of functional group tailored peptides on the LbL film containing functional nanomaterials such as growth factors and drugs.

5.5. References

(1) Chiti, F.; Dobson, C. M. *Annual review of biochemistry* 2006, *75*, 333.

(2) Dobson, C. M. *Nature* 2003, *426*, 884.

(3) Wang, C. X.; Yang, A. H.; Li, X.; Li, D. H.; Zhang, M.; Du, H. W.; Li, C.; Guo, Y. Y.; Mao, X. B.; Dong, M. D.; Besenbacher, F.; Yang, Y. L.; Wang, C. *Nanoscale* 2012, *4*, 1895.

(4) Lesne, S. E.; Sherman, M. A.; Grant, M.; Kuskowski, M.; Schneider, J. A.; Bennett, D. A.; Ashe, K. H. *Brain : a journal of neurology* 2013, *136*, 1383.

(5) Dorr, A.; Sahota, B.; Chinta, L. V.; Brown, M. E.; Lai, A. Y.; Ma, K.; Hawkes, C. A.; McLaurin, J.; Stefanovic, B. *Brain : a journal of neurology* 2012, *135*, 3039.

(6) Kalia, L. V.; Kalia, S. K.; McLean, P. J.; Lozano, A. M.; Lang, A. E. *Annals of neurology* 2013, *73*, 155.

(7) Stone, D. K.; Kiyota, T.; Mosley, R. L.; Gendelman, H. E. *Neuroscience letters* 2012, *523*, 167.

(8) Li, H.; Zhang, F.; Zhang, Y.; He, J. H.; Hu, J. *Acta Bioch Bioph Sin* 2007, *39*, 285.

(9) Hamley, I. W. *Angew Chem Int Edit* 2007, *46*, 8128.

(10) Mobley, D. L.; Cox, D. L.; Singh, R. R. P.; Maddox, M. W.; Longo, M. L. *Biophys J* 2004, *86*, 3585.

(11) Dai, B.; Kang, S. G.; Huynh, T.; Lei, H. Z.; Castelli, M.; Hu, J.; Zhang, Y.; Zhou, R. H. *P Natl Acad Sci USA* 2013, *110*, 8543.

(12) ChooSmith, L. P.; GarzonRodriguez, W.; Glabe, C. G.; Surewicz, W. K. *J Biol Chem* 1997, *272*, 22987.

(13) Kakio, A.; Nishimoto, S.; Yanagisawa, K.; Kozutsumi, Y.; Matsuzaki, K. *Biochemistry-Us* 2002, *41*, 7385.

(14) Zhang, S. G. *Nat Biotechnol* 2003, *21*, 1171.

(15) Scheibel, T.; Parthasarathy, R.; Sawicki, G.; Lin, X. M.; Jaeger, H.; Lindquist, S. L. *P Natl Acad Sci USA* 2003, *100*, 4527.

(16) Chiti, F.; Calamai, M.; Taddei, N.; Stefani, M.; Ramponi, G.; Dobson, C. M. *P Natl Acad Sci USA* 2002, *99*, 16419.

(17) Otzen, D. E.; Kristensen, O.; Oliveberg, M. *P Natl Acad Sci USA* 2000, *97*, 9907.

(18) Pratt, L. R.; Pohorille, A. *Chem Rev* 2002, *102*, 2671.

(19) Raman, B.; Chatani, E.; Kihara, M.; Ban, T.; Sakai, M.; Hasegawa, K.; Naiki, H.; Rao, C. M.; Goto, Y. *Biochemistry-Us* 2005, *44*, 1288.

(20) Whitesides, G. M.; Grzybowski, B. *Science* 2002, *295*, 2418.

(21) Zhang, F.; Du, H. N.; Zhang, Z. X.; Ji, L. N.; Li, H. T.; Tang, L.; Wang, H. B.; Fan, C. H.; Xu, H. J.; Zhang, Y.; Hu, J.; Hu, H. Y.; He, J. H. *Angew Chem Int Edit* 2006, *45*, 3611.

(22) Zurdo, J.; Guijarro, J. I.; Jimenez, J. L.; Saibil, H. R.; Dobson, C. M. *J Mol Biol* 2001, *311*, 325.

(23) Li, H.; Zhang, F.; Zhang, Y.; Ye, M.; Zhou, B.; Tang, Y. Z.; Yang, H. J.; Xie, M. Y.; Chen, S. F.; He, J. H.; Fang, H. P.; Hu, J. *J Phys Chem B* 2009, *113*, 8795.

국문초록

아밀로이드를 포함한 단백질의 응집체에 대한 연구는 최근 의학, 식품, 나노 과학, 연성재료과학 등의 다양한 분야에서 주목받고있다. 특히 아밀로이드는 단백질의 베타병풍구조 간의 수소결합에 의해 형성된 고도로 정렬되고 안정한 나노 구조체로서 넓은 범위의 산도, 고농도의 염, 온도, 단백질 분해효소 등의 외부의 환경에 대해 저항성을 나타내며 실크나 강철과 견줄 수 있을 정도로 우수한 기계적 물성을 가지며 비교적 용이하게 다양한 기능기를 부여할 수 있다는 장점이 있다. 또한 아밀로이드 섬유체 간의 복합화를 통하여 젤과 박막의 구조체를 형성하고 약물 등의 기능성 물질을 담지 할 수 있기 때문에 기능성 소재의 재료로써 그 잠재력이 크다. 따라서 본 공학박사 학위논문에서는 생체적합성을 갖는 우유 단백질 중 하나인 카파-카제인을 이용하여 아밀로이드를 조립함에 있어서 그 형성속도와 구조를 제어하였고 응집모델을 제시하였으며, 다층적층법 기반의 아밀로이드 나노복합체 박막의 구현에 대해 논하고자 한다. 제 1장에서는 아밀로이드의 물리적 화학적 특성과 아밀로이드 나노복합체 박막을 형성하기 위한 방법 중 하나인 다층적층법에 대해 설명하였다.

제 2장에서는 카파-카제인의 아밀로이드 형성기전에 미치는 요소와 각 요소가 아밀로이드 형성에 미치는 영향을 규명하였다. 아밀로이드의 형성에 있어서 핵-의존성 응집기전을 따르는 일반적인 단백질의 경우 핵의 형성속도가 아밀로이드 형성속도를 결정하는 반면, 이황화결합에 의해 복합체로 존재하는 카파-카제인의 경우 이황화결합이 환원되어 카파-카제인의 단분자화가 아밀로이드 형성에 가장 큰 영향을 끼친다는 선행연구의 제안을 바탕으로 본 연구에서는 다량체로 존재하는 카파-카제인에 디티오트레이톨 (1.4-dithiothreitol)을 이용하여 카파-카제인 분자간의 이황화결합

을 환원시켜 단량체로 변환 후 열처리를 아밀로이를 조립함으로써 이황화결합의 환원에 아밀로이드 형성에 미치는 영향을 확인하였다. 또한 반응 온도와 카파-카제인의 농도가 아밀로이드의 형성 속도와 아밀로이드의 길이 및 그 형태 구조를 제어할 수 있다는 확인하였으며 원자간 힘 현미경을 통하여 정밀하게 분석함으로써 카파-카제인의 아밀로이드 형성 기작 모델을 제시하였다.

제 3장에서는 용액 내에서 조립된 카파-카제인 아밀로이드의 표면 전하의 종류와 세기가 외부 환경의 산도에 의해 제어된다는 것을 확인함으로써 이 성질을 이용하여 다층적층법 기반의 아밀로이드와 고분자전해질로 형성된 아밀로이드 나노복합체 박막을 구현하였다. 카파-카제인 아밀로이드는 카파카제인의 등전점 범위와 동일한 범위에서 등전점을 가지며 산 조건에서는 양전하로, 염기 조건에서는 음전하를 띄었다. 따라서 산 조건에서는 음전하를 갖는 고분자전해질과, 염기 조건에서는 양전하를 갖는 고분자전해질과 정전기적 인력을 기반으로하여 나노복합체 판상형 박막과 캡슐을 구현할 수 있었다. 특히 산 조건에서는 pH에 따라 이온화도가 변화하는 약고분자전해질과 이온화도가 변화하지 않는 강고분자전해질을 이용하여 다른 특징을 갖는 박막을 형성함으로써 아밀로이드와 고분자전해질의 상호간 인력의 차이가 아밀로이드 나노복합체 박막의 두께 성장과 표면의 거칠기에 미치는 영향을 규명하였다.

제 4장에서는 다층적층법을 기반으로 카파-카제인과 약고분자전해질을 포함하는 다층박막을 형성하였으며 다층박막 내에 포함되어 있는 카파-카제인은 외부자극에 의해 특정 조건 하에서 아밀로이드로 변환됨으로써 실시간 (in-situ) 아밀로이드 나노복합체 박막을 구현하였다. 약고분자전해질과 카파-카제인은 모두 외부 환경의 산도에 의해 전하밀도가 조절되기 때문에 산도를 조절하여 박막 내에 존재하는 카파-카제인과 약고분자전해질 간의 상호작용의 세기가 약화되도록 유도하였고 카파-카

제인의 이황화결합을 환원시키고 열처리함으로써 아밀로이드의 조립을 유도하였다. 또한 박막의 단면을 관찰함으로써 아밀로이드가 박막의 표면뿐만 아니라 박막의 내부에서도 형성되었으며 아밀로이드 가닥끼리 서로 얽힌 채로 균일하게 분포되어있었음을 확인할 수 있었다. 지금까지의 아밀로이드를 이용한 나노복합체 형성에 관한 연구에서는 아밀로이드를 기계적 물성을 향상시키는 강화제로 사용하기 위해 용액 내에서 먼저 아밀로이드로 조립한 다음 매질에 첨가시켜주는 방법으로 아밀로이드 나노복합체를 구현하였지만, 본 연구에서는 다층박막 내에서 아밀로이드의 조립을 유도함으로써 최초로 실시간 아밀로이드 나노복합체 박막을 구현하였다.

제 5 장에서는 아밀로이드 나노복합체 박막을 이용하여 새로운 나노재료 플랫폼을 구현하기 위해 박막에서의 아밀로이드 형성 이후의 조합현상에 대한 연구를 수행하였다. 아밀로이드의 형성속도 측면에서는 용액 내의 동일한 조건에서 생성되는 카파-카제인 아밀로이드의 성장속도에 비해서는 느렸지만, 그 평균외형길이는 3 배 이상 증가하였으며 나노복합체 박막의 표면에서 형성된 카파-카제인 아밀로이드는 반응시간이 증가하면서 아밀로이드 섬유가닥 간의 조합으로 아밀로이드가 서로 꼬이는 형태를 보였으며 그 두께 또한 증가하였다. 이러한 현상은 용액 내에서 생성되는 카파-카제인 아밀로이드의 형성과정에는 나타나지 않은 현상으로, 박막 내에 고집적되어 있는 아밀로이드 간의 상호작용으로 인해 발생하는 것으로, 이황화결합의 환원과 반응온도가 카파-카제인 아밀로이드 간의 조합에 미치는 영향을 규명하였다.

주요어: 기능성 박막, 다층적층법, 아밀로이드, 카파-카제인, 고분자전해질, 나노복합체

학번: 2009-31263